Aalto-yliopisto
Insinööritieteiden
korkeakoulu

Rodrigo Prieto Padilla

Selective Laser Melting of Silica Glass Powders

Master's thesis, which has been submitted as a thesis for examination for a Master's degree.

Espoo 09.11.2018
Supervisor: Professor Jouni Partanen
Advisor: Niklas Kretzschmar

Author Rodrigo Prieto Padilla

Title of thesis Selective Laser Melting of Silica Glass Powders

Master programme Mechanical Engineering **Code** MEN.thes

Thesis supervisor Jouni Partanen

Thesis advisor(s) Niklas Kretzschmar

Date 09.11.2018 **Number of pages** 109 **Language** English

Abstract Additive manufacturing (AM) has recently amassed great media coverage thanks to its unique capabilities and its appeal towards practicality; contrary to popular belief, these technologies have been used or developed for decades and are continuously improving. Currently, they have managed to allow a new method for fast prototyping, and new practices for producing complex structures with relative ease.

The variety of AM technologies currently available is large and employs different approaches to the process. Similarly, a multitude of materials are available for production which further broadens the reach of AM products. There is however, a lack of success in the field of glass AM as there have not been many significant developments in the field which would make this process as versatile as with other materials. Furthermore, the produced components with current glass AM methods do not fulfill the requirements that traditionally-manufactured glass components require, thus preventing these developments from getting past the experimental phase.

This study attempts to give a better understanding of the causes for these limitations, as well as provide a solution to these recurring issues by testing theories which presumably could solve them. This process was systematically and qualitatively documented and a conclusion, as well as an own attempt to solve recurring problems, is detailed.

Keywords AM, 3D printing, Selective Laser Melting, Glass AM, Process Parameter Optimization, Inspection

Acknowledgements

I would like to thank those who supported me during the development of this thesis as well as throughout the extent of my studies.

To *Jouni*, *Niklas*, *Sergei*, and *Sven*, your guidance and encouragement to pursue such an ambitious topic made it possible for me to enjoy this process.

To everyone at *ADDlab*, thank you for all those tips and tricks you taught me while doing my experiments. Specifically, to *Meng*, thank you for making me part of the team, and to *Olli*, thank you for your endless patience.

To my *dad*, I would have never been an engineer if you were not one.

To my *mom*, I would have never followed my dreams if you had not followed yours.

To *Elli*, you were there during the whole process and helped me stay sane.

To *the three of you*, thank you for your endless support and constant encouragement; none of this would have been possible without you. You all know and experienced how challenging it was for me to study something I do not understand in a language I do not speak, yet you never let me give up.

I dedicate this thesis to you.

Helsinki, October 10, 2018

Rodrigo Prieto Padilla

Glossary and acronyms

3D scanner	Device used for replicating 3D shapes digitally
3DP	3D printing
Ablation	Material removal by means of evaporation
Absorptance	Ability of a material to absorb energy
AM	Additive manufacturing
Annealing	Heat treatment to modify material properties
Balling	Formation of spheres during the powder-melting process
BJ	Binder Jetting
Build-plate	Surface upon which prints are deposited
CAD	Computer-aided design
CNC	Computer numerical control
Deflection coil	Magnetic device controlling the XY direction of an electron beam
DFA	Design for assembly
DIY	Do it yourself
Extrusion	Material-feeding by pushing feed through a fixed gap
FDM	Fused deposition modeling
FEM	Finite element method
Fly-cutter	Rotating end of a mill used for subtractive material-shaping
Galvanometer	Laser-beam XY movement device
G-code	Numerical control programming language. Interprets STL files as movements
Hatch distance	Distance between the center-lines of two scan lines
Hausner Ratio	Value used for indicating the flowability of a granulated material
Internal stress	A force within an object, unaffected by external influence
IoT	Internet of things
JIT manufacturing	Just-in-time manufacturing
Kiln	Oven chamber used for chemical processing with adjustable temperature
LAM	Laser AM
LAS	Lithium aluminosilicate
Lean methodology	Manufacturing methodology focusing on increasing productivity
LENS	Laser-engineered net-shaping
LOM	Laminated object manufacture
Rayleigh instability	Phenomena explaining the separation of liquid streams into separate balls
SGC	Solid ground curing

Sintering	Joining of softened and liquefied material without full melting
SLA	Stereolithography
Slicer	CAD-model processing software for slicing objects into layers
SLS	Selective laser sintering
XRD	X-ray crystallography

Contents

1 Introduction

Additive manufacturing (AM) comprises multiple manufacturing practices used to describe different technologies which have been appearing over the years. It is a process most often beneficial for low-scale production, with little technical knowledge, and with lower initial costs; it is a user-friendly approach to product development [1].

It has seen a rapid evolution throughout its long history. Currently, AM has evolved from being an experimental prototyping tool into an ecosystem providing tools for the manufacturing of components which cannot be done with traditional methods; likewise, it has seen a slower, yet marginal increase in manufacturing of final components rather than proof-of-concept prototypes [2].

When compared to traditional manufacturing methods, AM benefits from simplified processes involved in the completion of a product. Similarly to traditional methods, CAD skills, a basic understanding of the technology being used and its limitations, and general properties of the material being used are required to develop a prototype for printing. In comparison, traditional methods generally require machine lengthier operation skills, post-processing, safety regulation compliance, and manual per-material adjustments [3].

Fundamentally, the term AM elucidates its layered nature; components are generated by added layers changing cross-sectional areas according to the geometry of a product.

The term AM has perceived a slight, yet accelerated, displacement brought-on by the more common term “3D printing”. This is largely due to the mass consumer-oriented marketing behind the term 3D printing, whereas AM is frequently associated with technical or industrial processes. Gebhardt [2] goes as far as to claim that the term 3D printing will replace AM altogether given how it is easier for people to picture it when it is associated to well-known technologies like paper printing as well as its close relation to 3D modeling programs which makes-up a large part of the base functionality of the process.

It is widely considered that a 3D model is more useful than a drawing or technical specification sheet; not only do models contain all the dimensional information necessary to recreate a product, they also can be manipulated and modified to better understand the

product and to iterate with ease. Furthermore, models are necessary regardless of the existence of drawings or technical sheets to validate the product before production.

Amongst the benefits of implementing 3D printing in manufacturing, is the possible cost and time reduction of production lines. Some parts of a product can often introduce complicated procedures into the production. Odd shapes or complicated-to-machine components can significantly increase the costs of production by reducing speed or having the need for complimentary steps. Some components of a product might also not need higher-quality procedures to be produced and can easily be replaced by less-costly 3D printing processes [4].

AM is characterized by some unique traits. Their production requires no tooling unless post-processing is applied and can be produced in any orientation. Their production is possible thanks to STL (stereolithography) files which allow printing by means of algorithms which communicate the movement steps necessary for the material to be generated with precision. Additionally, printed components often have visible layers which can be identified as curved perimeters throughout the component when produced with fluid deposition processes or a porous structure when produced with powder-based methods.

The extent of materials which can be produced via AM processes is currently extensive enough to cover many material groups, yet glasses are still under-researched and thus, under-developed. The field of research of glass melting is not new yet lacks the extensive development which can be seen with other materials. Additionally, selective laser melting of glasses is nearly non-existent.

Most research done in the field has focused on testing different parameters of laser-powered sintering machines to further understand their effects and variations with glass materials; these materials come in powder form. The parameters most often tested are combinations of laser scanning-speed and laser power however, other parameters such as layer-height, powder-shape, hatch-spacing, laser spot-diameter, energy density, wavelength, and qualities of different materials have been tested as they are important to the field.

Per the findings of most research on the field which has been done between 1997 and 2017, a comprehensive understanding of the factors affecting these results has been achieved and these learnings are applied in this paper to try and produce pure SLM printed glass components. The focus of this study will be on applying these learnings and previously tested parameters, on silica powders with a gran size between 2-20μm. These powders are a suitable material given their very-low thermal expansion coefficient and glass temperature, yet high hardness and yield strength when compared to other glass materials.

The structure of this paper will first cover AM and attempt to give a clear understanding of the mechanisms present in the forming of new components produced with these technologies. Subsequently, its history, types, and a thorough explanation of glass AM, specifically, will be presented.

Next, the research methods will be described and introduced to help understand what is intended to achieve as well as the procedures standardized for testing the obtained results. This will finally be concluded upon with the actual results from the experimentation process and an analysis will be made to assess the relevance of the results.

2 Additive Manufacturing

AM has undergone multiple transitions and has been called by multiple different names. One of the first names for it was Automated Fabrication which emphasized the principle of automation as used for fabrication of products. This term however, quickly became a super-group of different technologies involving automation, usually powered by computers, which did not follow the principles that AM does [3]. Another term related to AM, yet not as common, is Freeform Fabrication which allures the unique capabilities of AM.

Currently, the term AM is the de facto industry standard for 3D printing processes as it better visualizes the nature of the process.

This technology has been righteously deemed as a revolutionary approach to traditional manufacturing. It has amassed large amounts of media coverage and has fueled controversial discussions on the future of manufacturing and the disruptive potential of AM. Amongst its immediate benefits are production infrastructure.

In this chapter, a deeper description of the principles behind AM, the different technologies currently existing, and the benefits and disadvantages of using AM will be discussed.

Current product manufacturing paradigms are designed and optimized for large production quantities; by principle, when designing a product, costs of designing the assembly line for it, procurement of assembly equipment, manufacturing regulations, molds, and multiple other related costs are inputted into the equation of calculating the estimated cost of producing a unit of a product. This happens worldwide and is the basis of mass production.

When discussing AM, this whole scheme is ruptured and disregarded which can be both beneficial and crucially disadvantageous; current product distribution chains are not designed for this type of manufacturing, and such disruptive processes need a buffer-period to be adapted to current infrastructures; this takes even longer and is harder if current infrastructures are to be replaced altogether.

Just-in-time manufacturing and lean methodologies are more recent paradigms which somehow are more adaptable and open for change; their intrinsic nature dictates so and therefore makes them ideal candidates for the AM revolution; this however, is not the case of older traditional manufacturing methods. Traditional manufacturing is based on many different principles, most of which rely on middle to long-term plans involving a vastly larger number of stakeholders and running/up times of machinery as well as inventory storage costs.

First, producers contact suppliers of components and raw materials needed to produce the product. To find a distributor, it is necessary to go through a procurement phase where suppliers are evaluated (usually based on market performance). Once a supplier is selected and all components are procured, the assembly of the component begins. This step itself requires the planning of the assembly line, resource allocation, and fulfilment of physical space needs. Afterwards, the product is forwarded to distributors which will be the point of contact for the customer. Not only is this process convoluted, it also involves multiple third parties and steps which are not directly affecting, and most often are unknown, to the customer (Figure 1).

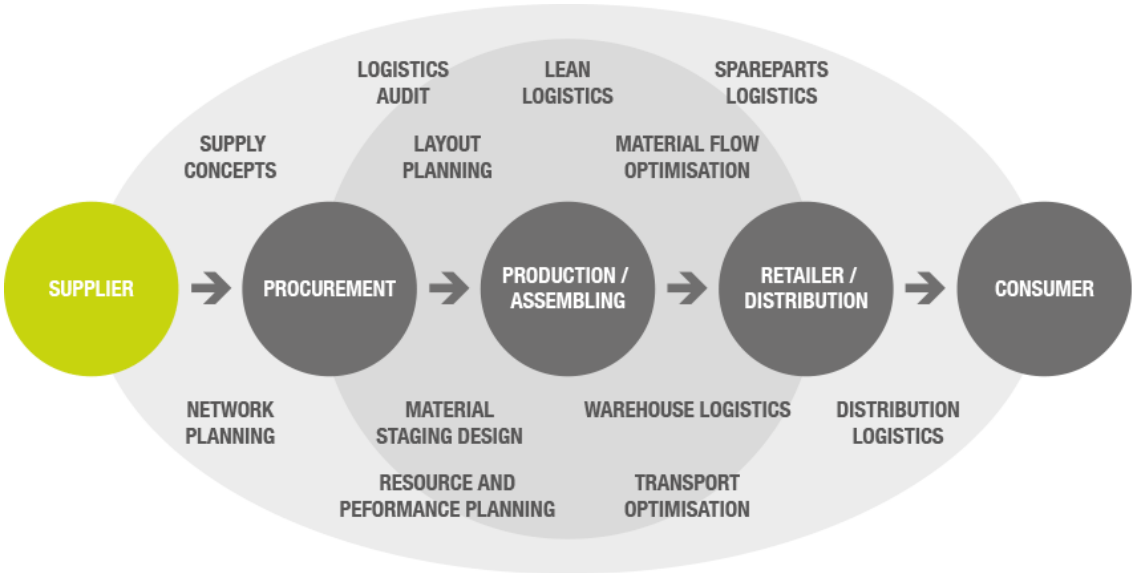

Figure 1: Manufacturing process for traditional methods [5]

When comparing this to AM-based production, the only step is production since the consumer produces the item itself. To understand this better, it is necessary to understand

the product design process first. Initially, products are born with an idea which aims to solve a problem. Once this concept is born, the idea undergoes a lengthy research phase where its physical attributes and manufacturability are evaluated, and its production is planned for (Figure 2).

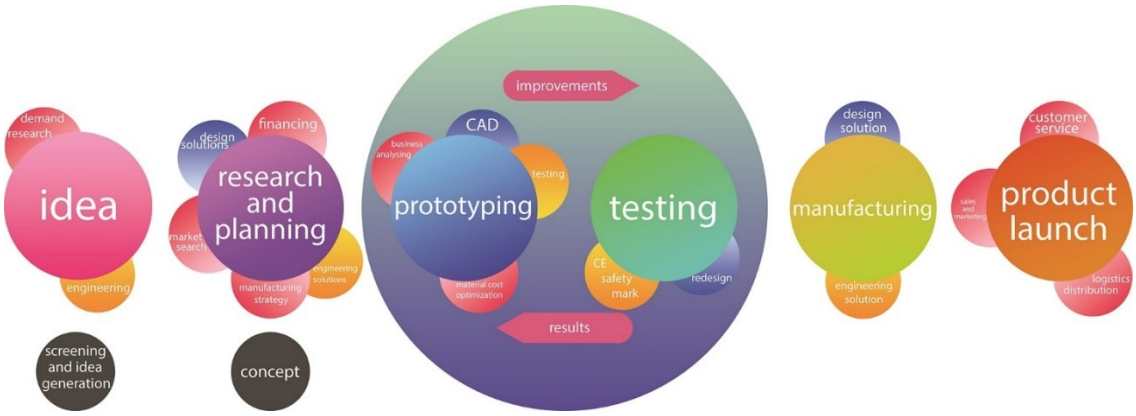

Figure 2: Product development cycle, from idea to launch

Next, the prototype is built and tested. This is a continuous process which often involves multiple iterations which improve on the results obtained from previous versions. Afterwards, the finalized product is optimized for manufacturing and moved into the assembly line. This process involves assembly of the product, distribution to warehouses and retailers, and the transportation between these. Finally, the product is launched, leaving support as the only responsibility of the producer.

On the contrary, if we analyze this process from an AM perspective, the product goes directly from idea to the user, thus enabling faster interactions and direct cooperation between the source and destination. It is clear to see how the invention of AM as a solution to the lengthy process involved in traditional manufacturing has succeeded. While not without flaws, it is rapidly amassing a customer database and rising in popularity; the discovery of new technologies in the field and optimization of existing ones are fueling its market share.

It is also useful to compare this technology to computer numerical control (CNC), another computer-aided manufacturing process. Fundamentally, they stem from the same concept; by inputting a path into a computer, a mechanism moves in steps following a path which creates a shape. It does so by moving a tool through a path which, unlike AM,

removes material from an initial volume. These paths are programmed with computer-aided software and calculated from a 3D model. As can be foreseen, this technology has major constraints which are not present in AM such as features within features, moving components, and processing from all directions, are not possible.

AM systems have existed for a longer time than most people are aware; they became slightly popular during the 1980s with multiple patents filed in Europe, USA, and Japan. While there were some large companies making great advancements coming out of USA, most new companies come out of other countries. In Europe, EOS (Germany) has had the largest impact in the industry with their powder bed fusion systems, yet multiple other European countries have been developing their own brands, often with innovative new technologies to offer. Currently, the three original developers of rapid prototyping, Solidscape, 3D Systems, and Objet Geometries, are still the leaders in the field.

Recently, AM technologies have seen an increased effort to introduce them into industrial manufacturing to replace existing processes. The rationale behind this is mainly supported by four trends:

- Faster prototyping: design and monetary constraints have pushed designers to find new ways to test prototypes cheaper. With 3D printing, this has mostly been successfully accomplished and increasingly implemented in the industry. With current technologies, it is possible to test near-perfect replicas of the final product with similar materials.
- Low production volumes: when mass production is not needed, or customization is, 3D printing enables producers to easily and rapidly modify the product on demand and adjust to the customer's requirements. This increases value for the customer and manufacturer, broadens the manufacturer's market, and decreases the risk of production errors caused by faulty molds.
- Complex components: by nature, AM technologies enable the creation of shapes which are not possible using traditional manufacturing methods. This is mainly due to overlapping or concentric features, gravity constraints with bridging elements, or other complicated shapes which cannot be processed due to tool or equipment constraints.

- Customization: As mentioned before, customizing components to meet the customer's needs is easier done with 3D printing thanks to its rapid prototyping nature. The process involved in moving from idea to product is drastically shortened.

2.1 History

When discussing AM, it is easy to picture machines following a set of steps pre-programmed by a computer. The steps tell the machine where to be, where to extrude from, and at what time precisely in a manner that conforms what we know as AM; however, the origins of layered manufacturing date back as far as the 19th century. In the year 1892, topographer J.E. Blanther filed a patent (Figure 3) for a process where he built 3-dimensional landscapes by consecutively superposing layers of sheets. While this might not define AM, it follows the same holistic approach to creating 3D structures out of multiple 2D shapes [6].

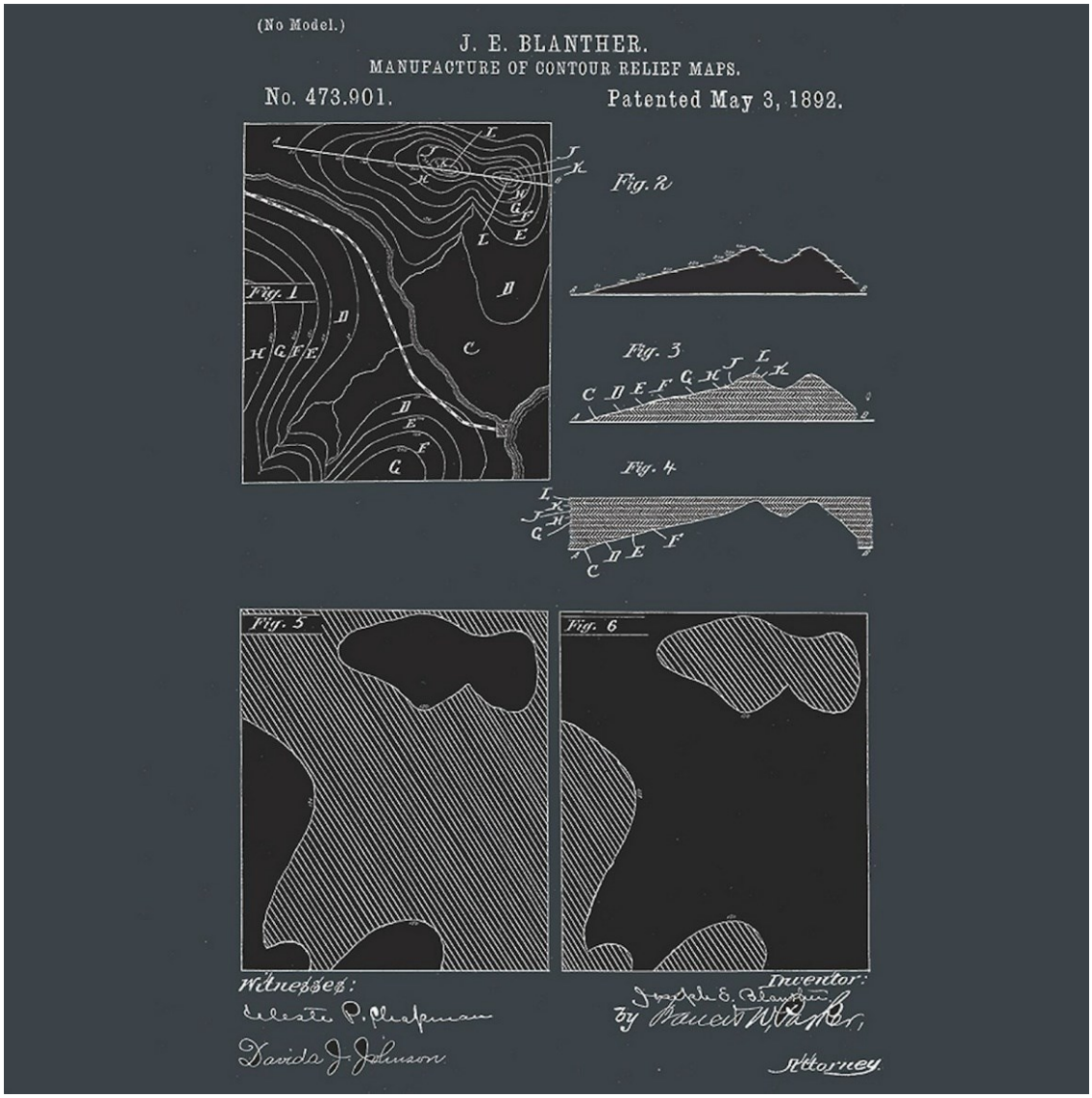

Figure 3: Patent image taken from J.E Blanther's "Manufacture of contour relief maps"

Discussions about AM began during the 1950s and first attempts at creating solid objects by curing photopolymers with a laser took place in the 1960s, yet actual development and recorded discoveries did not happen until the 1980s. During this time, patents from Asia, Europe, and North America were applied for with similar processes based on layer-by-layer AM described.

Later that decade, three more companies, Helisys (LOM), Cubital (SGC), and DTM (SLS), were born of which only DTM still exists and only so as part of a merger with 3D Systems. Furthermore, Stratasys (FDM) was born and MIT group patented the process of 3DP. Both latter technologies are widely used currently, yet all the previously mentioned

companies employ the same basic AM principle by means of different procedures. Finally, in the 1990s, inkjet binding was developed by Sanders.

During the 1980s, the first demonstrations of the AM process took place, however the first successful one was developed by Sanders (now Solidscape) in 1994 called the ModelMaker, a Jet Fusion printer of liquid wax. Soon after, 3D systems introduced the Actua 2100 which used the same principle and was later revised and renamed as the ThermoJet.

Binder printing methods were mainly developed during the 1990s by MIT; they commenced with 3DP processes wherein binders are deposited onto a bed to form cross sections. This technique has led to many current methods for AM of polymers and metals.

The rise of low-cost 3D printers began in 1996 when Stratasys introduced the Genisys (FDM), 3D Systems introduced the Actua 2100 (Inkjet), Z Corp. introduced the Z402 (Inkjet), and Schroff Development introduced its paper-lamination system. Later that decade, metal printing with lasers (LAM and LENS) and stereolithography were introduced by Aeromet, Optomec, and Autostrade respectively.

In the 2000s, AM by curing photopolymers has been of focus. This process is beneficial to multiple different AM fields as it enables the production of components with materials which were not usable before. By mixing a photo curable resin with powders of the desired material, it is possible to harden, and then melt away the binder resin; logically, the melting point of the material bound by the resin needs to have a higher melting point than the binder. These technologies started seeing increased use in the early 2000s, namely developed by Objet Geometries. Their system jets the photopolymer through a print head with 1,500 nozzles [7].

2.2 Operating Principle

AM systems can be interpreted as “manufacturing methods which are able to produce 3D components without the use of cutting tools, molds, or manufacturing aids”. AM focuses on simplification and approachability.

AM works together with computer-aided design (CAD) to make manufacturing precise, repetitive, and iterative. CAD models are 3D sketches made with 3D modeling software

which enables the creation of structures based either on mathematical formulas, free-form shaping, or 3D scanning. These models are stored as stereolithography (STL) files which contain a description of the 3-dimensional geometry contained within the model. This information is necessary for the printer to process and convert the model into a G-code.

G-codes are essentially a set of steps and locations for the print-head to situate itself at a specific moment during the printing process. Much like paper printers, the extruder, nozzle, laser, or 3D printing device follows these instructions to deposit or solidify material in succession and create layers. One by one, the layers are created and added upon until the full 3D object is done printing. All these calculations are done by algorithms written by the printer's developer which usually calculate all the parameters necessary to make the print stable and functional. Many machine developers allow for custom settings to be tested; custom infill densities, layer thickness, print speed, extrusion/deposition frequency, etc. This usually comes with benefits and setbacks; while offering increased customization and better research testing capabilities, failures have a higher occurrence rate.

The intrinsic principle behind AM is better depicted by the 3D puzzle in Figure 4; the 3-dimensional shape consists of multiple 2-dimensional outlines which are put together to make a lower resolution 3D shape. The resolution is directly dependent on the thickness of each layer. In this example, a larger number of thin layers would give a higher resolution whereas a lower number of thick layers would give a lower resolution; this is the case with pixelation which take place when transitioning from analog sources to digital ones. This effect is often termed the stair-step effect as it is analogous to the way steps form a staircase [2].

Figure 4: Puzzle toy following the principles of AM [2]

2.2.1 Generalized Process Chain

From a holistic point of view, AM is seen as an easy to approach process at manufacturing which requires less effort than its traditional manufacturing counterparts. While this is true for the most part, the operator still needs to go through multiple steps to achieve results. It is also necessary to mention that steps can vary considerably when utilizing different technologies or even with different machines which function under the same logic.

3D modeling was not created to empower 3D printing. In fact, 3D modeling has existed and being implemented in design decades before AM was first implemented and has been a staple in engineering and architectural design since Ivan Sutherland developed Sketchbook, the precursor of 3D modeling. Currently, most mass production processes employ 3D modeling to improve reliability and design iteration, improve communication between stakeholders by reducing times and increasing precision, and for improved preservation of original idea concepts.

3D models however, are not 3D-printing-compatible files; they first need to be converted to STL files. The term STL comes from STereoLithography as coined by 3D Systems in

the 1990s. This file format contains information on the geometry of the model alone and excludes version history and precise information on structure. The precision of the STL file can be adjusted when exporting to include less or more triangular faces which directly correlate to build quality and finish.

Given the digital nature of AM, it is easy to modify the component extemporaneously. Some modifications require editing the actual CAD file to add, remove, or modify features of the component; other modifications such as flipping, scaling, unilateral warping, and density can be modified even after the file has been converted to STL format. This enables producers and creators to easily adapt a product to specific needs with reduced processing times and involvement from both ends [7].

The following steps constitute the general phases of the process:

2.2.1.1 CAD model and its creation

First, a digital 3-dimensional recreation of the product needs to be created; a CAD model. This model will be the basis of the print and the concept on which iteration takes place. A 3D model is essentially interpreted by a computer as a set of surfaces, lines, polygons, or extrusions of surfaces which together conform a solid component.

2.2.1.2 STL & conversion

For a 3D printer to recognize the CAD file and be able to interpret it, it is necessary to convert it to STL format. While there are other supported formats allowing for 3D printing, STL has amassed a near-absolute control of the field.

Most industrial or professional 3D printers will be able to interpret the STL file directly as they have an in-built STL-interpreter however, most consumer printers do not. Consumer printers usually require for this step to take place in a computer which does the calculations and simultaneously converts the STL file to a G-code (Figure 5).

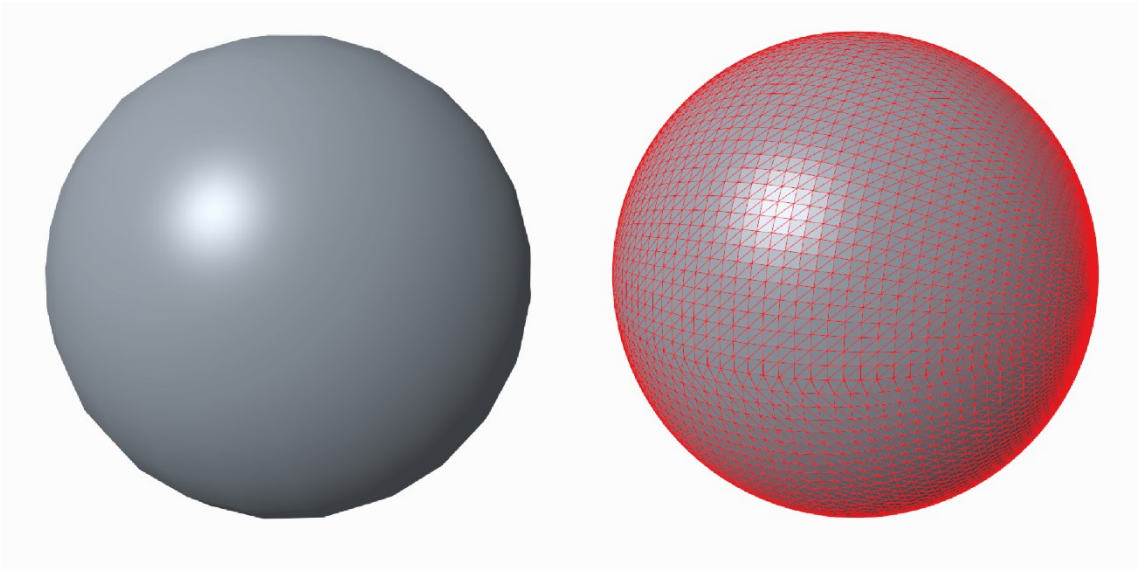

Figure 5: Tessellation process of a sphere

2.2.1.3 G-code & creation

Conversion to G-code takes place using either a 3D model slicing application or directly with the printer's built-in software.

When converting to G-code, the first step done by the interpreter is to verify the file is correct. This is commonly done with a graphical interface where the operator can visualize the 3D model (often with quality loss) and modify it on-demand. This is done so that the object can be multiplied, rotated, inverted, or scaled as desired to fit the requirements. Multiple parameters can be modified at this stage which also affect the properties of the final print by altering the way the print is made (more in section 2.3.2).

2.2.1.4 Machine set-up

During the printing process, it is necessary for the operator to both create a digital model of the part, and physically set-up the machine for the process. Norm is that most require material to be introduced into the printer, printing surfaces or beds to be cleaned, and parameters to be selected. This step varies radically amongst different technologies and thus will be further discussed in section 2.4.

2.2.1.5 Printing

The main step of the process; 3D printing starts, and the components are built. During this step, the G-code is interpreted by the machine and the print head and build-plate move

accordingly. Layer thickness defines the Z-axis step-distance while the shape of the layer defines the movement of the X and Y axes.

The process defines the binding method between layers; each layer is joined to the previous one by means of a binder which can either be an external substance used as an adhesive, or the print material itself before it is solidified. This causes the layers to be naturally bound together structurally.

Once again, the length of this step varies greatly with different technologies and different machines. Prints can last from seconds to weeks depending on the amount of material being printed, process used, and efficiency of such.

2.2.1.6 Print completion

The component is removed from the printer. The printing process is completed, and the component is completed or nearing completion. If present, support structures need to be removed. These can be made of either the same material or a different material.

Support structures printed with the same material are common as the material is readily available and the parameters need not be changed or a second extruder need be introduced; inversely, different-material supports require specialized printers which allow this, yet are often preferred if available as they are easier to remove or have special properties which are desirable.

It is recommended to evaluate the situation and proceed with caution as different processes often require different precautions; heat-based processes often need a cool-down time to prevent deformation, resin-based require a resting time to let the liquids drain, and some other processes simply result in components too hot to be handled.

2.2.1.7 Post-processing

This step is often unnecessary or overseen as many applications do not require post-processing. Should it be required, it consists of application-specific steps; there are commonly polishing, abrasive finishing, sanding, or coating. It is necessary to evaluate the need for post-processing or the benefits of it; selecting a higher print quality (more thin layers rather than less thick layers) can marginally increase the print time necessary to achieve a similar result as can be with faster post-processing.

2.2.1.8 Completion and usage

At this stage, the process is finished, and the component is ready for use.

2.2.2 Design in AM

Designing for manufacturing and assembly has traditionally meant considering the multiple aspects of the long chain of events which take place for a product to be produced. This involves considering stakeholders, assembly lines, running costs, down-time costs, and many other factors which affect the final production costs and capabilities of the process. This means that designers constantly are looking for new ways which improve on the formula and ideally reduce these costs by adapting new technologies into the equation.

If we look back at the trends which shaped the controversial design paradigm-shifts of the 20th century, we have two main theorems which vastly improve on traditional formulas and do so by innovating on the process and reducing the number of steps taken to complete a product. These are Design for Assembly (DFA) and Lean Manufacturing.

Intrinsically, Design for Assembly is a methodology which aims at improving the workflow of the process of assembling a product by simplifying the process and making it more controlled and less cumbersome. This method uses multiple numerical algorithms which calculate the cost of various manufacturing processes and recommends ways to improve. These processes range from casting, transporting the part along a conveyor belt, and even the costs related to the downtime of changing tools [8]. At its core, it focuses on considering the assembly line when designing a product. This intends to reduce the costs and work done by simply tweaking aspects of the component.

Lean manufacturing on the other hand, is a production balance between individual-component crafting, mass production, and their related advantages and setbacks. It aims to reduce the variability and lack of variety of mass production while marginally increasing the yield capabilities of craft production. It does so by implementing methods which use less resources than mass production. Furthermore, mass production focuses on the principle of reducing the amount of failures while achieving a good-enough quality while lean explicitly focuses on perfection and aims to optimize the process to achieve it.

While perfection is never actually reached, lean producers do have an increased efficiency and product quality when compared to traditional mass production methods [4].

It is clear to see how AM follows the tracks of both these methodologies and acquiesces the backbone of manufacturing simplification.

When applied to DFA, AM basically gets rid of most processes:

- Tools do not need to be changed or replaced often;
- Personnel is reduced; sometimes down to 1 person;
- Storage space is minimum as only raw material needs to be available;
- Transportation through an assembly line can be removed;
- Actual assembly of the components of a product can be fully removed.

Likewise, AM follows Lean Manufacturing guidelines:

- Less resources, materials, and processes are used;
- Customizability is available;
- Various costs are reduced during production [1].

At this point, it is useful to understand the actual process when designing for AM including its tools, CAD design considerations, and print parameters and limitations. By applying DFA methods to AM, optimization can take place even within the same method.

To begin with, the AM technology to be used must be considered and its limitations kept in mind. When using photopolymerization or powder bed technologies, for example, features requiring support need not be considered as these technologies enable printing without them, whereas other methods, such as FDM, require support when printing features with an overhang angle higher than 45 degrees. Similarly, the orientation of a component can drastically change the physical properties achieved upon completion.

2.2.2.1 Support

Supports are necessary when printing features which create an overhang or any shape which cannot hold its own weight due to gravity. These supports are generally present as

vertical poles onto which the feature rests and are more weakly attached to the print to allow for easy removal during the post-processing step.

The generation of support structures directly affects the time-efficiency of the printing process, as well as the technology needed for the manufacturing of a component. This parameter however, cannot be avoided with many 3D printing technologies. Thus, the printing process needs to be ascertained based on needs and limitations of the process before production.

2.2.2.2 Orientation

The orientation of the component requires careful consideration and comparison due mainly to its relation to printing time and print properties. The time it takes to print the component when placed under two different orientations varies greatly and is, once again, related to support structures since the amount of them needed is linked to the orientation.

Second, the mechanical and optical performance of the product is affected under different orientations. If we think of an FDM-printed component, the layers are extruded on top of each other and the molten material itself acts as adhesive however, if we compare the strength given by this adhesion to the strength given by the continuously created layer, the first falls short in mechanical properties. Similarly, such adhesion layer does not give the same optical results as other surfaces given its flatter and more tightly-packed nature.

2.2.2.3 Resolution

This parameter is one of the main selling points of new 3D printing machines developed with existing technologies; having smaller layer-thicknesses directly relates to higher print-accuracy. Inversely, a higher count of layers means longer printing times. The resolution is determined by the step distance in the Z-direction which is irrelevant of the XY cross-sectional shape.

An analogy which can better explain this is the processing of 1-megapixel images compared to 10-megapixel images. The latter will look sharper and carry more detail but will take a longer time to render. This holds true for all AM technologies and is usually the main factor affecting print-speed.

2.2.2.4 Infill density

Infill density is the amount of material which will make up the structure within the print. To better understand this, it is necessary to understand how 3D print are empty shells which have a level of material filling to give it strength and weight. This infill usually has a square, or hexagonal grid pattern which gives it strength while keeping its weight low. The higher the infill the stronger and heavier the product is (Figure 6). Usually, this needs to be considered per the specific needs of the product.

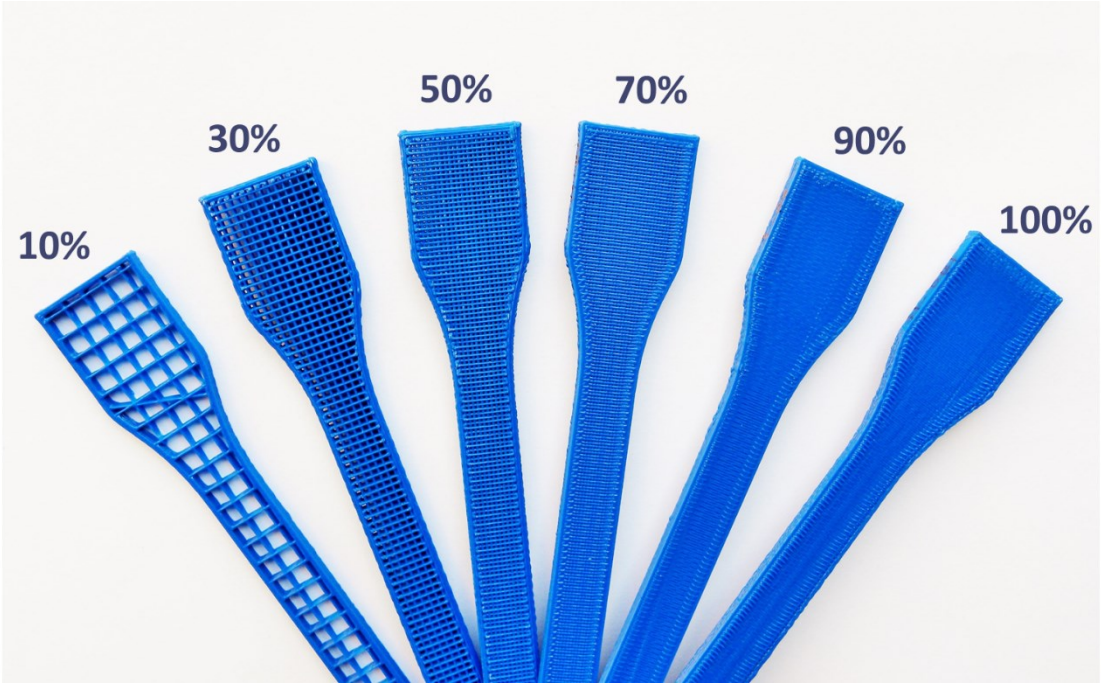

Figure 6: Infill percentage of an FDM print [9]

2.2.2.5 Scanning speed

Scanning speed is the name given to the speed of the moving extruder head, laser beam, or powder deposition nozzle. Most printers keep this parameter locked or recommend the user to use the printer with default settings as it usually is pre-calculated to be optimal for fastest speed without compromising the print quality. If this parameter is set higher than possible, the print will become non-continuous and failure will happen; inversely, if the scanning speed is too low, the print will simply take a longer time than is necessary and the material might become to fluid and not attain its right consistency.

2.2.2.6 Plate adhesion

This setting created a special layer at the beginning of the print which helps attach the component to the build-plate to keep it from moving. It also helps prevent distortion by creating a layer which is larger than the first print layer, thus creating a larger contact surface for adhering to the plate.

The print-time effects of this parameter are not that grave compared to others and usually are recommended if failure from lack of adhesion takes place (common amongst consumer FDM machines). On the other hand, plate adhesion often makes it harder to remove the component from the plate and sometimes ends with deformation or damage to the print when removing.

2.2.2.7 Material needs

Some AM materials require post-processing to get the best results out of them and some products require post-processing for specific purposes. These are highly dependent of the requirements of the final product, yet it is still possible to produce some product with different technologies, some of which can be faster if they do not require post-processing.

2.2.2.8 Shape optimization

Finally, as with traditional manufacturing processes, optimizing the shape by considering the application and machinery, helps reduce production times.

When utilizing 3D printing, some features which are usually present in traditionally-manufactured components, need not be added; these can range from hinges and screw holes, to multi-component assembly supports. If we consider the duct in Figure 7 for example, it consists of multiple components which need to be manufactured on their own and assembled together; if using 3D printing, it consists of one single CAD file which incorporates all the parts in one component, thus eliminating the need for assembly and reducing the amount materials needed.

Figure 7: Traditional multi-part component vs AM one-part component

Furthermore, software such as solidThinking's Inspire, help reduce the amount of material which needs to be extruded by analyzing the forces and moments which will be applied to the component and doing an FEM analysis to remove material in areas where it does not add strength to the component. This process goes even further with 3D printing where many constraints present in traditional methods are not present.

It is necessary to mention that 3D printing is only beneficial in some situations and traditional mass-production methods are still more widely used as they give larger yield capacities. Considerations on production batch sizes usually lead to choosing traditional methods and subsequent components added to the product sometimes make it impossible to employ AM. Also, there is a limited range of materials which can be used for printing; Glass, the focus of this research, not being one of them.

2.3 AM Process categories

AM processes can be categorized into two main applications divided by their uses: rapid prototyping, and rapid manufacturing (Figure 8). The first one focuses on enabling the user to prototype a product to test some critical features so that the product can move on to the next phase or directly extrapolated for assembly with traditional methods. The second one aims to describe the actual manufacturing of the final product using AM technologies without the need for additional processing. Additionally, rapid tooling is the process of creating fixtures or tools using AM, which allow manufacturing.

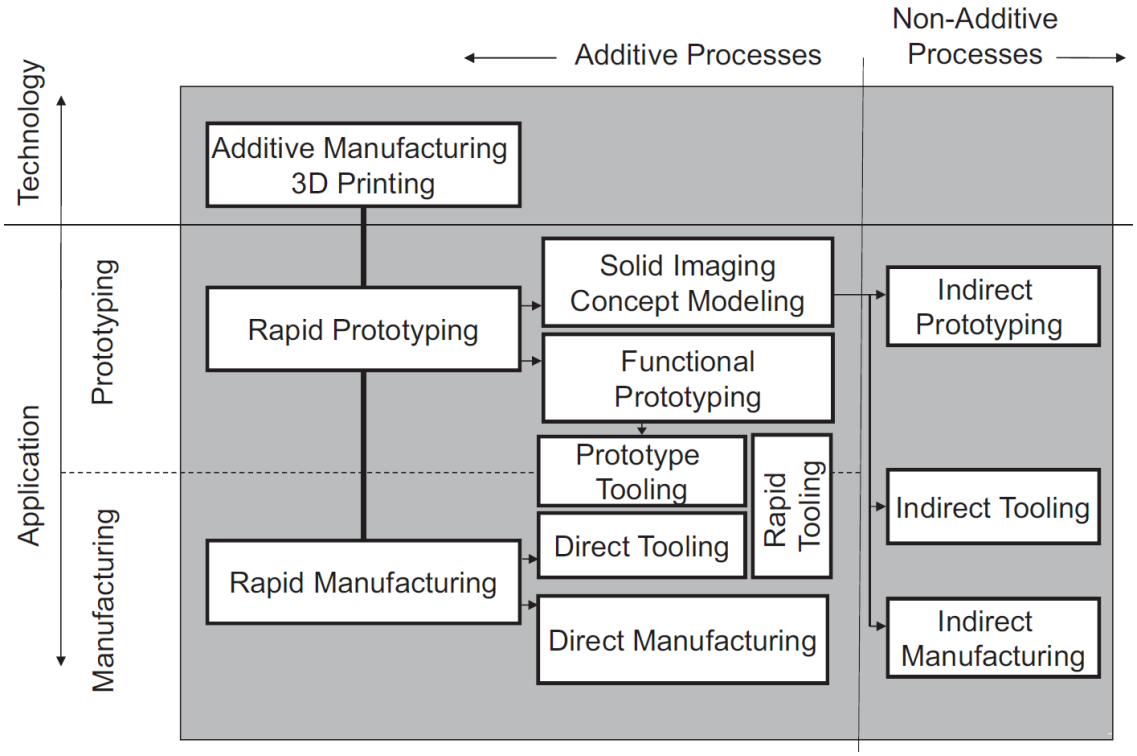

Figure 8: Subdivision of AM processes by application [2]

Rapid prototyping is furthermore subdivided into concept modeling and functional prototyping. As can be inferred, concept modeling focuses on giving a non-tangible concept its own physical interpretation; this aims to help better visualize the physical appearance of the final product. A functional prototype is produced to test an aspect of the product; these are mostly used to test the engineering design of the component.

Given the ever-growing amount and diversity of additive technologies, it is useful to group them under different categories which allure their intrinsic functional nature. While there are multiple different interpretations on what is the best way to group these technologies, the most common, and both ISO [10] and ASTM [11] standardized, groups them as described in the following subsections. It is worth mentioning that not all existing technologies are listed as there are many under development or focused on highly-specific uses which do not directly concern the scope of this publication.

2.3.1 Vat Photopolymerization

The process of photopolymerization is based the usage of radiation curable resins which basically harden once they meet a light source. These are generally cured with UV light,

which is not visible to the human eye, yet some are cured with light in different spectra which are visible.

Invented in the 1960s, photopolymers are used in multiple different industries thanks to their unique properties which give place for a variety of different applications which are not easily possible with other methods. These range from hardening coatings to liquid-filling of crevasses. However, it was until the 1980s that Charles Hull tested curing resins with a scanning laser like the ones found in laser printers. This experiment eventually led to the invention of SLA.

AM using photopolymers can be currently achieved with the following three methods.

2.3.1.1 Stereolithography (SLA)

Machines using this technology function by pointing a laser scanning exposure apparatus, also called a galvanometer scanner, at the resins to start the curing process and rapidly solidify them. These machines have a container where the resins are stored, an installation space, and a build-plate which moves vertically. The resin container fills-up the installation space and the head lowers until it is barely in contact with the resin. A laser then proceeds to "etch" the 2D topography directly on the resin, thus curing it onto the plate layer-by-layer. The laser is aimed on the surface by a mirror which is controlled by the computer interpreting the G-code.

Due to the nature of the curing process, components printed with this method tend to undergo minor shrinkage. This phenomenon has been reduced with the introduction of epoxy resins however, they require a longer curing time. Components printed with this method usually are structurally weak before the curing process takes place, therefore adding to the deformation phenomena.

Post-processing SLA components is lengthier than with most other processes. First, it is necessary to remove the print from the print bed and to remove the support material which is generated as legs of the same material added to the model; these need to be cut-off or broken-apart. Next, it is necessary to gently wash-off or sand-off the excess epoxy from the surface of the component. Finally, the component is put in an UV chamber for hours to finish the curing process.

Figure 9 depicts the operating principle of SLA AM.

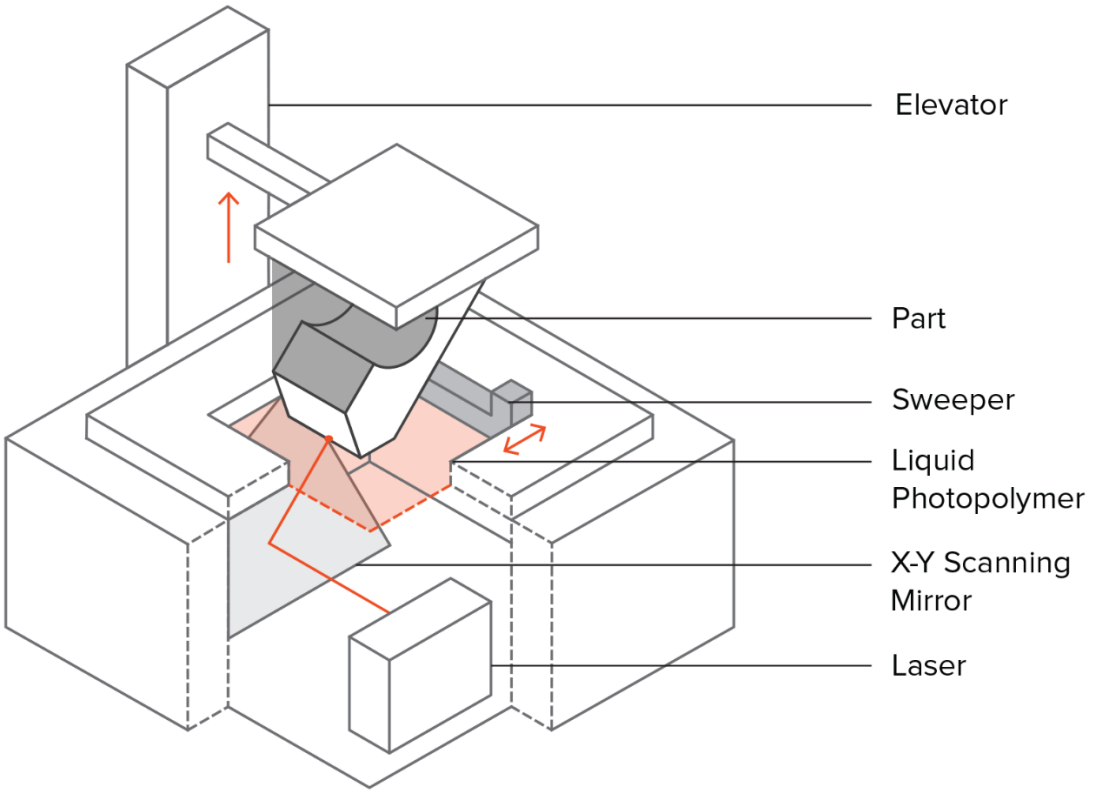

Figure 9: Graphical representation of the SLA process

2.3.1.2 Digital Light Processing (DLP)

While holistically like SLA, DLP functions based on a different process and aims to obtain different results. The construction and operation of the machines is overall the same; the difference lies in the light source. DLP machines replace the laser and mirror with a DLP projector.

Most projectors use Liquid Crystal Displays (LCDs) to shape color light sources into a combined image which is projected onto a screen via a lens. DLP projectors on the other hand, have a very different operating principle. These systems contain a chip called a Digital Micromirror Device (DMD) which contains millions of miniature mirrors which can instantly switch between ON or OFF positions. When in ON position, the mirror reflects the light through the lens, and when in OFF position, they do not. This principle has made DLP projectors attractive to video enthusiasts as they offer true-black color management with image reproduction, whereas LCD projectors still emit light in dark

spots. This also gives way to DLP printing, where light is shed on the resin only at the spots where the micro mirrors are switched ON.

DLP projectors have the potential of becoming the fastest AM technology, as they solidify a full layer at the same time rather than a single spot throughout the layer. This makes for a continuous process which can give very high resolutions in a short amount of time given a powerful-enough laser.

2.3.2 Material Extrusion

Material extrusion has become the most common consumer 3D printing process. It is inexpensive to produce, usually requires simple post-processing, and is approachable for average consumers. The process is based on the melting and extrusion of a material through a nozzle which hovers above a print-bed. This material which is being extruded can either be a solid filament-based material which is melted into liquid plastic, or a pre-mixed, viscous liquid which solidifies by means of heat or photocuring.

2.3.2.1 Fused Deposition Modeling (FDM)

By far, the most common extrusion process is FDM. FDM melts a filament of pre-fabricated material which often comes in large rolls. This material is molten to a point specific to the material being printed. There are many materials which can be printed with this method, yet they all have optimal extrusion settings which prevent the appearance of errors.

First, the filament needs to be inserted into the extruder. This extruder has a motor attached to it which moves the material forward and into the nozzle which is heated at up to 300 degrees Celsius; this temperature is reached by a heating element embedded onto the nozzle-head which receives a current regulated by a thermistor or thermal sensor. Subsequently, either the extrusion head moves on the X, Y, Z, or their combination of axes, or the platform does so to extrude the material in the exact location indicated by the G-code. Generally, a configuration where the head moves in the X-Y axes and the build-plate moves in the Z axis is common. After the layer is finished, the next layer is extruded on top of the previous one.

This type of printing is very common amongst consumers and individual enthusiasts as is marginally less expensive than other methods and can be independently developed thanks to the communities of RepRap and Marlin. These offer free tutorials for building or designing custom FDM machines and software for programming them, respectively.

While popular, FDM systems have various limitations which make them inefficient and unadaptable to many processes. They unequivocally require support material which can be printed from the same build material or different materials if a second extruder is available, and the material range is often limited mainly to plastic filaments and a few viscous materials such as ceramic powders.

An overview of the process is shown in Figure 10.

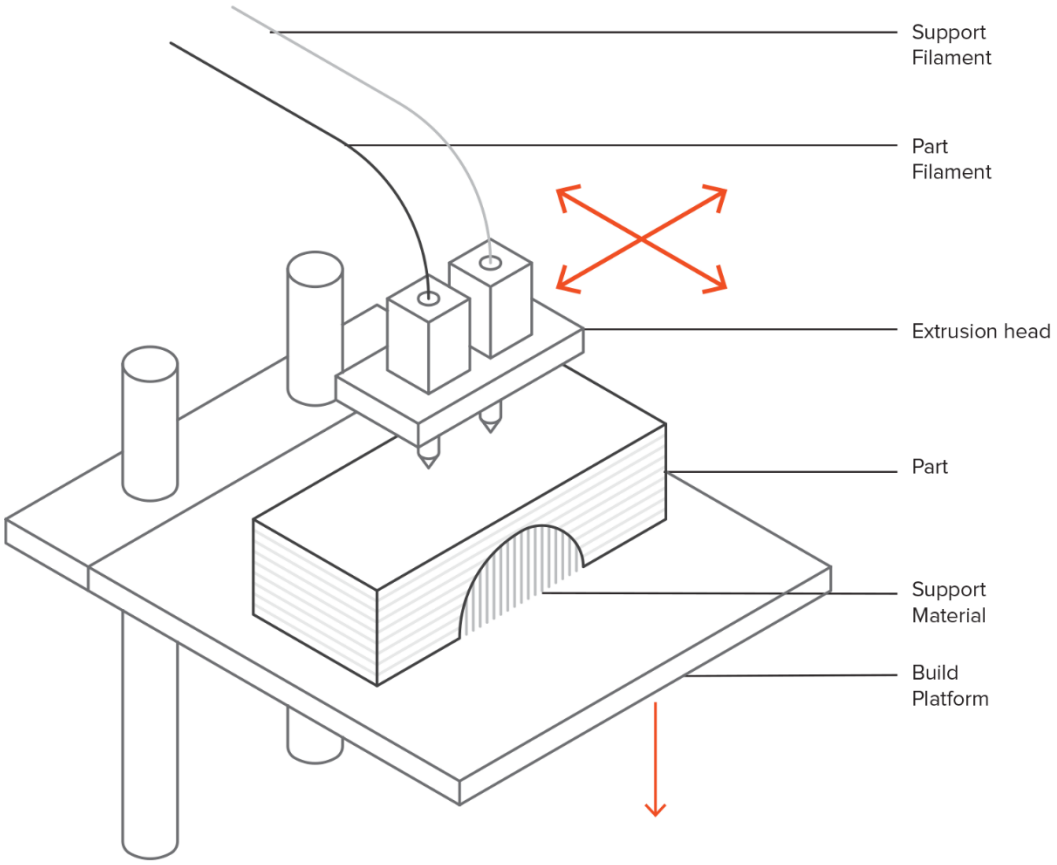

Figure 10: Graphical representation of the FDM process

2.3.3 Material Jetting

Material jetting is a process which follows tightly along the steps of traditional 2-dimensional inkjet printing. This process uses photo curable polymers or waxes deposited as droplets. Amongst its main benefits is the ability to print with different materials or colors at the same time, giving for a wide range of applications and a better adaptability.

2.3.3.1 Material Jetting (MJ)

Similarly-named, the base technology for material jetting prints layers upon layers. The print heads consist of jets which expel hundreds of solidifying droplets onto a build platform, which are cured with UV light. This, naturally, makes it a 1D extrusion process which makes it possible to print large prints at the same speed as smaller prints. Furthermore, if multiple items are printed at the same time, this process can potentially print faster than most other technologies.

This process requires supports which are made from soluble materials for removal during post processing and are printed at the same time as the actual component (Figure 11).

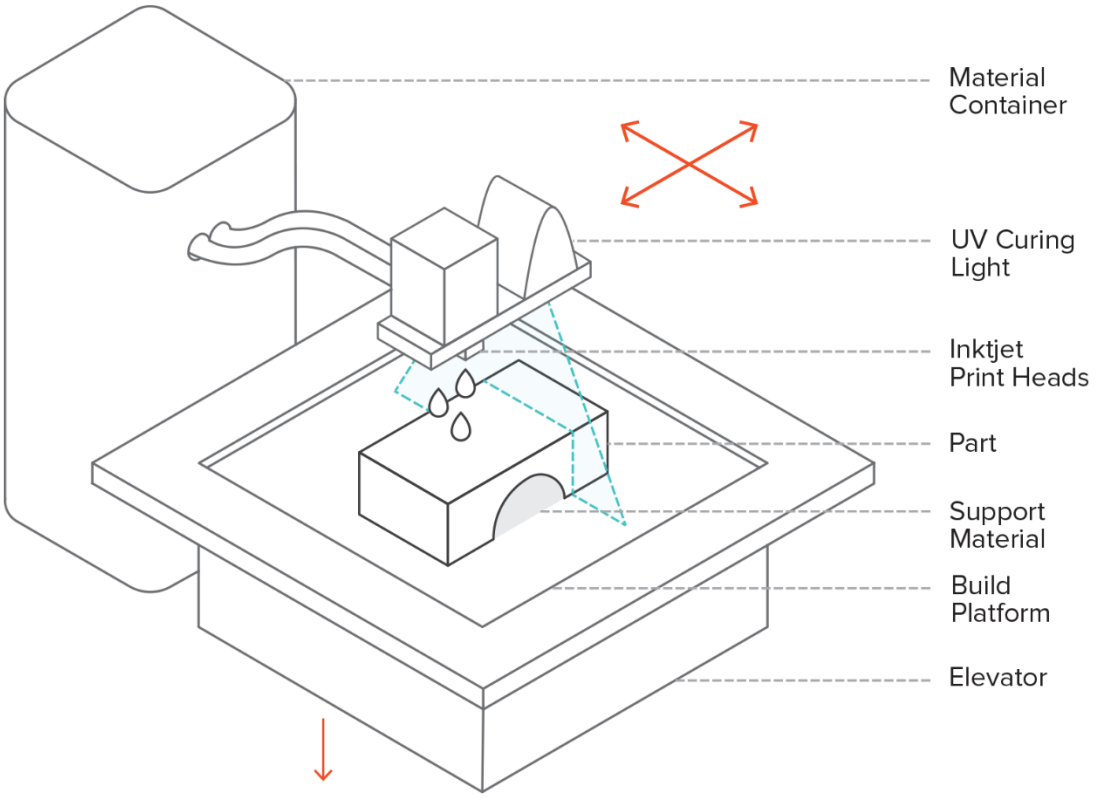

Figure 11: Graphical representation of the MJ processes

2.3.3.2 Nanoparticle Jetting (NPJ)

Like material jetting, this process expels inkjet particles which adhere onto each other layer by layer. The main difference is the addition of metallic nanoparticles to the liquid mix which help print with said material. After extrusion, the component is heated in a heating chamber to melt away the resin, and leave a solid, metallic part.

2.3.3.3 Drop on Demand (DOD)

Unlike other material jetting processes, drop on demand employs dual jetting-heads; one for a dissolvable support material, and one for the build material. Additionally, it is common to use fly-cutters to perfectly flatten the surface after each layer.

This technology is usually employed for lost-wax casting and mold making [1].

2.3.4 Binder Jetting (BJ)

Binder jetting is a hybrid AM system between powder-based and jet-based systems; it functions by jetting resins onto a powder bed, which solidify the powders and adheres

them together to form 3-dimensional components. This method does not require supports as the components lie on the powders, and does not necessarily need curing, as some binders solidify on their own [2].

The binders are colored liquids which are jetted onto a bed of powdered cellulose. The cellulose powder is contained in a chamber which is initially full. Next, the powder is moved onto another empty chamber, where the jet is adhered on to. Eventually, most of the cellulose powder will be transferred to the other chamber, where the product will be buried; once finished, the product is left to cure and eventually is dug-out from the bed and cleaned (Figure 12).

Post-processing binder-jetted components is lengthy and possibly destructive. Extensive care needs to be taken when removing the component from the powder bed, as well as when removing excess powder. Modern machines have a closed chamber with a build vacuum which helps remove the excess powder first instead of removing the component from it. Furthermore, some components need sand-blasting to remove the excess material in tight spots.

This process can be used for both sands and metals; sand models can be made with multiple colors by first jetting a binder agent, and then jetting a colored tint onto it, and are also used for casting. Furthermore, highly-fluent materials are infiltrated to the finished print to improve its mechanical properties.

Metal powders can be used in a similar manner to nanoparticle jetting; powders are bound together by means of a polymer resin which is later melted away in a furnace. This gives

a 60% metal density which can be later increased to 90% by using bronze to infiltrate the gaps [1].

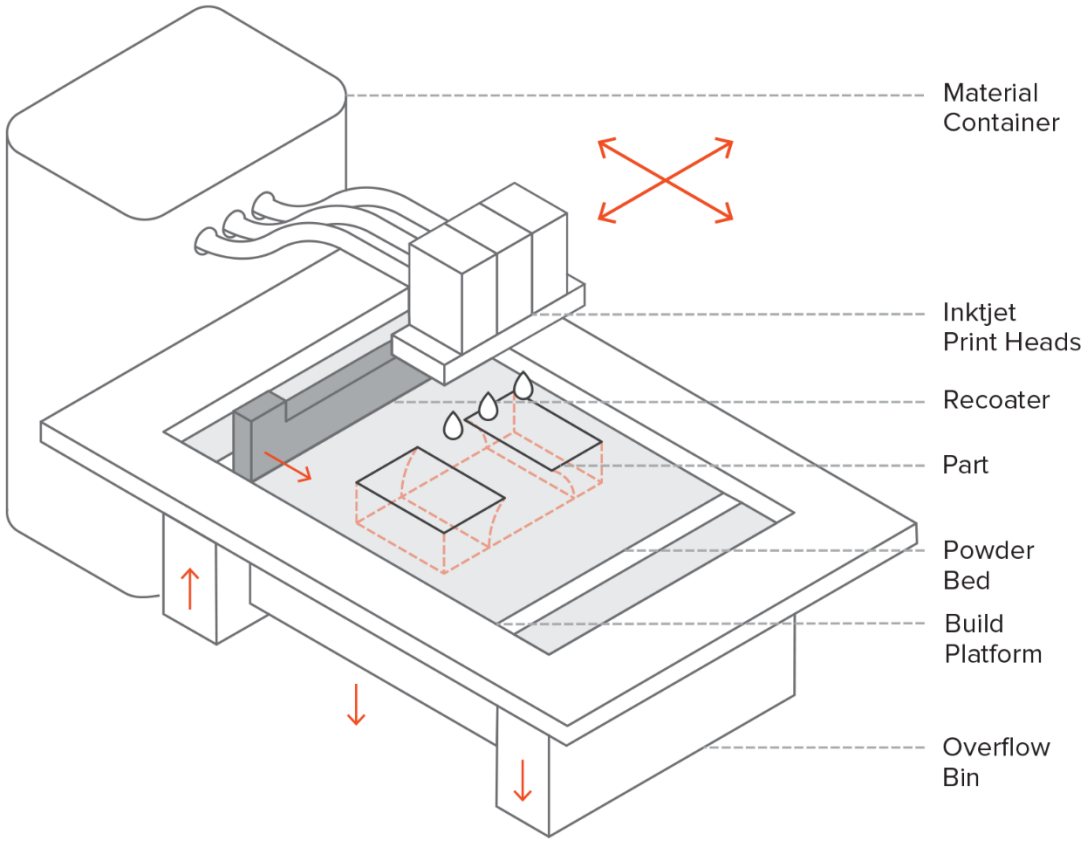

Figure 12: Graphical representation of the BJ processes

2.3.5 Sheet Lamination

One of the first commercialized AM technologies, this process is based on the principle of adjoining multiple material sheets (usually paper), cut out to the shape of each individual 2D cross-sectional layer. The sheets are bound together by means of an adhesive, thermal bonding, or clamping.

2.3.5.1 Laminated Object Manufacturing (LOM)

Commonly, sheet lamination processes are categorized per the order of their steps:

Bond-then-form processes first bind the sheets together, and afterwards cuts them to shape. This was originally achieved with adhesive sheets used for the process which do not need extra binders to be added; they simply require a heated roller to roll over them

to melt the binder. Afterwards, a laser cuts the shape on the last layer leaving the unused material behind as support cut into tiny pieces with a crosshatch pattern which are more easily removed (often with wood carving tools) than their uncut counterparts. Other processes use adhesive-free paper which is bound together with a resin powder jetted onto the sheets only where the component is being built which makes it easier to remove the excess material.

These processes have been used not only for paper binding but also other materials, including metals, which are glued to tapes which conform each layer of the component. These components are later heated to complete the sintering process (Figure 13).

Form-then-bond processes on the other hand, first cut the individual layers to shape and later are bound together. This process makes it easier to create components with internal features which would otherwise be hard or impossible with bond-then-form technologies due to removal issues. It is also impossible to cut into previous layers with this method, as each layer is first cut separate and later introduced into the previous layers. Conversely, this process requires external support creation which is both complicated and requires post-processing to remove using thermal or chemical processes.

Metal LOM processes are categorized as follows:

- Thermal bonding, where the sheets are cut into shape, assembled atop each other, and later heated until they bind to each other;
- Metal clamping, used mainly for simple components, where the sheets are not bound together until the process is finished. A clamp, bolt, or mechanical fastener is introduced to keep the components in place [3].

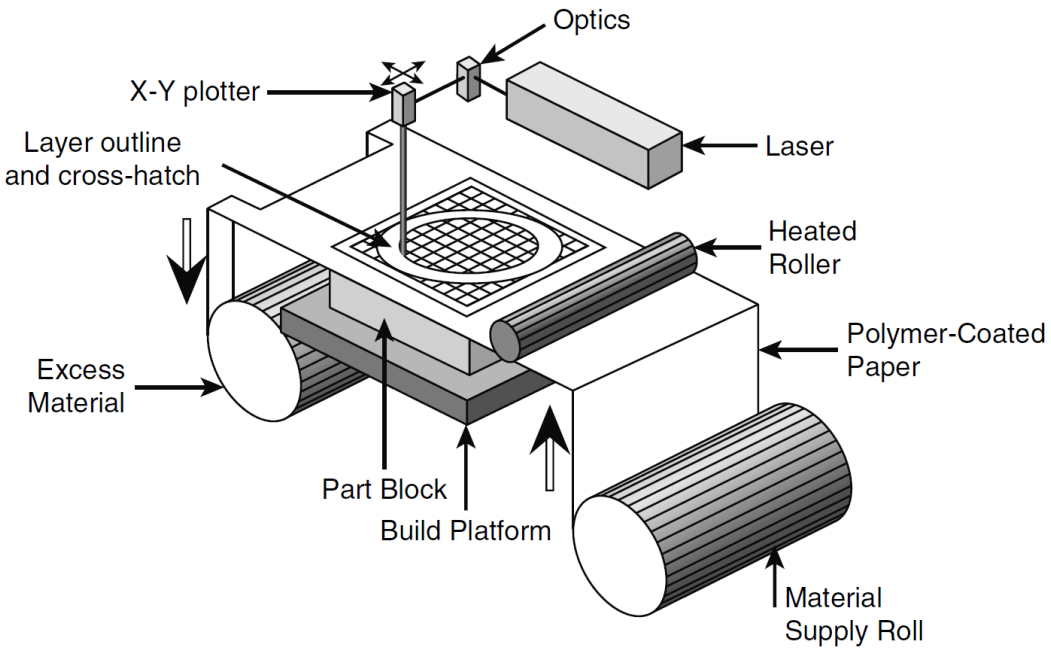

Figure 13: Graphical representation of the LOM processes

2.3.6 Directed Energy Deposition

Also termed Beam Deposition, these processes create metal parts by constantly feeding metal which is instantly melted and deposited (unlike powder-bed fusion systems). Metal is supplied either as a powder or a wire feedstock, and the melting device can be either a high-power laser or a focused electron beam (much like traditional welding methods). These components require support material if complex features with large overhangs are to be built [3].

2.3.6.1 Laser Engineering Net Shape (LENS)

With this process, metal powders are freely poured onto a building platform via nozzles supplied by cyclone powder feeders; here, a laser melts them. The streams are later cooled by means of heat induction. This whole process takes place in a closed chamber which is usually filled with inert gases which are recirculated and constantly monitored for quality.

Components produced with LENS technologies often reach higher tensile strengths and ductility due to grain refinement taking place in the process. This is rarely seen with AM technologies, as most components tend to have weaker links than their traditionally manufactured counterparts [2].

2.3.6.2 Electron Beam AM (EBAM)

Like LENS processes, EBAM utilizes an electron beam to melt continuous streams of metal powders or wire feed. Distinctively, this process utilizes an electron beam in a vacuum chamber to melt the metal material.

2.3.7 Powder-bed-based AM Processes

Powder-bed fusion processes have a long development history as they are one of the oldest AM technologies available and have a wide range of applications, as well as one of the most extensive material support catalogues. All powder-bed fusion processes consist of a roller or recoating-slider which spreads thin layers of powder from one feeding cartridge onto a build platform and subsequently onto a heating element which causes the fusion of the powdered-materials.

Like directed energy deposition methods, powder-bed fusion utilizes both lens-based and electron-beam-based fusion technologies to create the layers however, unlike them, the process does not consist of a constant stream or feed of material but instead features a bed of material-powders upon which the laser or electron beam is pointed at. The shape is created by scanning a pattern throughout the powder-bed where the powders convert into molten material which solidifies into a shape [3].

2.3.7.1 Multi-Jet Fusion

A recent technology developed by HP which focuses on depositing layers of multi-material binders onto a bed of powders selectively where fusing will take place and subsequently curing or sintering them in order to bind them [12]. This material also acts as a fusing agent which will improve the energy absorption from the heat-source. Likewise, a detailing agent is used at parts of the cross-sectional layer where fusion is not meant to happen, which reduces fusing to allow the creation of sharp, detailed features. This technology is said to be able to print 25% faster than traditional SLS machines due to reduced cooling [1].

2.3.7.2 Electron Beam Melting (EBM)

Like EBAM systems, Electron Beam Melting processes use high-energy electron beams to heat up materials and cause them to melt.

EBM processes require vacuum chambers to operate and utilize deflection coils to provide the movement for scanning. Unlike laser-based processes, energy absorption is not dictated by absorptance (a material's effectiveness in absorbing radiant energy), but by thermal conductivity (property of a material to absorb heat) instead [13]. Also, pre-heating is done with the electron-beam itself, which eliminates the need for additional heating devices; the electron beam quickly and briefly defocuses to create an area the size of the whole powder-bed to raise its temperature consistently.

Electron beams area streams of electrons traveling at speeds close to the speed of light. These beams can be affected by gasses present in the enclosure which deflect the beams and reduce its efficiency, thus requiring the use of vacuum chambers. The use of magnetic coils gives place for faster changes in speed and direction which improve the speed of the print.

The main caveat of EBM processes is its limitation to powders which conduct electric charges, thus limiting the process to conductive metals only. Moreover, the lower the conductivity of the material is, the lower the efficiency of the process is. Regardless, this process has some advantages over laser-based AM processes.

2.3.7.3 Selective Laser Sintering (SLS)

Selective laser sintering is a process whereby powders are added together by means of a moving laser which sinters them together (Figure 14).

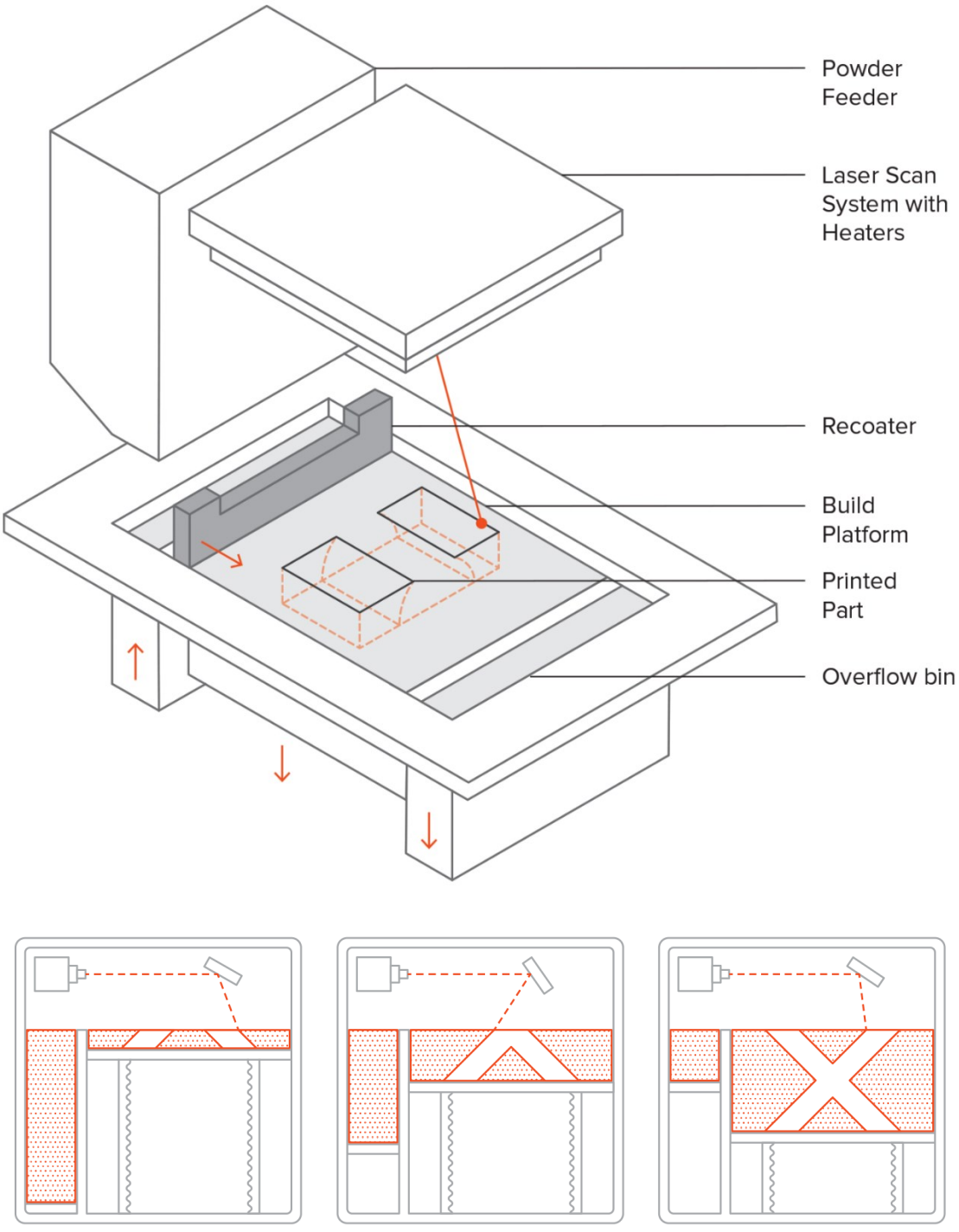

Figure 14: Graphical representation of SLS and SLM processes

To better understand the process, it is necessary to first explain the term sintering. Sintering is a process which utilizes heat and/or pressure to partially melt materials for adhesion. The main difference between sintering and melting is that melting forms a fully

molten stream of material, whereas sintering stops melting when the materials become soft and viscous enough to adhere to each other [14]. As can be logically inferred, sintering requires less energy and thus requires less time if external factors (laser power, technological implications, etc.) are not considered. Likewise, components produced with this method may not have as strong a bond as fully molten components since particles are adhered to each other rather than molten together, forming one single element.

These machines are aided by heated chambers (often heated by infrared lamps) which help bring the temperature of the powders close to their melting point, thus requiring a drastically lower laser power to reach their melting point. This heating also prevents deformation caused by rapid cooling of the components after reaching a melting point [3].

For the laser to scan the shape onto the powder bed, the laser-system is equipped with devices called galvanometers which are mirrors attached to the lasers which are moved by motors according to the layer pattern. Unlike deflection coils which can have instantaneous movements thanks to magnetic changes, galvanometers have a slight delay given their motor mechanics.

Laser-based systems do not employ vacuum chambers but instead utilize inert gases which are invisible at the laser's wavelength to let it pass through. Lastly, the efficiency of this process is limited by the thermal absorptance of the material.

2.3.7.4 Selective Laser Melting (SLM)

While nearly identical to SLS, selective laser melting differences itself by fully melting the particles together reaching a liquid phase rather than just partially melting them to adhere them together. This process often requires post-process re-heating while still on the heating-platform in order to reduce warping and structural weaknesses induced by residual stresses [1].

This process is often considered exclusive to metallic powders, yet this is erroneous as other materials can be added by melting processes. The lack of SLM research and products on other material powders, as well as the increased usage of this misnomer, have led most research done with SLM of non-metallic powders to be incorrectly termed as

SLS even if actual melting to liquid phase takes place. Another term often used to describe SLM of metals is Direct Metal Laser Sintering which, once again, is a misnomer as DMLS sinters the components together without them reaching a liquid phase thus enabling layer-homogeneity.

For correctness, the term SLM will be used to describe processes where melting to liquid phase of any material takes place.

2.4 Applications

While most generalized uses for AM have been mentioned before, it is useful to understand how those methods translate to actual tangible products. Some of these applications have already been developed and are currently available while some others are under development. These will be divided into sub-categories per the uses mentioned previously.

2.4.1 Rapid prototyping

AM is widely, and mainly, used for prototyping purposes. It requires little to no supervision or manual labor and gives a close impression of what the final product will be like.

Concept modeling, also known as solid imaging, serves the purpose of giving a physical model that allows the user to visualize the component without necessarily having any functionality [2]. This can be compared to traditional foam models which are usually hand-crafted or produced via subtractive prototyping methods.

Functional prototyping, on the other hand, has the sole purpose of proving that some functionality is present, and often does not include any of the visual aspects of the final product. These are mainly developed for engineering purposes [2].

2.4.2 Rapid manufacturing

For some purposes, the quality of prints is satisfactory for actual use. Under these circumstances, it is possible to produce final products utilizing AM only.

2.4.2.1 Initial investment and running costs

The production costs of components manufactured with traditional methods can rapidly increase if the equipment and tooling is not available. If we consider components which require specialized tools, machinery, or molds for production, costs rapidly increase. The initial costs for AM technologies, considering access to the machine is available, are generally lower than those of a full-fledged assembly line.

2.4.2.2 Low production volume

If only small amounts of the product need to be fabricated and the technology is suitable for the purpose, AM can reduce the overall costs of final production of a product given the extensive processes often involved in manufacturing given its simplistic approach. When printing, all that is needed is material for the machine however, these are more expensive than their raw, mass-production counterparts, and therefore it is necessary to make a cost analysis comparison taking into account the yield volume and costs-per-unit [6].

2.4.2.3 Decentralization

A large investment which is usually not needed when producing with AM is the rental and maintenance of a warehouse to store produced goods or assembly components. Furthermore, there is a need for space to install the machinery, assembly lines, space for the operators to work, and so on. AM only requires the storage space for the raw materials, the machines (usually much smaller), and possibly a small storage space for finished components.

This follows a JIT manufacturing approach and helps reduce down-times and increase reliability by reducing the number of suppliers involved in the finalization of a product.

2.4.3 Complex structures

Perhaps the most notable application of AM which has yet to be accomplished by other manufacturing methods is the easy creation of complex 3-dimensional structures with the only limitation being the resolution of the equipment used [3].

These can involve the creation of shapes surrounded by other shapes which are impossible to create with traditional tooling because of physical limitations. Moreover, the possibility

to combine moving parts in a single print enables the creation of new products while simplifying their production (Figure 15).

Figure 15: Complex shape manufactured with AM [15]

2.4.4 Customization

If we consider niche markets once again, there is a growing need for custom made components which traditionally requires lengthy periods of manual labor. Examples of these are mostly medical and can range from casts to dental prostheses; these require intricate and convoluted approaches if precision is to be achieved and, even then, they often fall short of the ideal results.

While not widely-used, AM has started to replace a few of these processes with more advanced and precise solutions; with help from 3D scanners, a near-perfect replica of a body part can be made and therefore a near perfectly-fitting cast or prosthesis can be created. Figure 16 shows a 3D printed cast which was tailored to fit the user's arm using less material and making it breathable and easier to remove while offering protection for the user.

Another benefit of customization capability is the possibility to modify components or have a database of modular shapes available to increase the catalogue offering for customers without incurring large investment costs or space needs.

Figure 16: 3D printed custom-made cast [16]

2.4.5 Repair

While limited to materials which can be created using AM methods, repairs of broken components created in batch or, which are otherwise no longer available, can be achieved. This can range from on-site repairs for structural needs to broken parts of medical equipment to assembly line elements [17].

2.4.6 DIY promotion

While less profit-oriented than the previous applications, DIY manufacturing has created a new paradigm where people's creativity has an increased empowerment fueled by AM technologies. Not only does this allow the free expression of an individual's creativity, it also gives access to open-source components which would otherwise be expensive or complicated to obtain [6]. This has also led to a surge in hardware startups which would otherwise not be viable due to the high costs involved in traditional prototyping.

Colloquially termed the "maker movement", this empowerment has also supported the creation of communities such as Thingiverse or GrabCAD which rely on open-source sharing of DIY components. The sole goal of these communities is to share creations freely and globally with ease.

2.4.7 Industry 4.0

Commonly called the factories of the future, industry 4.0 focuses on the automation and digitalization industrial processes by reducing human-related risks and costs and increasing the reliability and repeatability of results. This is done by constant automated monitoring and adjusting of processes, and IoT communication between the equipment.

The whole system is networked, and algorithms keep the systems running with minimal operator input.

Currently, AM is only beginning to approach the industry 4.0 context, yet it has a strong anticipated impact which is only logical given its simplified nature. By reducing the steps taken to produce a product, algorithms can be simplified and the risks of failure become lower [6].

2.4.8 Sustainability

When discussing the environmental effect of AM technologies, it is necessary to point-out the drastic differences between different technologies and materials used. Nevertheless, AM improves on many aspects of traditional manufacturing:

- On-demand production – only the necessary number of products is made, or batches are only slightly larger than necessary. Mass production can see a large percentage of produced components becoming waste.
- Material-use minimization – only the exact amount of material needed plus supports will be used; unlike subtractive manufacturing, there is no removal of excess material thus no waste is produced and supports, if needed, only constitute a minimal fraction of the volume.
- Reduced repair waste – often, repairing a component requires purchasing parts which come in sets containing more than one [6].
- Reduced material use – with the aid of shape optimization software, it is possible to create components which closely approach the mechanical properties of a component while using only a fraction of the material. Furthermore, AM benefits from the possibility to generate complex structures, thus having virtually unlimited design optimization freedom.

To the contrary, AM often has a higher energy consumption when compared to processes such as injection molding by up to a factor of 60. This is specifically targeted at SLS methods which require a high-power laser beam to melt the powders.

Also, some processes can be destructive to the powders, thus preventing the reuse due to hindered properties of the material. The reuse of powders which are not structurally-strong will lead to failed or short-lived components which generate more waste [6].

3 Glass AM

AM has become a trend in the industry and research is done constantly in many different fields to expand the technology into new fields by adding new materials. It is therefore surprising to see the lack of research and, mostly, discoveries done with glass AM. Given its wide-spread use and nearly unique set of properties, glass plays a major role in industrial processes and thus would be a good inclusion in the catalogue of materials which can be 3D printed.

The reasons why research has been deemed a failure so far is that the results do not carry the properties which make glass special, namely transparency and strength. While other materials can achieve similar or higher strengths, it is the combination of its properties which makes glass valuable [18].

The experiments in this paper attempt to accomplish the following:

- Generate optically transparent components (inclusion of failures might be present, yet the component is clear enough to allow seeing through).
- Generate components with a higher tensile strength than what has been achieved in previous research.
- Find the optimal parameters for SLM AM of glass powders to assist future research.
- Test the effect on porosity of powders with a particle size between 2-20µm.

Furthermore, this thesis focuses on one specific type of glass, silica, which has specific properties suitable for initial testing in the field of glass AM. This glass is characterized by having the lowest coefficient of thermal expansion amongst non-ceramic glasses, useful to prevent the creation of residual stresses in the finished components which make it susceptible to cracking.

This chapter will discuss all relevant research done in the field of AM of glass, focusing mainly on those which have been either successful, SLM or SLS-based, or using silica powders. Other relevant research, not-excluding metallic or plastic SLS, will be covered and their relevance will be brought-up. Consequently, the phenomena which have

historically impeded glass AM to succeed, will be discussed, explained, and analyzed to explain the factors related to their appearance.

3.1 Existing Research

It is necessary to understand the underlying issues and limitations of the material, the technologies, and the factors which affect the process.

Energy density, layer thickness, and particles size are factors which are user dependent and can be pre-established or studied to improve on what has been attempted before. These have had a major influence in the results and, in most cases, failure of the process, and they, together, give a good perspective on what parameters and properties will help improve the process to give successful results.

Balling, porosity, strength, and transparency, on the other hand, give the possibility to reverse engineer the results obtained by failure or success and analyze the conditions which made them happen. Given how a deep understanding of what is considered a failure is needed, it is necessary to fully understand the intrinsic behavior and appearance of these phenomena to better asses their behavior, thus explanations are given for each of these.

The research found on the specific field of AM of glass dates back to 1997 and continues up to 2017 with major breakthroughs or successful methods suggested only in 2015 [19] and 2017 [20] where FDM of molten glass powders via a kiln and SLA of photo curable-resin-added glass powders were achieved, respectively. These methods, while highly relevant and breakthroughs in the field, do not fulfill the ambitions of this publication which is to generate transparent, 3D-printed glass components utilizing only glass-powders and allowing for complex geometries by use of powder-bed technologies.

Table 1 offers a good assessment of previous research, parameters used, and their results.

Table 1 Optimal parameters per previous research

Material	**Parameters (only recommended ones are shown if available)**	**Source**
Borosilicate glass	Hatch-spacing – 120-180 Laser power – 5-9	[21].

	Layer thickness – 2000 Particle size – 30 Processing – post-process heating Scanning speed – 300-550	
Fused quartz	Laser power – 20, 10 Layer thickness – 500 Particle size – 100 Scanning speed – 2, 1 Spot diameter – 500, 250	[22]
Fused quartz	Laser power – 20, 9.3 Layer thickness – 500 Particle size – 100 Scanning speed – 1, 0.9 Spot diameter – 1000, 500	[23]
Fused quartz	Laser power – 21 Layer thickness – 200 Particle size – <20 Scanning speed – 0.9 Spot diameter – 1000	[24]
Unspecified glass	Laser power – 100 Layer thickness – 500 Particle size – <500 Scanning speed – 50	[25]
LAS	Laser power – 20 - 100 Layer thickness – 3000 - 5000 Particle size – 38 – 63, 63 - 90 Processing – post-process heating at 1000 C recommended	[26]

	Scanning speed – 10 - 200 Spot diameter – 300	
LAS	Hatch-spacing – 200 Laser power – 10 - 50 Layer thickness – 150 Particle size – 63 - 90 Processing – post-process heating at 850 and 1000 C Scanning speed – 50 - 200 Spot diameter – 300	[27]
Soda-lime	Laser power – 15-50, 30-50, 35-50 Layer thickness – 1000 Particle size – 1-37 Processing – annealing recommended Scanning speed – 10-30, 5-20, 5-15 Spot diameter – 70, 200, 350	[18]
Soda-lime	Hatch-spacing – 50, 100 Laser power – 100 Layer thickness – 500 Particle size – <500 Scanning speed – 50	[28]
Soda-lime	Laser power – 60 Layer thickness – 150 Particle size – <100 Processing – post-process heating Scanning speed – 67	[29]
Spodumene glass-ceramic	Layer thickness – 100 Processing – post-process heating at 950	[30]

AlSi10Mg	Hatch-spacing – 50 Laser power – 100 Layer thickness – 40 Particle size – <120 Processing – post-process re-melting Scanning speed – 500	[31]
Gold	Hatch-spacing – 80 Laser power – 50 Layer thickness – 100 Particle size – 24 Scanning speed – 65	[32]
Nickel	Hatch-spacing – 100 - 800 Laser power – 190 Layer thickness – 50 Particle size – 30 Processing – post-process re-melting Scanning speed – 100	[33]
Nickel alloy	Layer thickness – >2000 Particle size – 100 - 160 Scanning speed – 5 Spot diameter – 3000 - 4500	[34]
Stainless steel	Hatch-spacing – 100 - 800 Laser power – 190 Layer thickness – 50 Particle size - 20 Processing – post-process re-melting Scanning speed – 100	[33]

Stainless steel	Hatch-spacing – 100 Laser power – 195 Layer thickness – 40 Particle size – 37.13 Scanning speed – 800	[35]
Stainless steel	Hatch-spacing – 70 Laser power – 150 Scanning speed – 700 Spot diameter – 50	[36]
Stainless steel	Laser power – 50 Layer thickness – 50 Particle size – <20 Scanning speed – 140 Spot diameter – 70	[37]
Stainless steel	Hatch-spacing – 140 Laser power – 100 Layer thickness – 30 Processing – re-scanning Scanning speed – 400	[38]
TiAl6V4	Hatch-spacing – 100 Laser power – 122 - 190 Layer thickness – 100 Particle size – 53 Scanning speed – 500 Spot diameter – 2000 - 5000	[39]
Nylon	Hatch-spacing – 125 Laser power – 60	[40]

	Processing – post-process re-melting, re-scanning Scanning speed – 13000	

Next, relevant findings from the research detailed in the table is presented.

Post-treatment of borosilicate powders in an oven increases the density of components achieving near full density (96.4% at 800 C for 6 hours) but introducing warping from shrinkage (17%). Stripes or chess exposure patterns reduce strength as they tend to break along the lines [23].

Reducing the layer thickness of fused quartz powders helps minimize loss of productivity since reducing it by a factor of 2 has the same effect as reducing the scan speed by a factor of 4. Reducing the layer thickness improves the bonding between the bead and substrate if laser evaporation is not present, yet for too small powders, laser evaporation removes more mass than is added.

The detachment of a bead's border can provoke additional porosity; this can be minimized by reducing the layer thickness which facilitates heat diffusion to the substrate or reducing the scanning speed which increases the heating period. Porosity also is a remnant of an incomplete heating process (sintering). According to the equation:

$$\frac{d}{\mu_s} > \frac{\eta D}{\sigma} \; where;$$

d is the spot diameter;

u is the scanning speed;

η is the viscosity;

D is the particle diameter;

σ is the coefficient of surface tension.

Increasing the beam diameter and decreasing the scanning speed and particle size should reduce porosity. Powder size is related to pore size, thus finer powders will give smaller pores [24].

The edges of a layer detach from the support which can be fixed by re-melting. Thinner layers remove the issue altogether since they facilitate heat diffusion through to the support. Halving the layer thickness equals a 400% reduction in scan speed. Reducing the layer thickness should be universally better if there are no large mass losses by evaporation. Defects present cannot appreciably reduce strength [25].

Precise control of laser temperature helps improve print quality and smaller particle sizes help achieve this. The lower the thickness of the powder layer, the better the quality of the consolidated layer due to more uniform heating and reduced porosity. Finer powders consolidate faster. Incomplete powder melting due to low power can lead to pores. Components had very low bending strength. Smaller powders would fill up the layer more thus giving strength [26].

For an unspecified glass, printing of a complicated helical shape with detached coils was possible. Small diameter variation [27].

The occurrence of balling when using LAS powders is due to the material's need to minimize free surface energy through surface tension. Slower speeds (100W – 10mm/s) give for a smaller separation between balls and less-radical balling phenomena than at faster speeds (20, 50, 100W – 100mm/s). Ball milled powders give more consistent results than ground. At 75W and 10mm/s, balling does not occur, yet Rayleigh instability appears. Larger particle sizes lead to balling; Prevention of balling happened at small particle sizes between 2 and 20μm.

Melt-depth increases with higher energy density. Higher energy density gives smoother results. At low energy density (20W – 200mm/s), layers do not bond sufficiently to provide structural strength. At intermediate density (30W – 150mm/s), balling was greatly reduced, and bonding improved slightly. Also, it achieves low viscosity. At high energy density (50W – 50mm/s), balling occurred, and pores appeared as well as darkening of the part; darkening was reduced after post-treatment in a furnace and achieved full melting meaning high viscosity.

For bulk parts, layer thickness was 150μm as thinner layers resulted in previous layers breaking off or displacing. Prevention of balling only possible at particle ranges of 2-

20μm but also cause vaporization which produce pores. Molten material forms a u-shape meaning material goes away from the center. The cause for this could be the Marangoni effect where surface tension gradients occur (possibly formed by temperature gradients in the laser spot). Smaller powder sizes have a larger energy absorption area. They also are more prone to ablation (empty spaces by evaporation). Deeper melting cannot happen with larger particle sizes.

Pores perpendicular to laser direction. Higher power makes deeper and less interconnected pores. In powder metallurgy, capillary forces introduce liquid into the pores between powder particles. Previous research attributes pore generation to the Marangoni effect because of surface tension gradients on the melt pool surface. Rapid cooling after melting traps the pores. High laser intensities caused no pores. Highly-viscous glass cannot adapt to the shape of previous layers and due to flowing towards the center, thus forming pores.

Poor laser energy absorptivity detriments the qualities of the product. Interlayer strength plays a really important role in ultimate strength. Produced samples did not have enough strength due to bad bonding between layers. Intermediate energy density gave a stronger bond. Annealing helps remove darkening partially [28].

Balling can be prevented when powders are melted at low and medium laser energy densities. At powers under 20W with a scanning speed of 200mm/s, particles coalesced by viscous flow. Increasing the laser power or decreasing the scanning speed gave continuous tracks. Using 30W at 150mm/sec gave a smooth surface with no balling but layers started curling. The balling phenomenon in metallic powders can be avoided using particles with a size smaller than 10μm and with proper control of laser parameters. Coalescing by viscous flow. Smaller powder sizes let capillary forces penetrate the pores by improving the viscous flow [29].

Fused soda-lime balls-up due to surface tension. Parts with a layer thickness of 0.5mm had significantly higher transparency than those with 1mm [20].

Balling can be avoided using small diameter powder particles. After reaching a point where the energy density gives a good melt track, further energy density increasing leads to excessive heat which causes balling. Excessive energy density leads to imperfections such as balling or bubbling of the molten liquid. Minimum layer thickness must be thicker than the particle size to prevent uneven deposition (gaps). It also needs to be deep enough to adhere to the previous layers but small enough to reduce thermal stresses, thus 500μm was used [30].

The strength and density of the component can be increased with post-process sintering in a furnace [31].

For spodumene glass-ceramic, swelling of the surface and darkening worsened with thicker layers. 50-micron layers had larger pores than those in 100-micron layers. Strength decreases with layer thickness increase but stay the same if post-process heat-treated. Due to a lesser need to penetrate, thinner layer thicknesses overcome the surface tension of the melt and prevent the top surface from forming a hump. Crystallization takes place at lower thicknesses due to higher heat penetration. Thinner layer thicknesses worsened pore formation as vaporization took place. After heat treatment, the 100-micron parts were stronger due to larger pores present at 50μm, and 150μm had weaker layer bonds. Percentage of pores decreases when layer thickness increased. Vaporization took place in thinner layers because of excessive heating. Thinner layers are more prone to pore formation due to the reduced amount of solid. All samples failed due to brittle fracture. Heat treatment strengthens but made them more brittle in crystalline state. Strength decreased with thicker layers. Strength of different thicknesses after heat-treatment gave similar results. Further heating gave further strengthening. Initially, flexural strength decreased as layer thickness increased due to degrading interlayer bonding which reduces heat penetration. Smaller pore size and better inter-layer bonding gave stronger samples. Strengthening with heat treatment was due to phase transformation in the material. Sintered particles at the surfaces give low flexural strength [32].

Higher scan-speeds promote capillary instability leading to splashing of liquid droplets in AlSi10Mg. Balling captures powder which is not melted and thus creates pores. Oxidation

promotes pore generation with metals. Trapped gasses can cause porosity, this happens at slow scanning speeds. Metallurgical pores can appear if hatch spacing is too large as powders do not overlap to fill the area. Keyhole pores arise from rapid cooling which does not allow for molten metal to fill the gaps. Slow or too fast scan speed cause pores due to different reasons. The area in-between gives best results. Overlapping scans reduce pores but do not fully remove them. The densest results (97.74%) were achieved with single unidirectional scans but 99.82% can be reached with double unidirectional scans at different laser powers. Keyhole pores contained powders which had not melted [33].

Good melting of gold powders achieved at powers higher than 35 W with speeds slower than 60mm/s. A length to diameter ratio of $L/D > 2.1$ causes balling. Balling at <60mm/s could be due to slow solidification allowing spreading of the molten track. The laser penetrates through the pores, reaching the interior of the powder. The lowest porosity values were achieved at 65mm/s which is neither the highest nor lowest speed used. The thinner the layer thickness, the less pores appeared. Hatch spacing had a near negligible effect on porosity [34].

Reducing oxygen content in Nickel powder SLM reduces balling behavior. Higher energy densities and surface re-melting can aid. Balling can be lessened by reducing scan-line spacing. If balling occurs in the first layer, gaps are created through which the following layers fall, thus creating uneven features. A lower oxygen content drastically reduces the appearance of balls. Overlapping of scan tracks does not affect big-sized balling. A smaller layer thickness enabled better wetting, thus reducing the presence of balls. Re-melting removes existing balls to a good extent. High-intensity gives better melt continuity due to well-wetting. At a layer thickness of 50μm, pores were not present, yet at 100μm they appeared and prevented wetting [35].

As for nickel alloys, the molten particles pulled solid particles into the sphere adding imperfections on its surface. The balling process takes place when the laser passes through gaps in the powder layer and melts the underlying layer. The probability of balling increases with the increase of length and the decrease of layer thickness. The laser penetrates through pores in a layer thus interacting with lower layers [36].

In the case of stainless steel, higher scan speeds might apply more shear stress to the liquid thus creating larger surface tension which in turn promotes ball formation and capillary instability which causes splashing of droplets.

Energy density is affected by both laser power and scan speed. While having an identical energy density, one with a higher laser power will give higher densities than one with a slower scanning speed. Also, higher energy densities altogether give larger densities. High energy densities at slow speeds and low powers give pores yet smaller ones, thus indicating energy density is not a good indicator of print quality. Porosity was maximum at 0.4% with energy densities of 44-81 J/mm3 but highly increases below 44. Also, at constant energy density, powers above 120 came in the highest at 0.4%, and quickly rise when it reaches 95. Porosity follows different formation mechanisms: At high speeds, balling occurs probably due to unstable melting. High speeds apply more shear stress to the liquid phase generating higher surface tensions [37].

Pores are caused by gas entrapment. Pores generated by balling prevent new layers to fully fill. Un-melted particles were observed within pores. Ultimate tensile strength and elongation to failure need to be weighed; There must be a good tradeoff assessment. Building direction can improve the yield strength. Possible to obtain fully-dense components with a higher ultimate tensile strength and elongation to failure than with conventionally made components [38].

The greater the value of P/V ratio, the larger the re-melted vector is [39].

Parts connected to the base plate have high stress levels in the range of their yield strength; Parts detached do not but suffer from warping. Stress levels are related to part height. Stresses are larger perpendicular to scan direction. Laser heat treatment post-processing reduces stress. Substrate plate heating reduces residual stress [40].

Thermal differences across the melt-pool of TiAl6V4 powders prevent the proper wetting of the underlying substrate thus leading to balling. It worsens with low viscosity. Excessively high or low energy densities steeply increase porosity. The best results were obtained with an energy density of 117 J/mm3 which are close to optimum 120 J/mm3. 3D tomography reveals that the pores generated at excessive densities have trenches

which may be stress concentrators. On the other hand, insufficient energy densities reveal sharper shapes and cracks. It is recommended to have energy densities slightly larger than those for minimal pore generation to prevent cracks. Porosity is usually correlated to energy density. The lowest porosity for different values takes place at 117 mm/s, 85 hatch distance, 165W, and focus distance of 1. Velocity, then power, exerted the highest effect on porosity. Hatch distance had the smallest effect. The ideal speed was 500 mm/s giving a porosity of 0.042± 0.008% with lower and higher speeds increasing porosity. Small hatch distances lead to re-melting which does not affect much unless hatch spacing is too small due to excessive heating. Excessive or too low energy densities give poor results. Porosity can increase due to partially melted, entrapped powder particles sticking to the edge of the melt pool. Pores generated at excessive energy densities possess trenches which act as stress concentrators [41].

Pores happen with Nylon powders because of poor small bonds or un-sintered powders. Trapped air causes pores. Printing direction affects the efficiency of heat strengthening methods. Vertical orientation (which is generally better for Nylon) gave stronger prints [42].

Per the results documented by the authors which are written in the chart, a few patterns can be seen which suggest positive results if tested. The following apply to glass powders and should give satisfactory results:

1. Post-process treatment of the component either by re-melting it past its melting point to remove residual stresses or re-scanning each layer after melting at a slightly lower energy density to prevent fast-cooling and thus preventing residual stresses from happening, remove darkening, and increase material density.
2. Having a layer-thickness as small as possible whilst abiding by the rule of $H > 3D$, where H is the layer thickness and D is the particle diameter, to improve bonding between layers to improve strength and improve heat diffusion which reduces porosity, to prevent detachment of the edges, and increase transparency.
3. Using powders with a size <20μm should prevent the occurrence of multiple defects such as porosity, improve the layer fill-up to increase strength, and increase viscous flow thus letting capillary forces penetrate pores.

4. Using powders with a size >2μm to prevent porosity due to evaporation.
5. Reducing scanning speed instead of increasing power to increase the heating period and prevent porosity and prevent balling.

There have been only a few promising results in the field of AM of glasses. The most relevant of which are:

- FDM of glass powders melted in a kiln and extruded onto a moving platform [19]
- SLA of photo-curable resin-induced glass powders with post-process removal of the resins by melting [20]
- MJ of translucent resins polished and coated during post-processing to create optical lenses [41]

The process suggested in this paper improves on the previous methods by using only glass powders, which increases simplicity and potentially reduces costs, and allowing for printing of complex shapes with overhangs which are supported by the powder bed.

3.1.1 Balling

Balling is a common side effect occurring in melting processes where particles form spherical clusters or "balls" instead of continuous streams of molten powder. This is often accredited to the viscosity of the material which increases the surface tension and capillarity of the material thus trying to attain a shape which does not counter these forces. This is a major issue commonly found while testing the SLM capabilities of multiple materials; in this case, glass powders.

Figure 17 shows the consequences of this phenomenon and how it gives poor print quality and failures while attempting to print smooth surfaces. It is necessary to mention how balling is not the only phenomenon involved in layer failures, yet it is the most common.

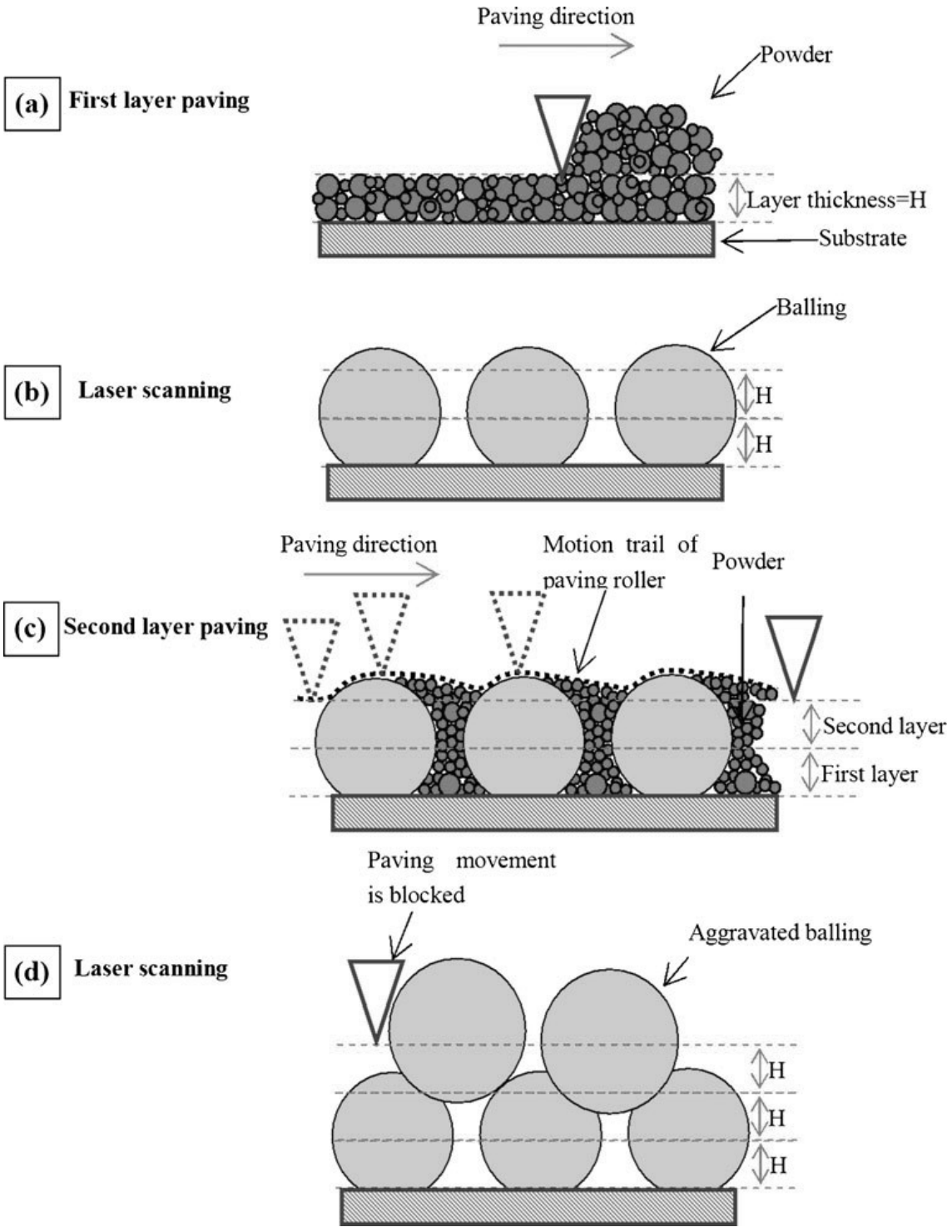

Figure 17: Graphical representation of problems derived from balling in multi-layer prints [33]

Li [33] suggests that heat is irregularly distributed through the layer since top particles are sintered quickly when compared to deeper particles. Strong contacts are formed

between these particles due to their surface melting and capillary action closing them together which shrinks the component.

Balling prevents the formation of constant tracks of molten material which ultimately gives place to porosity; this porosity detriments the mechanical and optical properties of printed components since they become more prone to cracking thanks to increased brittleness, and prevent the formation of fully solid, transparent components.

The most frequently suggested approach to prevent this phenomenon is to use smaller particles which require lower laser powers and allow for smaller layer thicknesses; thinner layers in turn reduce the dispersion of molten particles and are more resilient to the penetration of following layers.

Other approaches involve using lower energy densities, mainly from slower scanning speeds, to allow for the molten track to achieve full fluidity and slow cooling which prevents bubbles from becoming trapped in the layer. Also, preheating the chamber to a temperature nearing the melting temperature prevents fast cooling and therefore impedes surface tension from forming balls.

Finally, post processing the component by reheating or re-melting removes bubbles, increases density, and releases residual stresses. This is recommended not as a prevention method but as a remedy.

3.1.2 Evaporation

It is often hypothesized that large material voids take place during the process thanks to evaporation of the glass powders or their composing elements. This process is called ablation and can cause empty pockets of air to be introduced in the print which eventually translate to pores void of glass which detriment the quality of the print.

Khmyrov hypothesizes [22,23] that the Gaussian distribution of heat within the laser beam causes an energy density flux which increases the evaporation rate in the center of the beam while causing minimal damage in the outer rings. If the beam energy flux were to be constant throughout the whole perimetry, evaporation rates could be discarded if the correct parameters are found which soften the glass enough for viscous flow, yet do not heat it up for boiling and subsequent evaporation to take place. Likewise, an even

evaporation throughout the whole layer means a consistent layer height is achieved throughout its entirety.

Furthermore, Manob [26] stipulates that small-enough particles (<2μm) will have marginally higher evaporation rates than their larger counterparts, thus recommending a compromise between evaporation and balling by utilizing a particle size distribution in the range of 2-20μm.

3.2 Silica Glass AM

Khmyrov's research [22–24] is seemingly the only available one on silica glass powder SLS or SLM, thus making it the most interesting and relevant to test assumptions against. Furthermore, in his latest paper, he utilizes powders with a small mean particle size distribution which approximates the desired particles range for testing. Lastly, crack-free lines were accomplished which are seemingly transparent.

Using smaller powders, thinner layers, and slow speeds are continuously recommended to reduce balling phenomena and porosity.

3.3 Persisting problems and misnomers

It is evident that utilizing smaller particles in the range of 2-20μm is considered by other authors to be beneficial to improve the quality of printed components, yet it has not been thoroughly tested. It is unclear as to why this happens, yet it can be hypothesized that both material availability and lack of research on the relation between particle-size and porosity could be the culprits.

This paper attempts to consolidate these assumptions by testing under the constraints most recommended by previous research.

While most papers referenced in this thesis seem to agree on the same conclusions, there is a constant wording of "higher energy densities" or "lower scanning speeds" which do not have a tangible numerical measurement which indicated a range optimal for bonding. These vague terms happen because a range of energy density is used which can be from X to YX while others use a range from <X to <YX, thus making words such as low or high improper.

To rid of these misleading terminologies, measurements will be accounted for in energy density, scanning speed, or laser power ranges.

4 Research materials and methods

This section comprises the entirety of the experiment design, the hypotheses being tested, and the desired results to be obtained from the process.

To test the hypotheses proposed in previous research papers, the author's own hypotheses, and the validity of the results, a deeper understanding of the desired qualities and a comparison to traditionally manufactured components is necessary. These will furthermore help understand the acting mechanisms behind the processes and possibly explain any failures, should they happen.

The "goal" for the experimentation is to achieve the printing of an optically transparent glass components using a laser and a galvanometer by means of selective laser melting. The level of transparency does not need to be high enough for precision optics; a degree of transparency which allows an average adult to read text through it is enough. No previous research has managed to accomplish this, therefore there is no starting point to compare the results to or to improve on; the experimentation in this thesis is merely an attempt at succeeding where others have failed to prove or disprove the hypotheses postulated by them for the sole purpose of the advancement of AM of glass altogether.

This glass printing research process began marginally earlier than the actual laser melting of particles. It was first necessary to determine what properties are desirable for the process which increase the quality and reliability of printed components thus making them more useful. Then, it was necessary to analyze the properties of all glasses to find those which excel at the previously calculated parameters to later select the optimal one. Finally, locating a distributor which offers the specific material deemed to be optimal either at the correct powder size or close enough to allow processing to make them the right size.

During the SLM process, the powders will be targeted with the laser at varying powers, scanning speeds, and spacings as recommended by the referenced authors or as deemed suitable. The results will then be graphically visualized to find a "suitable melting zone" which optimizes the results. Also, powders will be pressed onto the substrate to increase the packing density and ideally obtain stronger components.

The tests will consist of melting single one-layer straight lines and circles on a glass substrate with varying parameters to find the optimal ones; these results will be inputted in a chart to determine whether energy density is a suitable parameter for estimating the quality of a 3D printed glass component. Afterwards, the optimal parameters resulting from these tests will be used to print 3-dimensional cylinders carrying the same dimensions as traditionally manufactured silica filaments/rods to test them in a 3-point flexural test machine for strength.

Additionally, 3D samples will also be subjected to post-treatment hardening by means of annealing in a kiln for an extended time at softening temperatures.

All samples will be analyzed under a microscope which makes it easier to visually comprehend the process and the faults present in each parameter combination. For simplicity, all samples will be analyzed under an optical microscope and, should there be a successful print, it will furthermore be analyzed with an SEM microscope. The reasoning behind this is mainly due to their availability and the time it takes to prepare each of the many samples for analysis.

The following sub-chapters offer an in-depth look at how each of these steps proceeded.

4.1 AM Technology Selection Methodology

The rationale for selecting this specific method for testing AM of glass is the possibility to utilize only the raw powders of the selected glass without the need to include resins or external materials to simulate the adhesion of the pure material. This substantially has the potential to generate pure printed components which keep the intrinsic properties of glasses yet have the value-proposition of creating complex shapes which are not possible with traditional glass manufacturing processes.

By method of discrimination, other AM processes can be withdrawn:

- Vat photopolymerization, material jetting, binder jetting, and multi-jet fusion require the use of resins or liquid-phase materials which can be hardened with light or adhere components together, thus introducing foreign particles and reducing purity.

- Material extrusion and directed energy deposition require the use of support material to create components with overhangs. This is hard to accomplish with components reaching high-temperatures and creates a rough surface finish which, with glasses, would detriment transparency, one of the most important properties of glass.
- Sheet lamination of rigid materials would not allow overhang features.

Electron beam melting would also be a suitable method however, SLM processes are more readily-available and at the time of this investigation, there was no access to such technology.

Lastly, SLS of glass powders has been investigated before with most results concluding that porosity caused by gaps between particles do not allow for transparency to happen and make the component structurally weak.

4.2 Glass Material Selection Process

To select a suitable material, it is necessary to comprehend the main causes for failures in previous attempts at SLM of glass. While most papers attribute this to the balling phenomena, it is the cause of balling which needs to be understood.

Balling is mainly attributed to thermal expansion, particle size, and surface tension so understanding why these happen and pondering of ways to diminish their effects is necessary.

Furthermore, it is necessary to understand why selecting a suitable material is such an important aspect to the results of the experimentation and how this process is done.

The main factor affecting the deformation and continuity of a print is the thermal expansion coefficient; not only does it affect the shape, but it also is directly linked to the structural strength of printed components due to the multiple cracks which most often arise because of it. Likewise, thermal expansion leads to residual stresses which increase the probability of cracks happening thanks to these forces attempting to balance themselves throughout the entirety of the printed shape.

To counteract this, the selection of a glass material which does not have such a large thermal expansion will largely aid in reducing the probability of failures happening. This process can be done by accessing material databases which allow for the selection and discrimination of materials based on their properties. Such software also allows the visual representation, graph making, and supply information on retailers of such material in different formats.

Probably, yet not so importantly, material hardness plays a role in the usability of the printed components. While this is not a requirement to get a functional 3D printed glass component, having a harder and stronger component will give the final product more use-case scenarios. Also, since most attempts at 3D printing glass so far have yielded very brittle and structurally weak elements, a weak material is not recommended.

Lastly, and somewhat regrettably, the availability of such powders plays a large role in the selection process. The fundamental goal of this thesis is to test the theory suggested by most other glass AM researchers that a particle size between 2 and 20μm is most suitable for printing as it will help counteract the effects of decreased density and increase wettability and consistent melting. This largely reduces the availability of glass powders.

4.2.1 Thermal Expansion Coefficient

Taylor [42] defines thermal expansion as the change of dimensions of a mass caused by a change in temperature at constant pressure. This mostly consists of mass expanding when heated and shrinking when cooled but this is not always the case as there are some materials which will shrink when heated and expand when cooled, respectively. For this thesis, we will only focus on those which expand when heated as is the case with all non-ceramic glass materials.

The thermal expansion coefficient, on the other hand, is a numerical value which acts as a multiplier to estimate the linear expansion the material will suffer. It can be calculated from the thermal expansion equation as follows:

$$\frac{\Delta L}{L} = \alpha_L \Delta T;$$

$$\alpha_L = \frac{\Delta L}{\Delta TL} where;$$

ΔL is the linear change of a unidirectional vector;

L is the original length of said vector;

α_L is the coefficient of thermal expansion, and;

ΔT is the linear change in temperature.

The units of the thermal expansion coefficient are $\frac{\mu strain}{^\circ C}$ which translate to the fraction of expansion a material undergoes for each degree of temperature ^{o}C or, if given the case, ^{o}F.

A lower thermal expansion coefficient reduces the probability of thermal shock which causes the printed segment to crack due to extensive warping when cooling which paired with residual stresses makes it very weak to withstand such deformations. In the case of glass materials, a coefficient which approximates 0 while keeping a positive value is desirable [18,21,24,26].

When comparing glasses to other materials which have successfully been printed utilizing SLS or SLM technologies, these materials do not necessarily need to have such a low thermal expansion coefficient as it mainly affects transparency of glass-printed components. While it is true that structural integrity, bonding between particles, and density are affected if thermal expansion causes cracks and balling, these materials are more resilient and most often require lower melting temperatures than those of Silica-based glasses.

The effect of thermal expansion on glasses can be easily explained when analyzing the crack-formations of glass windows; if windows suffer a thermal shock which makes them drastically change volume in just a portion of the glass, or if the glass expands faster than the metallic frame, the glass will crack to release the stress buildup caused from the temperature difference. This phenomenon is also the reason why some bridges are not fully attached on both sides but instead are only movement-locked in one direction and supported by expansion joints to allow for expansion to freely happen [43].

4.2.2 Particle Size

As has been noted before, utilizing a recommended particle size is the main hypothesis to be tested with this thesis. Most of the authors cited in this thesis recommend utilizing smaller powders while some of them even recommend a specific range under 20µm [24,26,27]. In comparison, other authors have mostly utilized particles in the range of 40-100 and > 200µm.

It is necessary to first understand the underlying mechanisms which make finer particles more suitable.

If we look at Figure 18, which represents an infinitely long volume, the void area is equal in both cases regardless of the particles size however, in real life, the mechanics of flow are favorable when voids are smaller, and more particles are molten since the void-to-material distribution is more even. Furthermore, if we consider the phenomena described in Figure 17: Graphical representation of problems derived from balling in multi-layer prints [33], more small particles are easier to smoothen-out than less large ones are. An analogy can be made to driving a car on an asphalt road versus driving a car on a cobblestone road; the finer particles of the asphalt road give a smoother ride with less bumps.

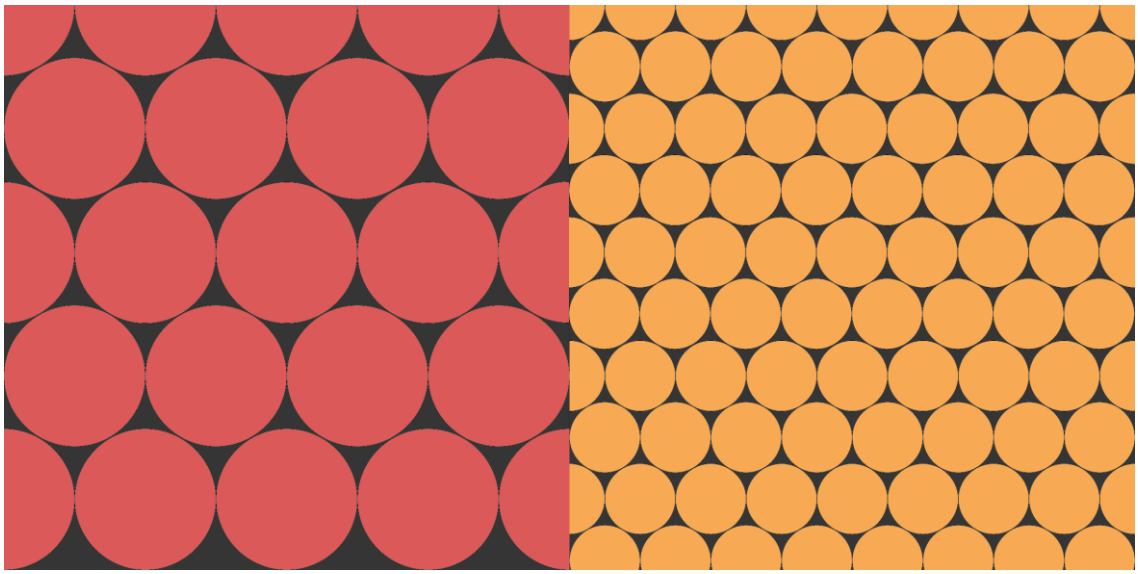

Figure 18: Void space. Left: Large spheres, Right, small spheres

Furthermore, according to Manob [26], a lower powder size-distribution gives for better flowability thanks to lower surface tension forces and increased viscous flow which prevent the formation of balls. This is further backed-up by his team again [27] where he mentions the capability of a molten track originating from smaller particles to better wet the desired area and not only create more consistent melt-tracks but also fill any voids present from the melting of previous layers.

4.2.3 Surface Tension

Surface tension is defined as the energy required to increase the surface area of a liquid due to intermolecular forces [44]; while this may sound relatively vague, it has a large effect on the probability of balling occurring. It can be seen in everyday phenomena as the main cause why liquid drops form. It is surface tension which causes all points within a liquid to exert a force on each other, which causes a strong force on the surface that helps it maintain its elliptical shape.

While all materials are affected by this phenomenon, the forces of surface tension vary greatly and drastically affect the wetting capabilities of elements used in 3D printing. Figure 19 gives an impression of the shape of droplets with different surface tensions. Glass, altogether, has a strong surface tension force which gives it a higher tendency to ball-up when compared to other materials.

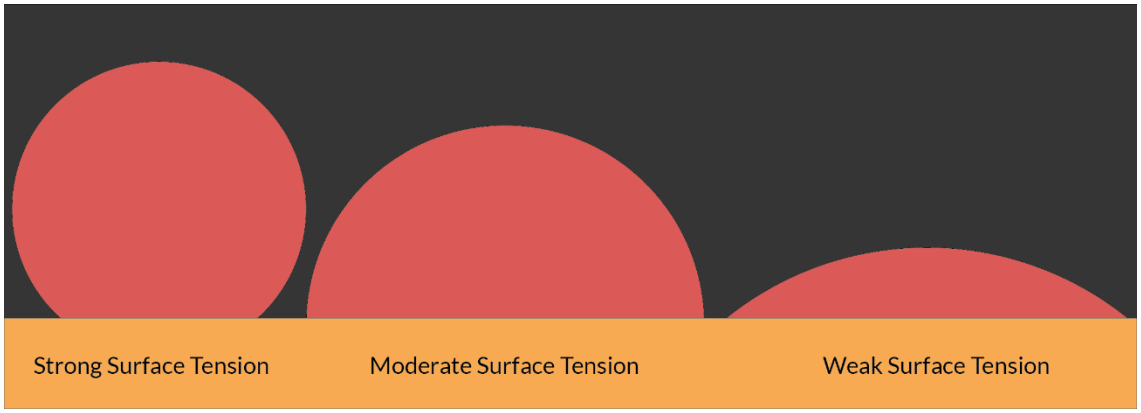

Figure 19: Visual representation of surface tension levels

Donaldson [45] defines wettability as the ability of a fluid to adhere to a solid surface in comparison to another control fluid. As can be inferred, surface tension plays an important

role on the wetting abilities of a fluid and thus needs to be taken into consideration when trying to understand the mechanisms and faults of SLM processes.

For reference, average surface tension values for common SLS polymers range between 12-18.4 mN/m [42] whereas glasses range between 200 and 320 mN/m [46].

4.2.4 Glass Temperature

While not a parameter which directly affects the quality of the print, the glass temperature or glass transition point is a temperature range during which glass, which is not a crystal, softens to become a true liquid; unlike most crystalline materials, glasses do not possess a melting point at which they instantly become liquid, they instead are defined by their glass transition temperature which is a gradual transformation [47].

Furthermore, some glasses, like pure silica, have extremely high glass temperatures which might limit the potential variations of scanning-speed-to-power analyses which can be done with a specific machine as is the case of Khmyrov who was limited to 40W [22] and whose research largely influenced this thesis. Fortunately, the machine used for these experiments has a maximum power of 100W, making glass temperature not a problem.

For reference, SLS polymers have melting temperatures lower than 200 ^{o}C while silica has a Glass Temperature range of 1290-1690 ^{o}C [48].

4.3 Testing

To provide quantitative and qualitative results on the experiments executed for this research, multiple properties of the printed components need be assessed by industry methods, when available, and by simple means of comparison to traditionally manufactured components of the same material.

In the case of strength properties of the printed components, multiple ASTM standards will be evaluated. These are based-off ASTM standard C158, titled “Standard Test Methods for Strength of Glass by Flexure (Determination of Modulus of Rupture)”.

Evaporation testing will follow a simpler approach wherein the initial density of a fully packed substrate-chamber of material will be assessed by measuring its initial weight and its weight after the SLM process.

Finally, the optical properties will be measured with a transparency meter if visually transparent objects are obtained.

4.3.1 Tools Used

The following is a list of all the software and hardware tools which were used to undertake the experimentation phase of this research; all of these are readily available (except when explicitly mentioned) to all students at Aalto University. Furthermore, the whole of the hardware tools used are presently available at the Aalto Digital Design Laboratory where most of this research took place.

4.3.1.1 CES EduPack 2017®

Perhaps the most relevant step to begin with is the selection of a material to test. This was easily achieved with CES EduPack 2017® which is a software which contains multiple teaching resources and, most relevantly, an extensive database of materials used in multiple industries, alongside their properties. This software also allows quick and visual comparisons of materials, material groups, or properties, to ease the selection process.

Furthermore, this software also provides information on most of the physical properties which will be studied and compared during this experiment, a comprehensive scientific detailing of each of them, and worldwide suppliers of said materials (if updated).

4.3.1.2 Creo Parametric®

Creo Parametric is a CAD design program which is largely used in multiple engineering industries; it is also the default engineering CAD software used at the mechanical engineering school at Aalto university.

For this project, Creo Parametric was used mainly for designing and 3D printing different holders and components in which glass substrates and/or glass powders were to be placed. Also, adapters and holders for use with the microscope are necessary to maximize efficiency and increase reliability and repeatability.

4.3.1.3 Ultimaker® and uPrint®

To print the 3D components designed with Creo Parametric, it was necessary to utilize the consumer level 3D printers available at the Aalto Digital Design Laboratory which are mostly a range of Ultimaker printers and one uPrint machine.

Ultimaker is a 3D printer manufacturer from the Netherlands which become an industry leader thanks to its resilient and relatively inexpensive FDM machines. Their machines are mostly targeted at consumers and prosumers.

For this project, only Ultimaker 2 Go machines were utilized as they have offered more consistent printing than other Ultimaker machines available at ADDlab, and their smaller print-bed was sufficiently large to print the necessary components, thus leaving the larger machines free for other students.

uPrint is an FDM printer offered by Stratasys. Compared to Ultimaker machines, uPrint has a marginally lower failure rate at ADDlab, can print ABS, and its support structures do not detriment the surface finish and precision of the component as much.

Keeping print precision and reliability in mind, a smaller print-bed was printed with the uPrint machine and retrofitted to the SLS printer to reduce the need for glass-powder material. While this was initially attempted with the Ultimaker machines, the precision and quality of the support material was not satisfactory, therefore it was necessary to use a higher-end machine.

To speed-up testing of different parameter combinations at equal layer heights, various substrate holders were designed which could easily be filled with powdered-material and allow for pressing.

Lastly, Ultimaker Cura, Ultimaker's 3D printing slicing software, was utilized to convert the CAD stereolithography model files (.stl) made with Creo Parametric to Ultimaker compatible G-code files.

4.3.1.4 Olympus BH-2 Microscope

To analyze the printed components and determine their structural shape, an optical microscope was used. Thanks to it being readily available, the Olympus BH-2 research-level microscope (Figure 20) is used while connected to a computer to allow for image capture.

Figure 20: Microscope setup

4.3.1.5 ShenHui 40W Laser Cutter

When necessary, a laser engraver/cutter is available which is useful for fast prototyping of holders or other components necessary for the process. This was only used for the fabrication of a holder

4.3.1.6 Aalto University's experimental SLS printer

The main tool used for this thesis is the student-built SLS printer available at ADDlab (Figure 21). Originally, it was intended to be used only for a mechatronics student class project but given its excellent performance, the project was further funded. Regrettably,

the machine has historically proven to have issues with repeatability of results when using low power, thus larger test-pools are suggested.

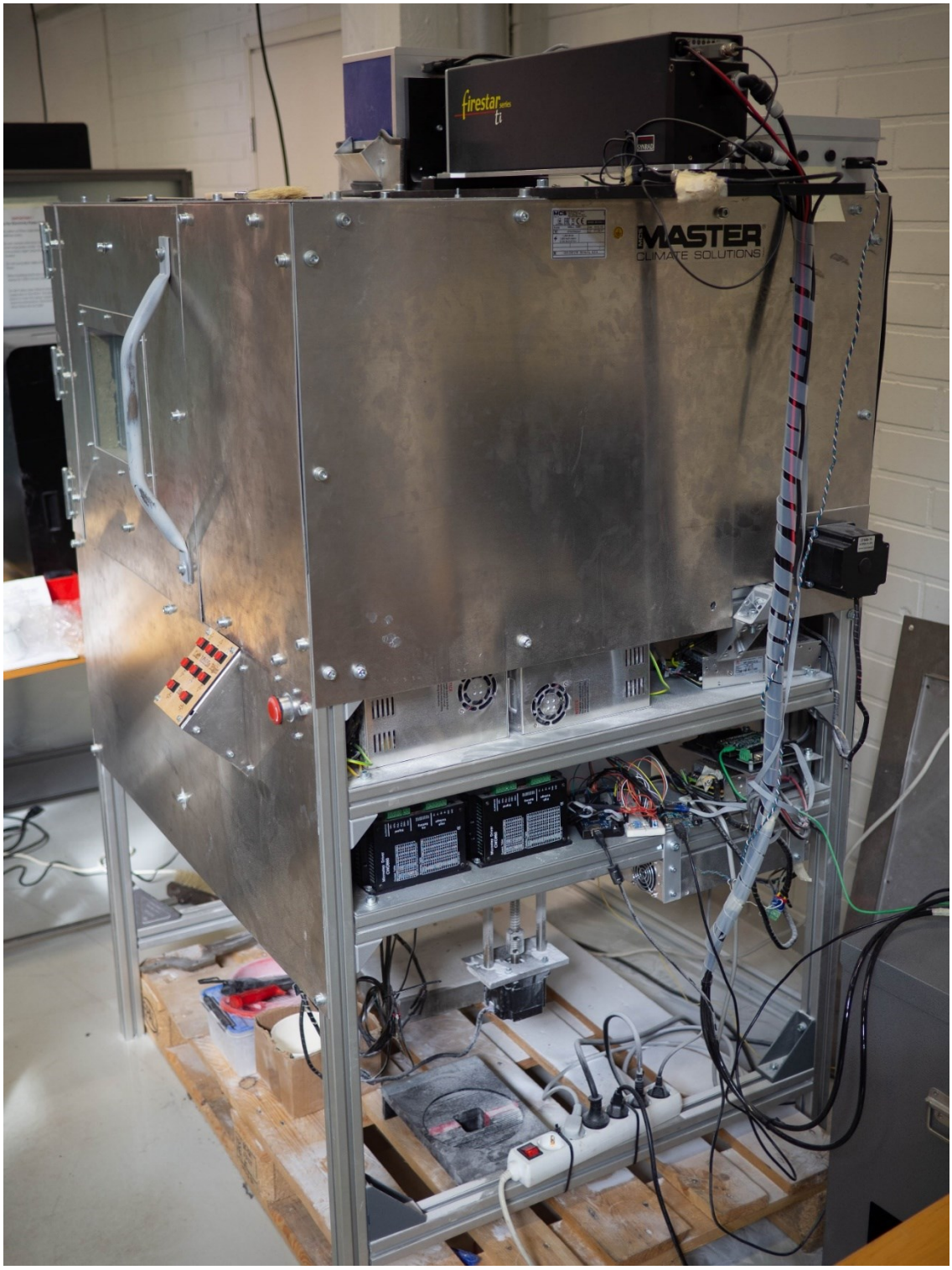

Figure 21: Aalto University's custom-built powder-bed printer

The specifications for the machine are as follows:

Laser power	100W
Laser Model	Firestar Ti series
Galvanometer standard	XY – 100
Print-bed dimensions (W x D x H)	300 x 300 x 220mm
Engraving software	RepliSLS 3D / BeamConstruct

4.3.1.7 RepliSLS3D

To control the printer, it is necessary to have an SLS software capable of controlling the galvanometer for it to track the patterned-layers onto the powder-bed. This is achieved with RepliSLS3D, a freeware capable of controlling both the galvanometer and laser present in the printer. This software also allows the creation and editing of imported SLS files to analyze and modify the way the print is made by controlling, for example, scan-pattern, hatch spacing, and a multitude of other SLS parameters.

4.3.1.8 Beam Construct

To simplify single-line and simple-shape tests, Beam Construct was used as it provides tools for creating simple shapes and adjustment of scan speed, laser power, hatch spacing, and hatch pattern.

While technically marketed as a laser-marking or laser-engraving software, it is ideal for this specific project as each layer can be scanned independently with varying parameters if desired.

4.3.1.9 3D printed and Laser Cut Tools

Thanks to both Creo Parametric and the 3D printers available at ADDlab, it was possible to produce custom-made parts to improve the efficiency of the process and to allow for faster repeatability of tests. The following components were made with such tools.

The holders shown in Figure 22 allows for the insertion of a substrate and still have enough space for either 250, 500, or 1000µm of material to be deposited or pressed.

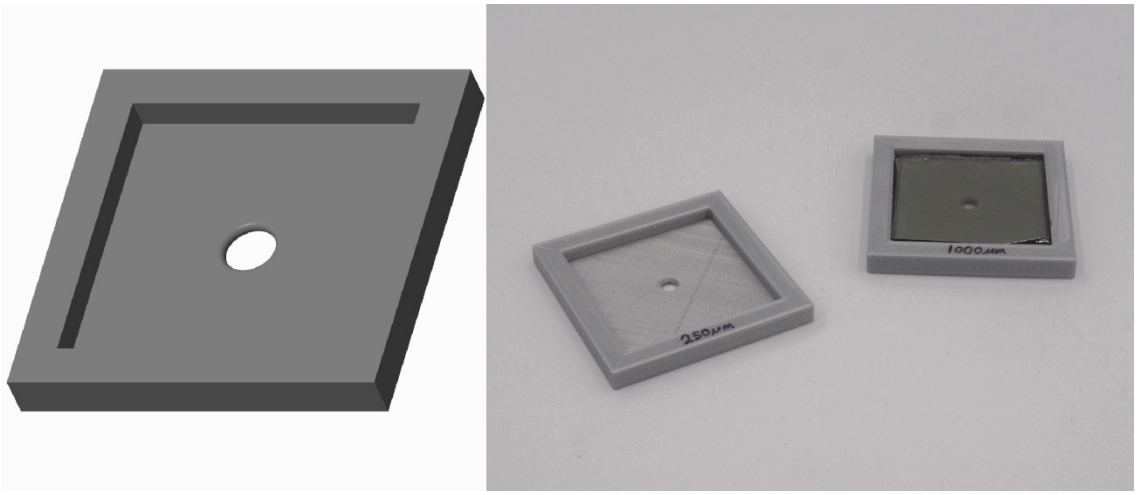

Figure 22: Sample holders and substrate placement

The holder shown in Figure 23 is designed to replace glass slides and be easily fitted onto the stage. This part also allows for light to pass through the substrate easily thanks to its minimal support structure.

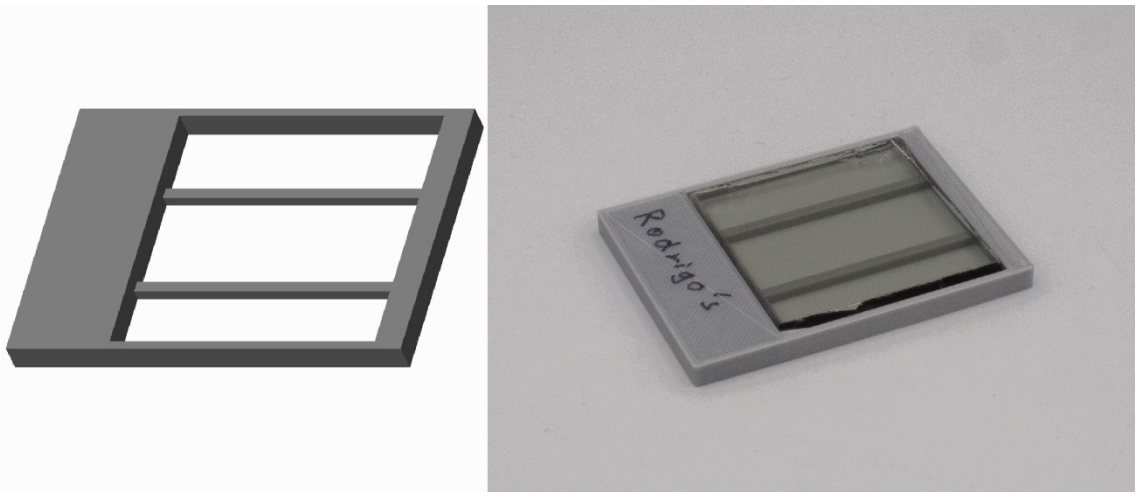

Figure 23: Platina replacement holder

The component in Figure 24 is a tool designed for pressing the powders tightly into the substrate holder to allow for testing printing with higher densities by pressing.

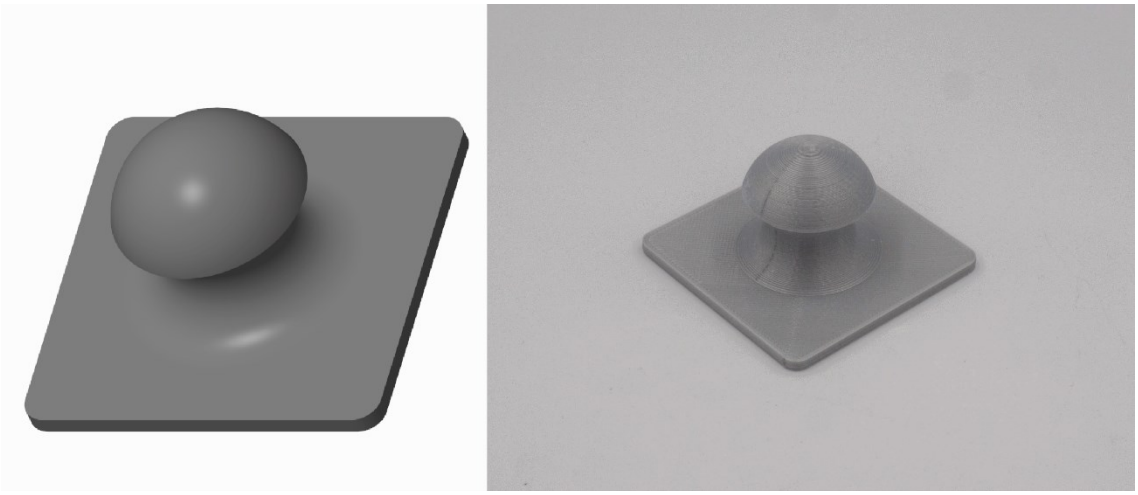

Figure 24: Pressing tool

Figure 25 displays a system to test printing of 3D cylinders in an automated fashion. Two iterations were made to include or exclude an aluminum rod in the central shaft.

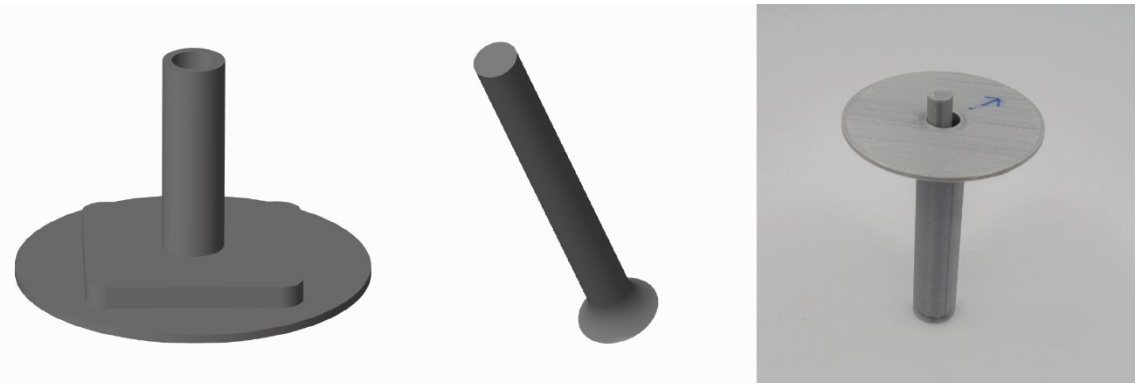

Figure 25: Cylinder holder

Figure 26 shows small 500µm thick rings made for testing of multi-layer pressed prints which would be added on top of each other to create a 10mm tall cylinder.

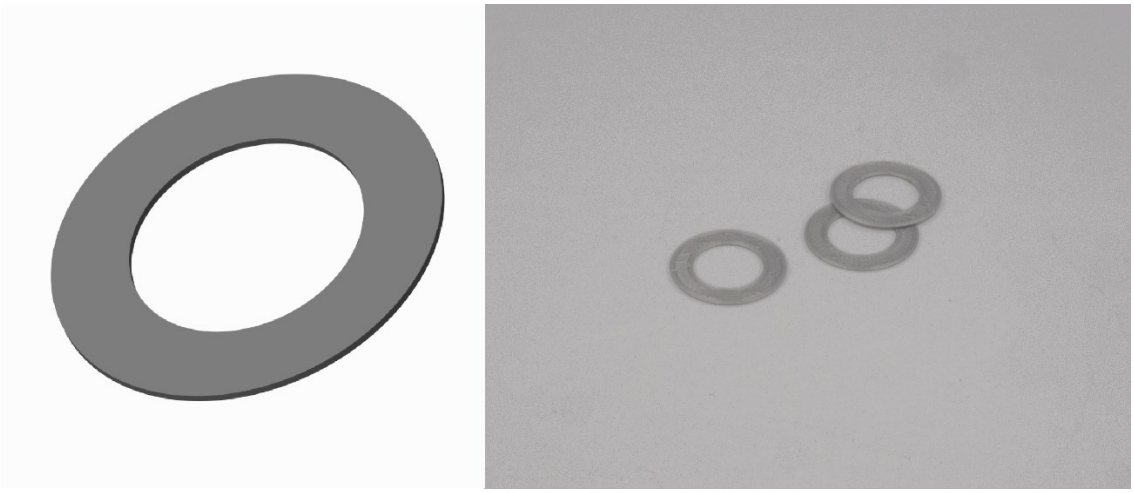

Figure 26: Rings

Figure 27 shows a laser-cut acrylic disc which serves the purpose of holding substrates vertically allowing the cross-sectional observation of print lines with a microscope.

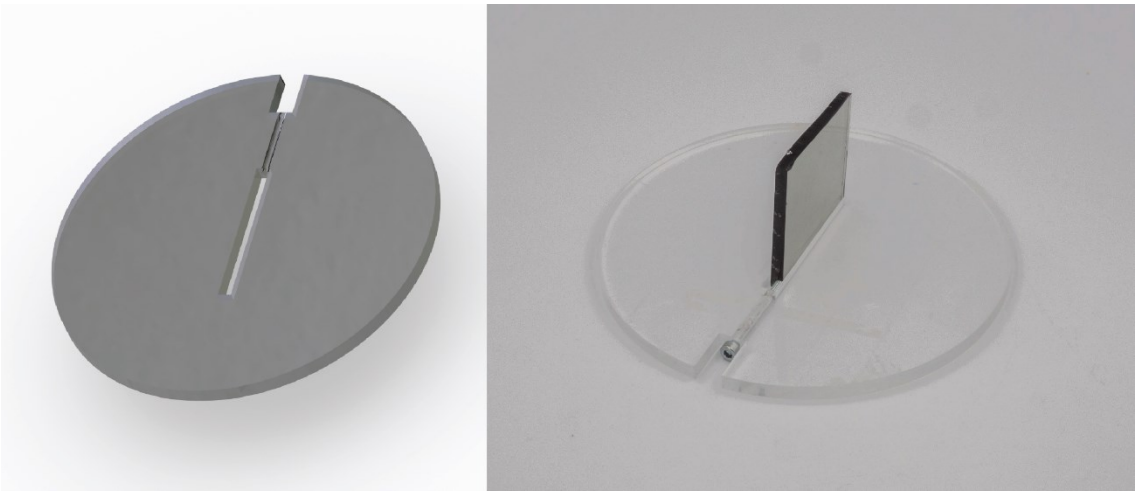

Figure 27: Vertical substrate holder

4.3.2 Energy Density

Energy density is theorized to be a parameter suitable for determining the sinter ability of powders. To test the correlation between energy-density and melt-uniformity, a grid such as the one showcased in Table 2 was made.

Table 2 Energy density at t=0.5mm and h=1mm: Horizontal axis - Power [W]; Vertical axis - Scanning Speed [mm/s]

	1	2	3	4	5	6	7	8	9	10	11	12
1	4.00	8.00	12.00	16.00	20.00	24.00	28.00	32.00	36.00	40.00	44.00	48.00
2	2.00	4.00	6.00	8.00	10.00	12.00	14.00	16.00	18.00	20.00	22.00	24.00
3	1.33	2.67	4.00	5.33	6.67	8.00	9.33	10.67	12.00	13.33	14.67	16.00
4	1.00	2.00	3.00	4.00	5.00	6.00	7.00	8.00	9.00	10.00	11.00	12.00
5	0.80	1.60	2.40	3.20	4.00	4.80	5.60	6.40	7.20	8.00	8.80	9.60
6	0.67	1.33	2.00	2.67	3.33	4.00	4.67	5.33	6.00	6.67	7.33	8.00
7	0.57	1.14	1.71	2.29	2.86	3.43	4.00	4.57	5.14	5.71	6.29	6.86
8	0.50	1.00	1.50	2.00	2.50	3.00	3.50	4.00	4.50	5.00	5.50	6.00
9	0.44	0.89	1.33	1.78	2.22	2.67	3.11	3.56	4.00	4.44	4.89	5.33
10	0.40	0.80	1.20	1.60	2.00	2.40	2.80	3.20	3.60	4.00	4.40	4.80
11	0.36	0.73	1.09	1.45	1.82	2.18	2.55	2.91	3.27	3.64	4.00	4.36
12	0.33	0.67	1.00	1.33	1.67	2.00	2.33	2.67	3.00	3.33	3.67	4.00

The values in this table follow the equation

$$E = \frac{P}{vht} \; where;$$

$$E = energy\ density \left[\frac{J}{mm^3}\right]$$

$$P = power\ [W]$$

$$V = scanning\ speed[\frac{mm}{s}]$$

$$h = hatch\ spacing[mm]$$

$$t = layer\ thickness[mm]$$

With $t = 1$ when printing single-line elements.

4.3.3 Evaporation Test

A simple mass comparison test will be performed wherein a substrate-holder assembly is filled with glass powders (similarly to how testing is done) and weighed pre and post printing. The weight of the holder, substrate, and excess material are then subtracted from the equation. Furthermore, to cope with possible human error, a circle with a diameter closer to the full side-length of the squared substrate will be printed.

4.3.4 Optical Properties

The last test will be for optical capabilities of the printed components.

To compare the transparency of the printed component when compared to traditionally manufactured Silica components, a transparency meter will be used. This device measures the ratio of light transmitted from one end to a receiving end; this is called transmittance and is measured as a percentage of light reaching the receiving end. If a material deflects light rays, they will not reach the receiving end, thus reducing the transparency of said material [49]. As can be expected, glasses have amongst the highest transmittance rates of all materials.

Testing this parameter will directly determine the feasibility of utilizing printed Silica components for applications such as optical lenses or eyeglass lenses.

Optically transparent, SLS printed glass components have not yet been successfully produced, therefore the closest reference is the powder-based binder-jetting experiment accomplished at KIT which achieved a maximum transmittance of 66% [19].

4.3.5 Three-Point Flexural Test

To have a quantifiable strength value which can directly be compared to traditionally manufactured components, a cylindrical rod will be printed which has the same dimensions of Quartz rods. Subsequently, a three-point flexural test will be conducted per the regulations of the ASTM C158 standard for “test methods for strength of glass by flexure”.

To run a three-point flexural test, a universal testing machine is equipped with two support pins or blades and one or two load pins as shown in Figure 28. The bottom pins serve the sole purpose of supporting the rod at an equal distance from the center. The top pin is

slowly lowered down onto the rod, exerting a constant, downwards force on the middle of the beam to allow it to deform. Meanwhile, the universal testing machine is recording the resistance curve to the force; upon failure, be it plastic deformation or cracking, the machine stops and outputs the values obtained at the last moment before failure.

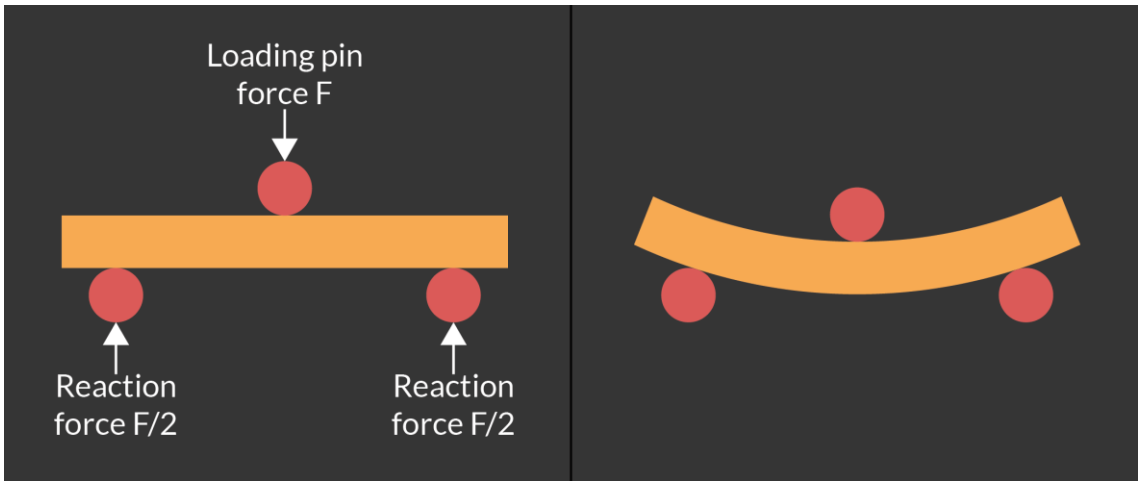

Figure 28: Flexural test diagram

The most relevant values obtained from the test are the flexural modulus and the modulus of rupture which indicate how well a material resists bending [50], and the maximum strain sustained by said material [51], respectively. This test however, is not flawless, as specific specimens might behave marginally different than others depending on their internal particle alignment and possible lattice-originating failure. For validation purposes, it is recommended to run the test multiple times on similar specimens to find a trend.

Fused silica has a flexural modulus of 71.2-74.8 GPa and a modulus of rupture of 198-218 MPa with a higher value meaning higher strength. For comparison, cast iron EN GJL 200 (commonly used for car engine blocks and break disks) has a flexural modulus of 103-120 GPa and modulus of rupture of 150-170 MPa [48].

5 Results

This section presents the findings of the experimentation process and the steps followed beginning with the material selection process until the final testing of printed components. Likewise, the obtained values, will be represented and any relevant graphics will be displayed to facilitate the comprehension of a concept or to visually prove the experimental results.

5.1 Material Selection

As the title suggests, and as has been repeatedly mentioned throughout this paper, the material group chosen is silica. A material comparison preceding the actual creation of this thesis was performed and its results are as follows.

By generating a material property chart with glass temperature and thermal expansion coefficient as X and Y axes, respectively (Figure 29), silica glasses have the lowest thermal expansion coefficient amongst all non-ceramic glasses (except for titanium silicate). Furthermore, no glass material has a large enough glass point which the SLS machine cannot reach, thus making the glass temperature parameter irrelevant (it is necessary to mention that, initially, borosilicate 7740 powders were chosen thanks to their having a lower glass point than silicates however, no powders were readily available, making it necessary to grind them from existing borosilicate instrumentation. This proved to be impossible given the lack of hard milling balls and jars or other grinding equipment).

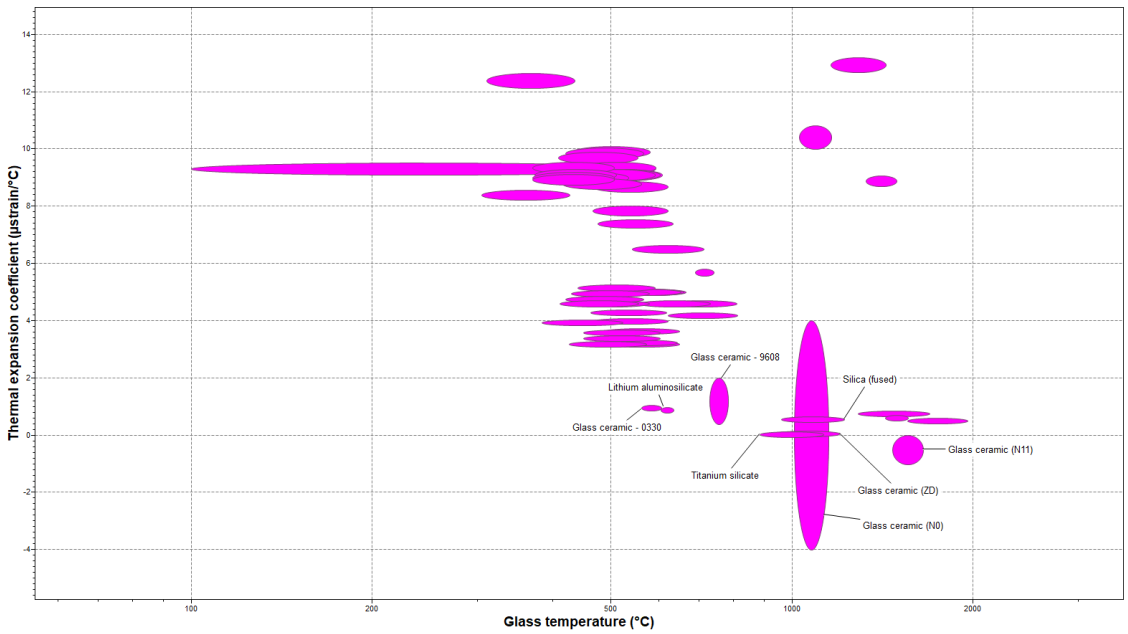

Figure 29: CES EduPack chart comparing Glass Temperature and Thermal Expansion Coefficient of glass materials

Next, to choose between titanium silicate and silica, their hardness was assessed where it was decided that silica would be better given its nearly fivefold harder surface (Figure 30).

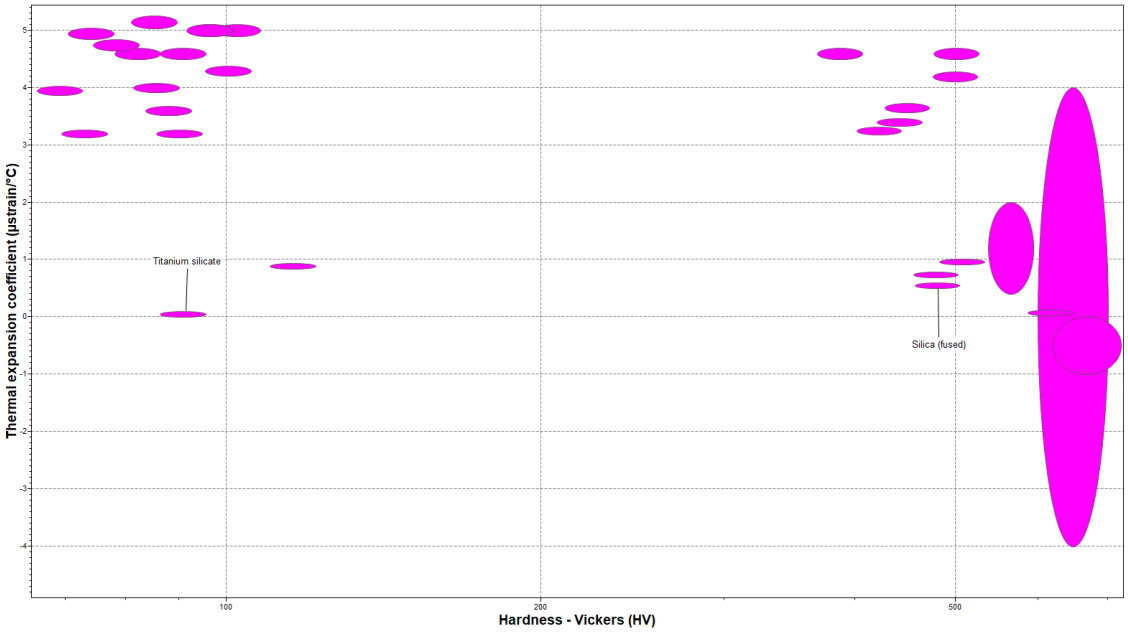

Figure 30: CES EduPack chart comparing Hardness and Thermal Expansion Coefficient of glass materials

Finally, powders both in the nanometric and micrometric scale were readily available from the Chemical Engineering department at Aalto University, so both were tested to determine a possible lower limit for particle size distribution. The following materials, all provided by Evonik®, were available:

Name	**Particle Size** $(\boldsymbol{D_{50}})$	**Density** $(\boldsymbol{g/cm^3})$	**Tapped Density** $(\frac{\boldsymbol{g}}{\boldsymbol{l}})$
Sipernat D 17	10µm	2	150
Aerosil 380	7 nanometers	2.2	50
Aerosil R 104	50 nanometers	2	50
Aerosil R 816	12 nanometers	2.1	60
Aerosil R 972	16 nanometers	2.2	50

When using such small powders, it is necessary to consider the flowability of the powders to prevent them from sticking onto the blade by agglomeration. This is measured by the Hausner Ratio which is utilized as a means of defining the flowability of solid granules of material if their bulk density (density of the material itself) and subsequent tapped density (density of a volume of material which is influenced by particle shape, particle size, and density of the material.) are known. It can be calculated from the following formula:

$$H_R = \rho_t/\rho_b \text{ where:}$$

H_R is the Hausner Ratio;

ρ_t is the tapped density, and;

ρ_b is the bulk density [52].

According to Carr [53], a Hausner Ratio up to 1.11 gives for excellent flowability; in the case of the available Evonik powders, the highest Hausner Ratio value is that of the

Sipernat D17 powder at 0.075, meaning that all available powders have excellent flowability.

Given its larger tapped density, Sipernat D17was chosen. This powder is a precipitated silica powder which is milled to obtain a mean D_{50} particle size distribution of 10μm, which is within the suggested range.

5.2 Single-Layer Samples

To have a direct comparison with the results achieved by most other referenced authors in order to prove or disprove the hypothesis that powders in the range of 2-20μm will give the highest density, similar tests were performed which will help standardize the procedure by having direct comparisons of results.

Multiple parameter combinations were tested to find the ideal printer settings to achieve a higher density and increased bonding, and to attempt to find a correlation between energy density and the aforementioned properties. This test was initially done with straight single lines which were analyzed under a microscope. Once suitable or optimal parameters were found, they were used to print circles which require more than one line to be printed. This second test is necessary to find the ideal parameters for hatch-spacing and line-count.

Finally, an attempt to print a cylindrical rod was made using all the optimal parameters found.

5.2.1 Straight Line

To follow the trend set by previous researchers (mainly Khmyrov [24]), a glass substrate was utilized upon which single, straight lines were printed. These lines are subsequently analyzed cross-sectionally and from the top to establish their shape, evaporation mechanics, and adhesion to the substrate.

The relevance of this test lies in pinpointing the absolute ranges in which sintering and viscous flow take place to generate better quality layers for further tests.

5.2.1.1 Procedure

Given the lack of knowledge regarding the ideal parameters to use for these specific powders, it was necessary to pinpoint the range within which they can be printed. This began as a simple experiment to narrow-down the distribution to a functional range with tests between 1 and 100 watts and scanning speed between 1 and 250 mm/s.

The first tests consisted of the powders resting on an acrylic bed without any tapping. A sample set of 16 parameter combinations was utilized to determine a suitable set for un-tapped powders with a nominal layer thickness of 5mm. The powers 1, 5, 10, and 15 watts were combined with the speeds 1, 5, 10, and 15 mm/s, out of which only the combinations 1w – 1mm/s and 5w – 5mm/s did not result in a single ball. This indicated that lower powers were necessary.

Furthermore, all the components printed with these settings resulted in large voids surrounding the sintered fragments which can be attributed to evaporation losses and a very low density (air-to-glass powder ratio). The latter was tested simply by tapping of the powders onto a substrate with a fixed layer-height as seen later in Figure 32 to increase the density by packing, which immediately saw an improvement in ablation reduction. This caused a shift of focus for tests to tapped layers only.

To automate this process, a pattern was made with Beam Construct which allows for multiple different parameters to be tested at once (Figure 31). The pattern was etched counter-clockwise beginning in the top-left gradient and allowed for testing of three times as many parameter combinations as before. The reasoning behind the outwards-facing pattern is to allow for analysis of the cross-section of the print components with a microscope.

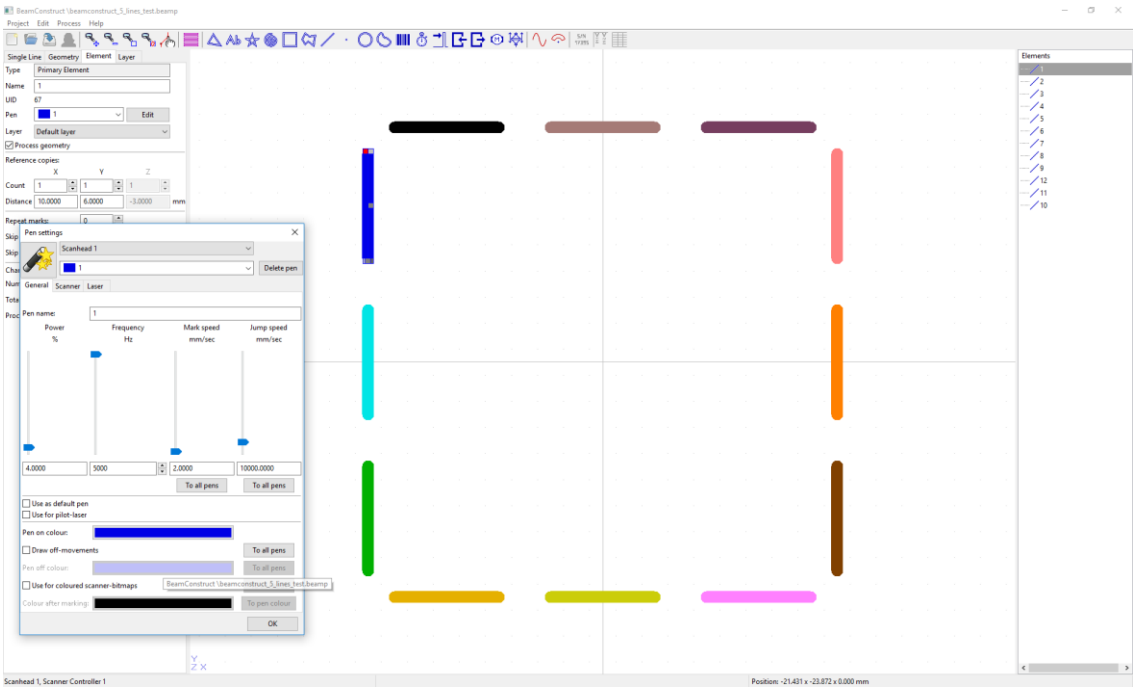

Figure 31: Beam Construct first sample

Tapped layers were set at a fixed layer-height of 500µm. To keep this constant, a squared perimeter was taped with multiple layers of masking-tape until the desired height was achieved and new tests patterns were devised to be printed on the substrate as shown in Figure 32. The red numbers, in this specific test, indicate the scanning speed and the blue ones indicate the laser power.

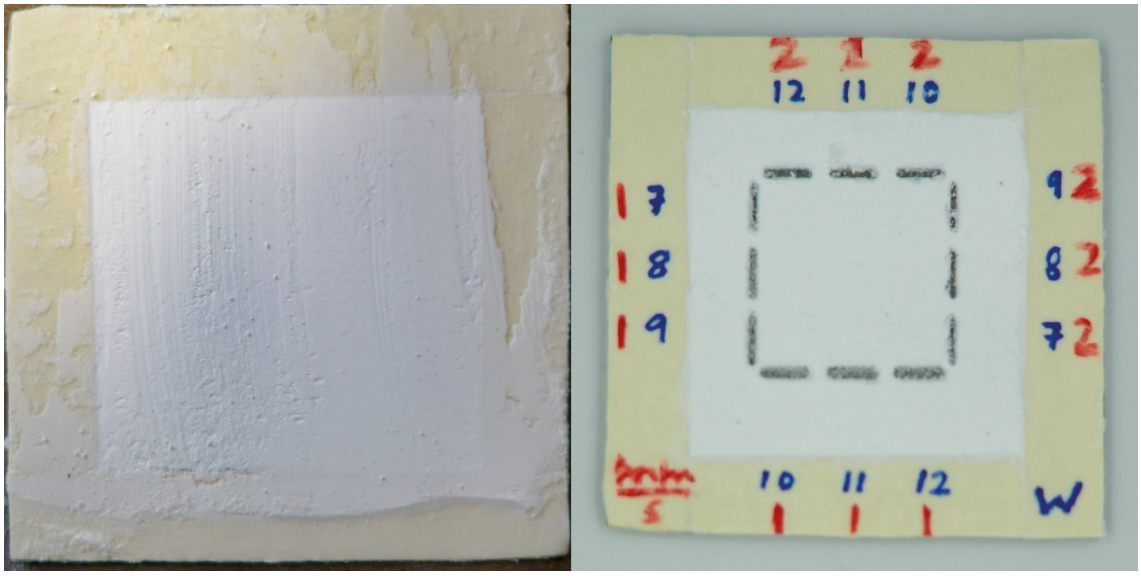

Figure 32: Left: Tapped/pressed powders on a substrate. Right: scanning-speed and power markings added

This however, also proved to be inefficient considering the large amount of parameter combinations estimated to be tested, thus the 3D printed holders mentioned in section 4.2.1.9 were introduced which allowed faster changing of substrates and all subsequent tests utilized a new pattern (Figure 33) which maximizes the line-count. This allows testing 21 combinations at once.

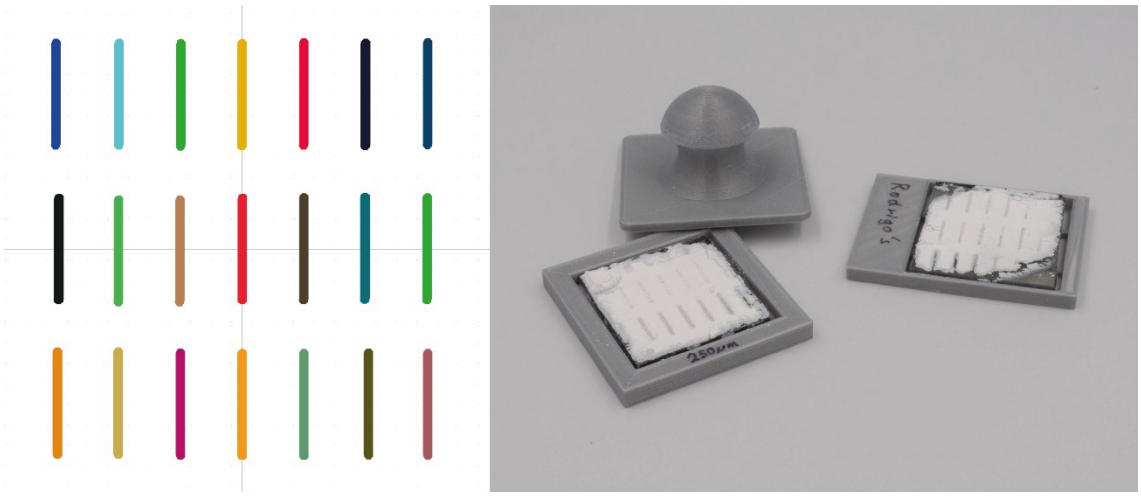

Figure 33: Single-line pattern and print samples

Furthermore, due to insufficient and irregular cooling between the molten pool of glass powders and the incident laser softening of the substrate, print-samples did not adhere to

the substrate efficiently (Figure 34) yet were showing promising results when observed from the top, thus all further single-line examinations were performed from the top.

Figure 34: Elevated end of a single-line with a 5x magnification lens

For samples with a layer height of 250µm, ablation was large enough to prevent the proper uniform melting of powders. Furthermore, powder deposition and pressing were complicated given the electrostatic forces present between the materials.

In the case of 1000µm-layers, the thickness was too large for the prints to adhere to the substrate at lower powers and using higher powers created thick, inconsistent print lines due to the temperature gradient of the laser beam. Therefore, all further samples were printed with a 500µm layer height.

The following tables enlist the parameter combinations tested which yielded partial or continuous print lines at different layer thicknesses.

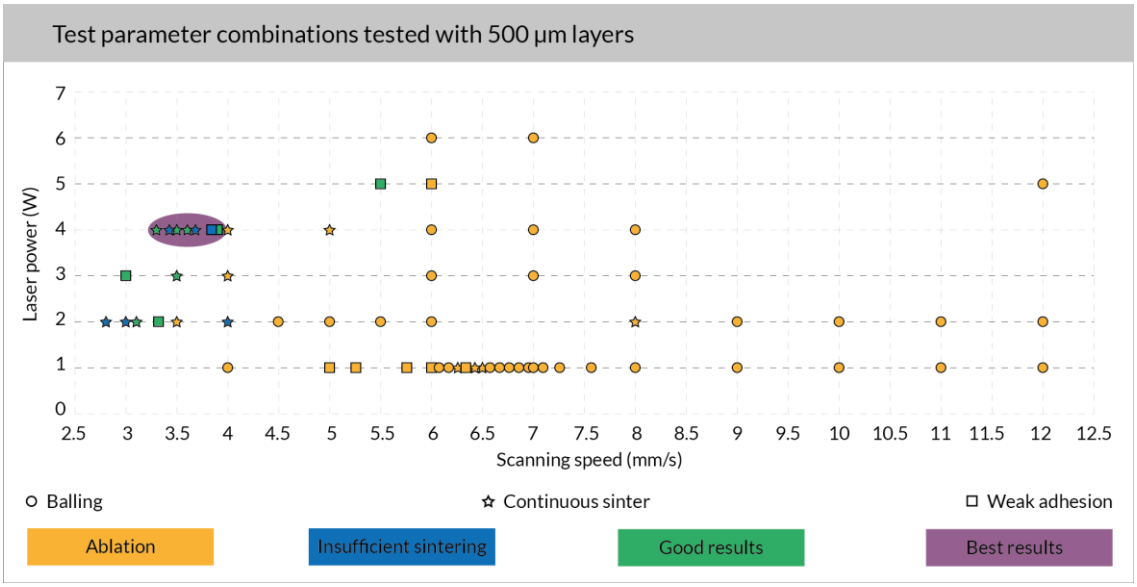

Figure 35: Tested parameter combinations for single-line patterns

Despite being suggested by previous research and extensively tested, the best results did not originate with the lowest scan speed or power. The most promising range took place with 4W at speeds between 3.3 and 3.7, peaking at 3.5. It is necessary to mention that more parameters than listed in Figure 35 were tested, yet only the ones which yielded suitable results are shown.

Furthermore, while energy density did present a trend, it cannot be reliably used to define the sintering capabilities since good results were obtained with both lower and energy densities, as well as bad results.

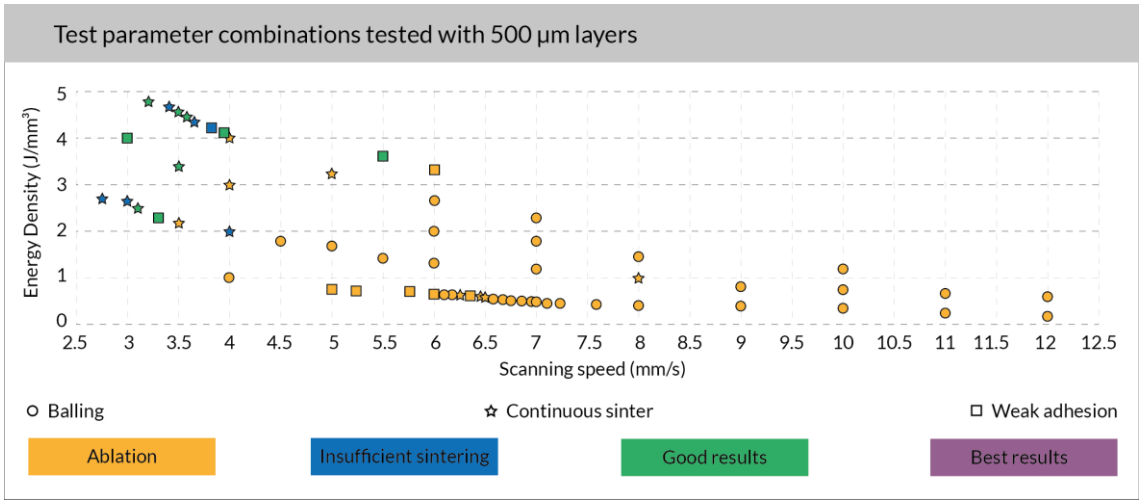

Figure 36: Energy density values at tested speeds

Examples of the phenomena taking place during the sintering process can be better appreciated form Figure 37. All sampled images are results of the experimentation process.

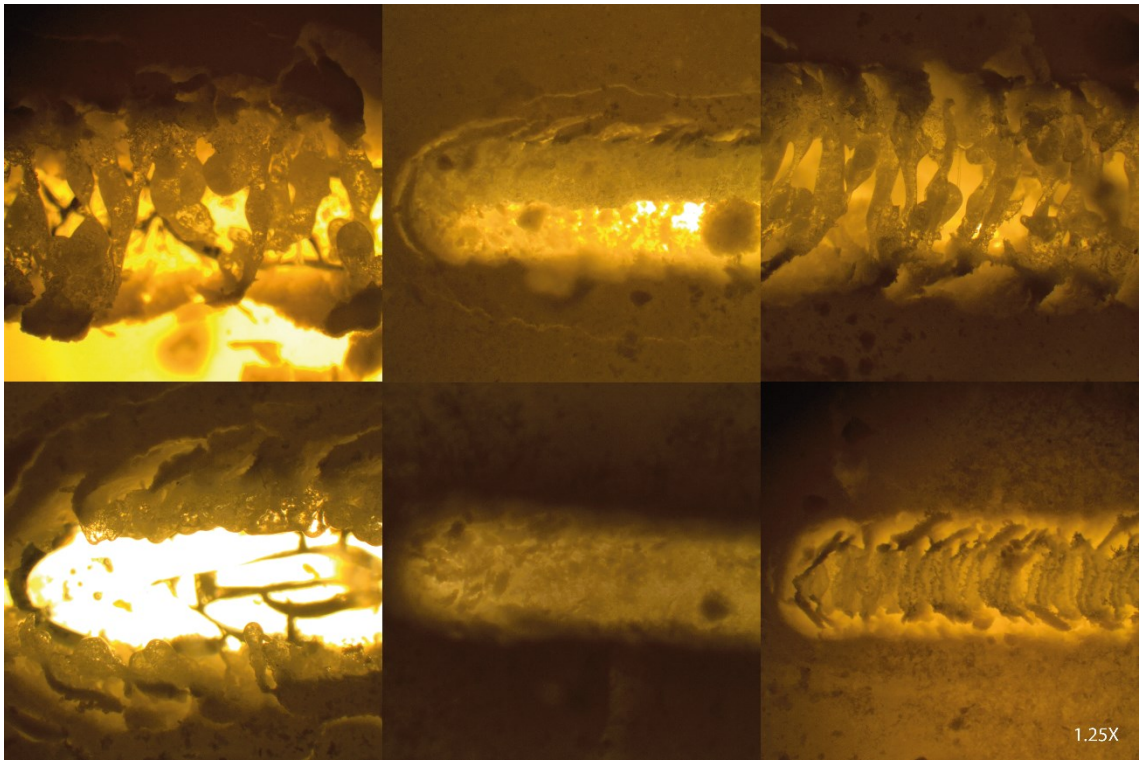

Figure 37: Top left - balling; top center - continuous sinter; top right - weak adhesion; bottom left - ablation; bottom center - insufficient sintering; bottom right - good results

Lastly, no relation could be made between energy density and print quality; similar energy densities were tested under different parameter combinations and did not yield similar results.

5.2.2 Circle

Having found an optimal set of parameters for straight lines, a new test was executed which consisted of filled circles using mainly, while not exclusively, the optimal parameters found before. It is necessary to first attempt printing a single layer of the desired 3D shape before attempting to print the full component given variability when changing shape and/or hatch spacing considerations which need to be considered which were not present before.

5.2.2.1 Procedure

To maximize efficiency, once again, a pattern with multiple circles was designed which allows for gradients to affect the surrounding area of the shape without affecting other nearby ones. This can be better understood from Figure 38.

Figure 38: Circular samples on a grid

Initial tests consisted of each circle having the same power and scanning speed parameters but with different hatch spacing and line-count settings, the best of which consisted of 0.5mm hatch spacing and 7 lines (default hatch spacing setting).

Having found the optimal hatch spacing parameters, the values obtained from the single-line experiment were put to test and the most relevant results are shown in Figure 39.

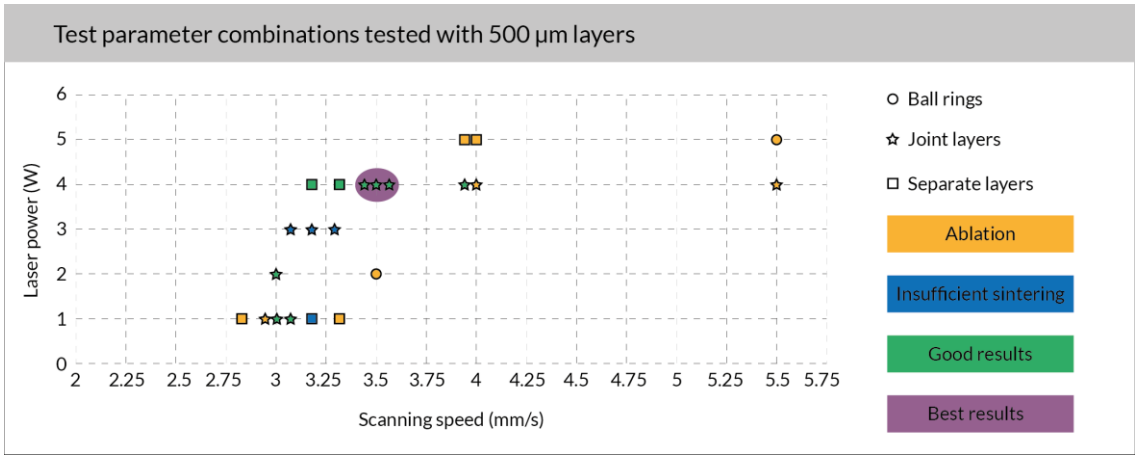

Figure 39: Tested parameter combinations for circle patterns

As was expected, the optimal results were obtained using the best results from the single-line scan tests. These samples had all concentric rings sintered together and had a more even distribution throughout the circle. On the other hand, no sample managed to print fully molten circles since, as previously mentioned, they all consisted of concentric rings. Furthermore, they all had residual powder attached to the surfaces if not fully sintered or presented themselves as fully sintered rings with large ablation between them.

Similarly to the single-line tests, energy density proved to be unreliable for parameter selection.

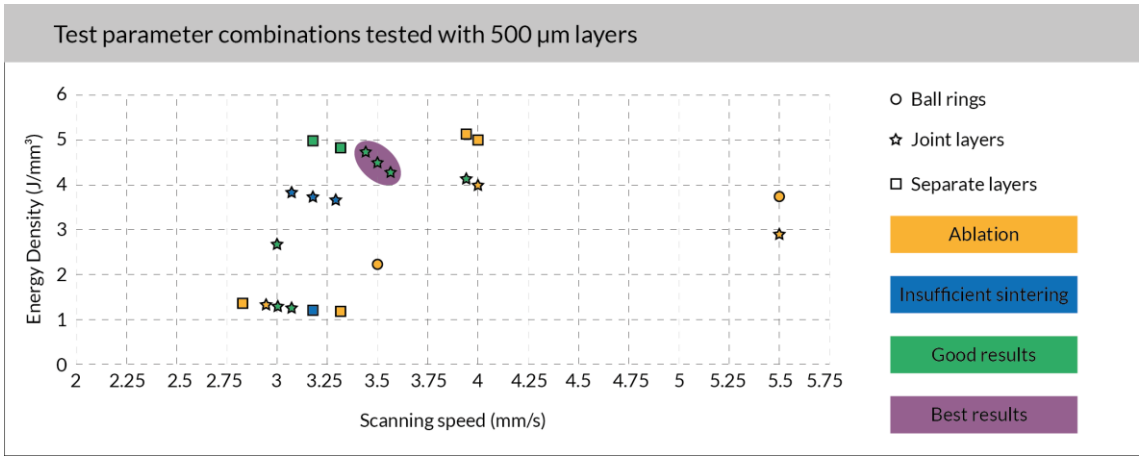

Figure 40: Energy density values for circles at tested speeds.

Examples of these samples can be appreciated from Figure 41.

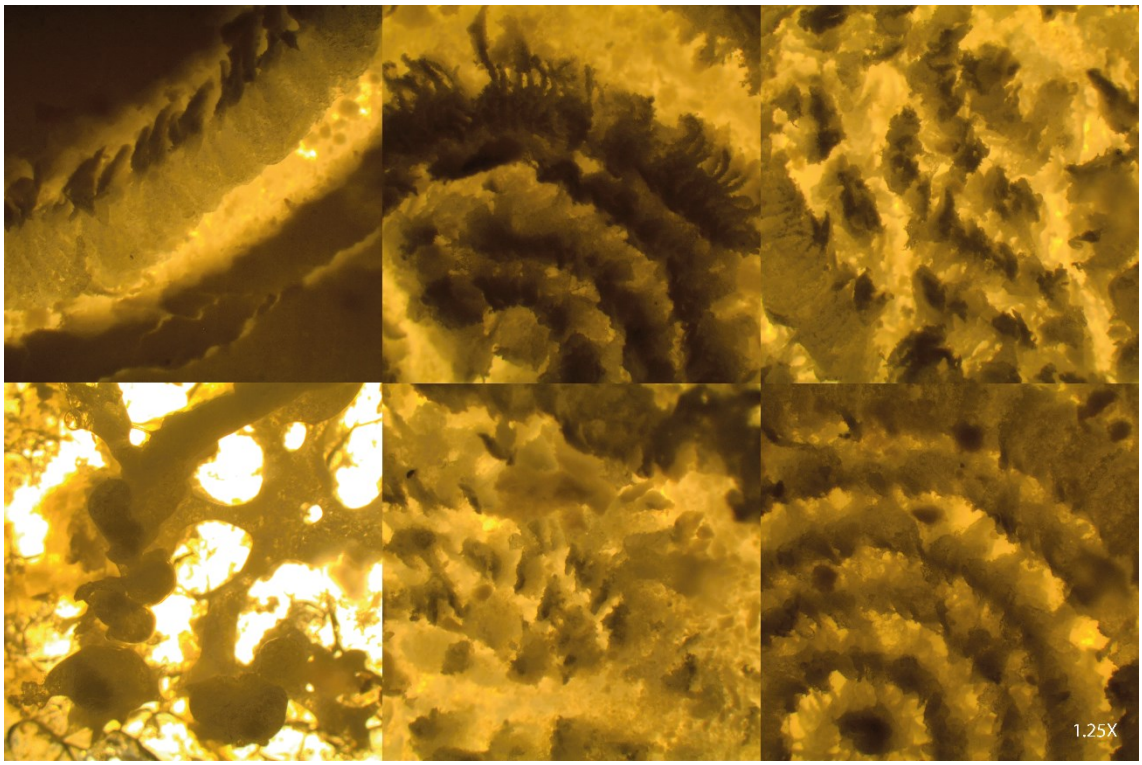

Figure 41: Top left - ball rings; top center - joint layers; top right - separate layers; bottom left - ablation; bottom center - insufficient sintering; bottom right - good results

5.3 Multi-Layer Samples

Initially, the rings pictured in Figure 26 were tapped, printed, and placed under subsequent rings which would act as holders for the next layers. This however, was rapidly discarded since curling and vertical displacement of molten powders made mounting on top of each other impossible (Figure 42).

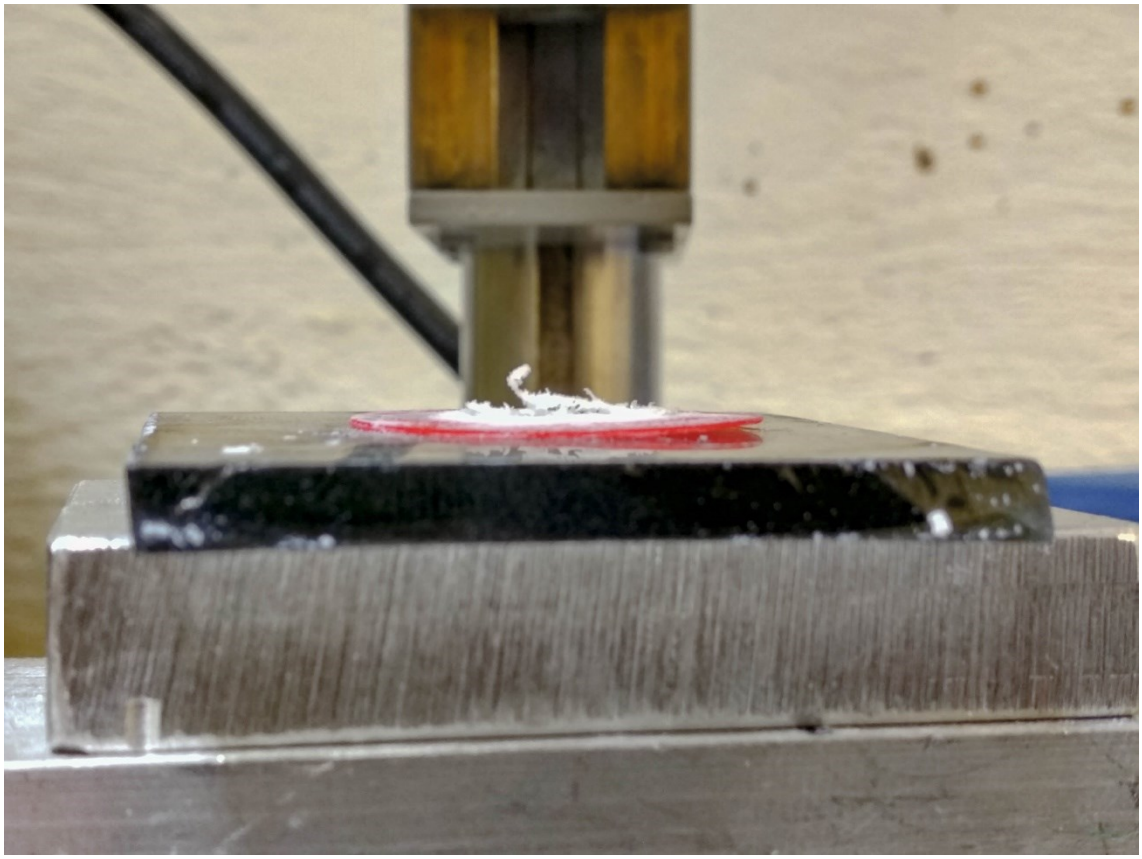

Figure 42: Vertical displacement or molten powders

Given the machine's large print area of 300x300mm, it was necessary to accommodate a smaller print-bed to reduce the material needs; this was achieved with a 3D printed platform with a smaller movable bed (Figure 43). While it was possible to continue testing with the previous set-up, the minuscule diameter of the cylinder required higher precision, and minimal deviation would not allow for printing of subsequent layers directly on top of each other. This, therefore, required a new system to be adapted to the existing machine which would take advantage of the automated bed-movement while still allowing for pressing of each layer.

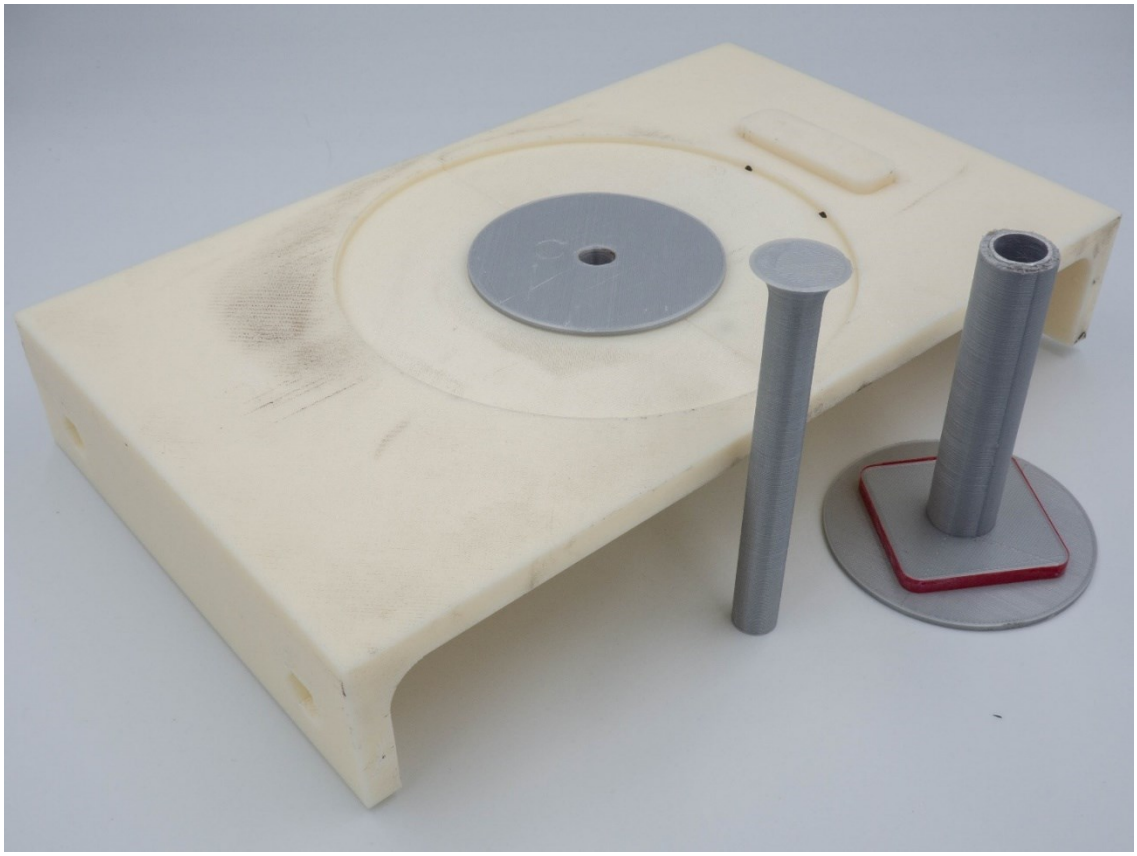

Figure 43: Print-bed size reducer with cylinder holders

The last test consisted of layers printed with the optimal settings followed by the manual addition and pressing of material for each subsequent layer until a full 3D printed rod was obtained. The model used for this process was processed with RepliSLS 3D and can be seen in Figure 44. It consists of a simple, standard rod.

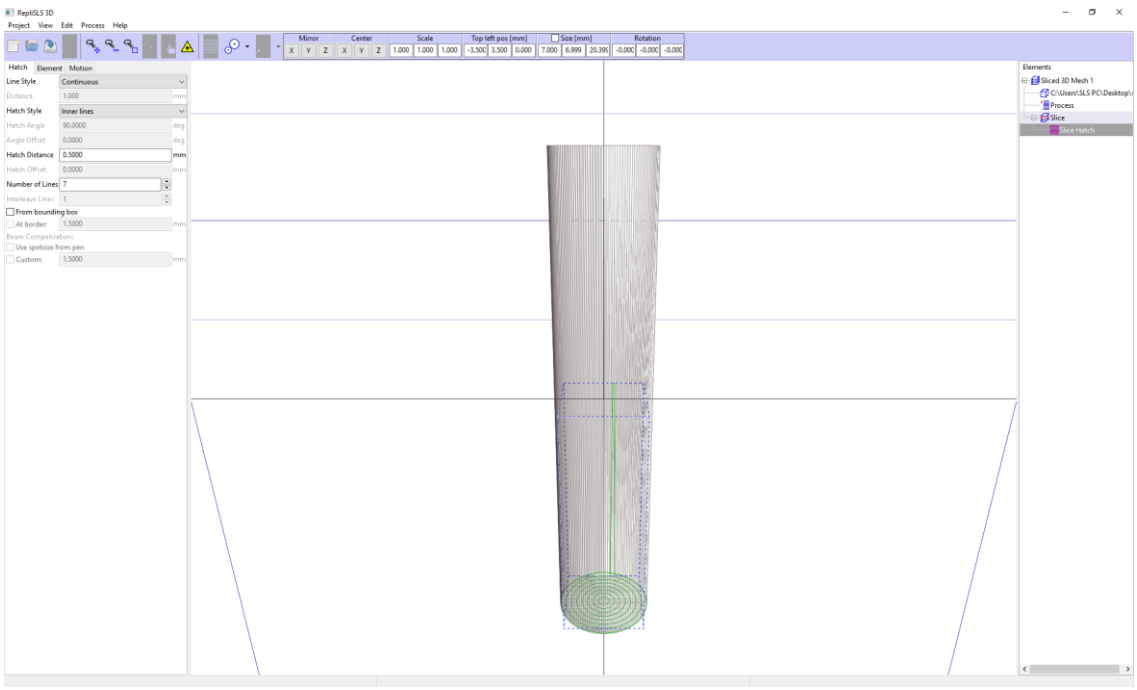

Figure 44: RepliSLS 3D interface with a cylindrical rod model loaded

Initial tests proved to be a failure with each subsequent layer experiencing extensive balling. Furthermore, printed layers were very brittle and would therefore break apart when pressing the subsequent layer. This led to testing with non-pressed layering once again. This test was conducted using the automated layer-depositing blade however, once again, this test failed as the powders agglomerated on the blade, probably due to electrostatic forces being generated due to friction between the powders, steel blade, and plastic bed. Finally, an aluminum rod was introduced into the cylindrical support as an attempt to reduce the electrostatic forces built-up within the rod however, this failed to improve the circumstances since electrostatic buildup took place before reaching the cylinder, thus retiring the testing of printing 3-dimensional structures.

5.4 Evaporation Test

The evaporation test was conducted using the same substrate arrangement used for ring, multi-layer print testing. Comparing the weight of 4 samples before and after the process proved that an average 11.039% of material evaporated during the process. This proves that evaporation losses need be considered when estimating the density of printed glass materials, yet do not represent such a marginal loss as has been predicted.

6 Discussion and Conclusions

The main purpose of this thesis was to test multiple hypotheses surrounding the concept of SLS or SLM printing of glass powders without any added substances, the most relevant of which are the possibility of achieving fully-dense prints by using powders in the range of 2-20μm and the possibility to increase the powder density by tapping or pressing each layer together. Likewise, yet to a lesser degree, the feasibility of using energy density as a parameter to define a linear set of parameters suitable for printing, was tested and further analyzed. The goal was to achieve optically-transparent components which require little-to-none post-processing for the manufacture of optical glass components.

Silica glass was selected as the material most suitable for these tests given its low thermal expansion coefficient which, in theory, should prevent cracks from happening when cooling. This material is also amongst the hardest of glasses, thus allowing a larger range of possible uses in various industries which require resistant materials. The selection process was lengthy and intricate which serves the purpose of validation of material choices.

This final chapter delves deeper into the mechanisms involved in the success or failure of the multiple tests undertaken by the samples and attempts to give a comprehensive explanation as to why these took place and how they can possibly be improved upon or fixed, in the case of failure, for future development of the field.

AM, contrary to common belief, is not a new technology, but has been under development for decades with large success in specific markets. While it is not fail-proof and mostly unsuitable for mass production, it is one of the most powerful tools available for fast-prototyping and as such has been implemented in various industries and by many mechanical designers. By tracing its development back to its recent wide-spread use and mass media-coverage, it can be understood that use-cases have been evolving and different materials and processes have been developed to enable its expansion into new markets. Perhaps the most relevant development in the field, considering the extensive use for modern prototyping industries, is that of consumer or prosumer-focused machines such as the Ultimaker line used for this specific thesis. These consumer products are inexpensive, thus allowing for a larger market-reach.

While many technologies, such as stereolithography and fused deposition modeling, have amassed the largest share of users in the consumer level, they have strong limitations and do not easily allow for printing of components without the need for support material. This is relevant because 3D printing should be a tool to enable either fast-prototyping or production of complicated shapes with a high-degree of precision; said precision cannot be accomplished when support structures are embedded within concentric components or leave traces of imperfections on the surface of components. Furthermore, selective laser sintering or melting technologies have what is perhaps the widest range of material capabilities and are easily adaptable for testing of new powdered materials. Similarly, binder jetting technologies allow for the experimental testing of new materials and composites more easily yet, unlike SLS and SLM, they require post processing if a binder material, different to the material to be bound, is used.

When utilizing AM technologies, it is of utmost importance to have a clear understanding of the capabilities and limitations of the technologies, as well as having a decent level of expertise in the creating CAD models for printing. While it holds true that these technologies aim to empower creators to easily create prototypes, a certain degree of knowledge is necessary. Many consumer-lever printer mistakes can be attributed to human error due to a lack of understanding of the limitations and/or the parameters available for printing. Likewise, it is necessary to comprehend the time-constraints one is faced with when using these technologies; while prototyping can potentially save time when compared to traditional methods for functional prototypes, visual prototypes can take longer than their traditionally-manufactured counterparts (a simple analogy can be made to grips of power tools modeled with modeling-foam vs 3D printing).

The field of glass AM is largely unexplored and mostly unsuccessful. While it has been researched for decades, it has not been so extensively. There have been two main successes in recent history in the field, they do not overcome all the limitations which have hindered the development of the field. One of them, which focuses on FDM of molten glass through a perforated kiln and deposited onto a moving bed, is victim of the main culprit of FDM technologies which is a need for support structures; if we think of the material used as the molten glass liquid it is, it becomes brittle when hardened, thus making it impossible for structure material to be removed. The second one, which

managed to overcome this problem, uses binder-jetting technologies to hold glass powders together with resins which need to be molten-away post-process; this, again, does not overcome one of the main hindrances of glass AM.

In the case of SLS or SLM of glass powders, perhaps the most promising results are those of Khmyrov who managed to print crack-free line-samples of quartz silica glass, or of Fateri who managed to print dimensionally-accurate samples. These two combined should give a promising future for the field of glass AM, yet they are not without caveats. In the case of Khmyrov, the samples are single-line prints which experience warping and evaporation losses, both causing considerable deformation of the component. Fateri's research, on the other hand, produced samples which were not optically transparent; while an attempt to improve on this with post-process re-melting proved helpful, they do not achieve the degree of transparency that is necessary for optical purposes.

The purpose of this thesis was to present the findings of experimentation processes performed on AM of glass powders using SLS or SLM technologies. The goal was to succeed where others have failed by creating optically transparent components with a higher-density and low balling or porosity. These phenomena affect the final quality of the print by making it opaque and structurally weak. The attempt was mainly guided by the hypotheses pondered by other authors claiming that powders with a particle size-distribution in the range of 2-20μm would effectively reduce balling phenomena present in particles with larger sizes while reducing ablation cause from the lower-density of smaller particles. Furthermore, pressing was tested to increase the density of each layer while decreasing the light transmission from the laser to previous underlying layers. To a lesser degree, other hypotheses, such as the possibility of utilizing energy density as a guide parameter for print quality, and the main causes of ablation, were examined.

Upon testing, multiple problems arose which made further research impossible however, hypotheses were tested, which could aid future research. The best sample produced can be seen from Figure 45.

Figure 45: Best sample produced

Testing a wide range of parameter combinations for single line scans was necessary to test the theory that particles with a D_{50} size of 10µm did not significantly improve on the results obtained with larger samples. While this does not mean that particles with a size in the range of 2-20µm are not an improvement, it does mean that size is not directly linked to the rate of success in printing components without porosity; it can be speculated form the results obtained and the phenomena observed, that the density of powders is of more relevance than any other parameter. The powders used for this experiment have a marginally-lower density than rods produced with the same material, thus intrinsically having air gaps in between particles which increase porosity. Furthermore, it is theorized that using smaller particles improves the flowability of the molten track, allowing to better wet the surface in an even manner, yet this was also not proven to be true since wetting was weak, and balling happened in each test however, to a lesser degree.

Energy density did not show a linear curve which would prove its relation to transition temperature yet, this assumption needs further testing as the energy density values used

in this experiment are marginally lower than standard in its category and testing with different machines would improve the reliability of this assumption.

It was observed during the tapping process that electrostatic forces tend to displace the tapped powders when sintered since the compression forces are released. Not only does this cause spattering but it also causes non-uniform melting gradients and patterns throughout the process thus limiting the dimensional-accuracy of prints. This force also made powders impossible to deposit onto the substrate with layer thicknesses smaller than 2000μm or tapped layer thicknesses smaller than 250μm. It is recommended to utilize a deionizing device to get rid of these unwanted effects.

Ablation caused by evaporation was proven to be true; by melting a specific area on a substrate and comparing the weight of the sample before and after the process, it was concluded that evaporation does remove a portion of material from the substrate, thus creating empty voids on the print area which will later be filled by subsequent layers being deposited and leading to failed prints. This loss however, is proportionally small compared to the density of the pool before processing.

Analysis of the samples which produce solid particles, mainly balls, showed micro-bubbles trapped within them (Figure 46). This held true for all different parameters tested which indicated that re-melting the prints in a kiln is necessary if optic-grade prints are desired.

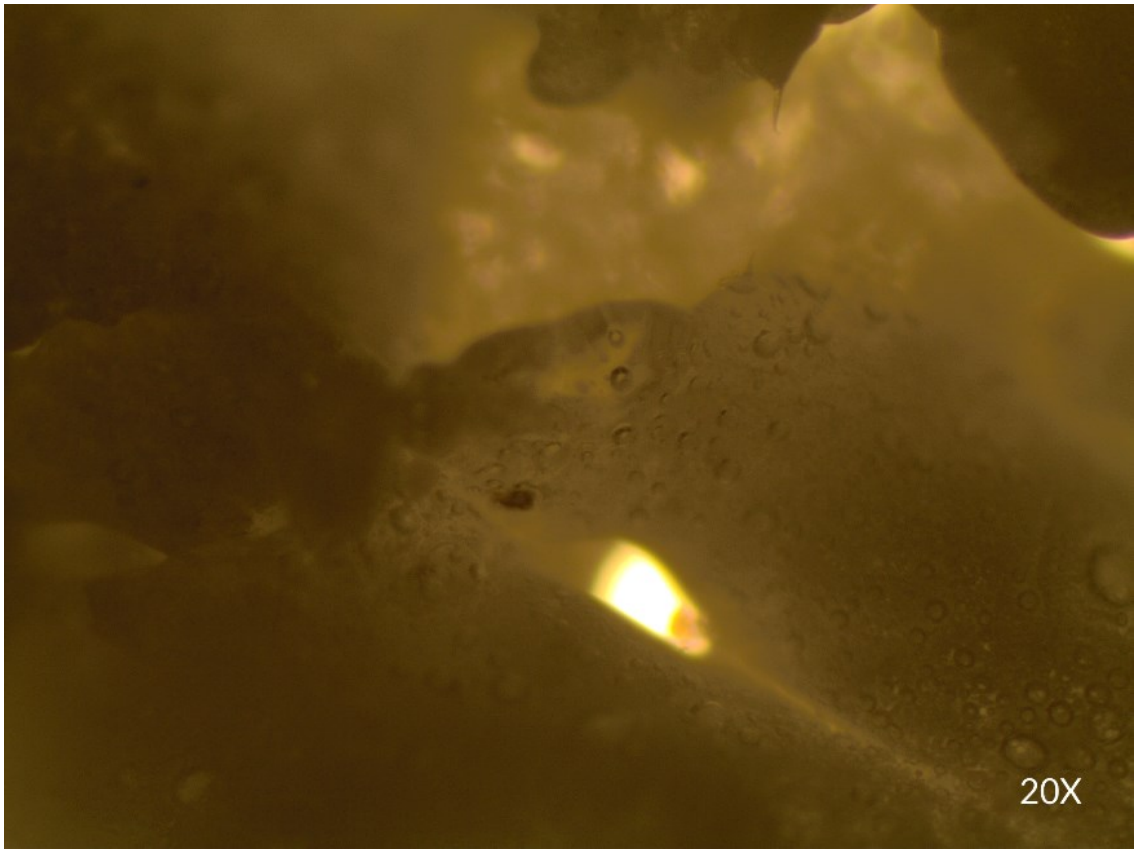

Figure 46: Micro-pores and micro-bubbles present in a sintered glass ball

7 Bibliography

1. Redwood B, Schöffer F, Garret B. The 3D Printing Handbook: Technologies, design and applications. Amsterdam: 3D Hubs; 2017. 289 p.

2. Gebhardt A, Hötter J-S. Additive Manufacturing: 3D Printing for Prototyping and Manufacturing. Hanser. Cincinnati; 2016. 591 p.

3. Gibson I, Rosen DW, Stucker B. Additive manufacturing technologies. Illustrate. Vasa. Springer International Publishing; 2010. 484 p.

4. Womack JP, Jones DT, Roos D. The machine that changed the world. Bus Horiz. 1992;35(3):81–2.

5. PCDN. Procurement and Supply Management Course [Internet]. 2018 [cited 2018 May 5]. Available from: https://pcdnetwork.org/event/procurement-and-supply-chain-management-course-3/

6. Ferdinand J. The Decentralized and Networked Future of Value Creation. 2016.

7. Gornet T. History of Additive Manufacturing. 2014;1–24. Available from: http://services.igi-global.com/resolvedoi/resolve.aspx?doi=10.4018/978-1-5225-2289-8.ch001

8. Boothroyd G. Product design for manufacture and assembly. Comput Des. 1994;26(7):505–20.

9. What is the influence of infill %, layer height and infill pattern on my 3D prints? [Internet]. 2015 [cited 2018 Nov 6]. Available from: http://my3dmatter.com/influence-infill-layer-height-pattern/

10. Iso S. Additive manufacturing . General principles . Terminology (ISO / ASTM 52900 : 2015) Tämä standardi sisältää eurooppalaisen standardin. 2017;

11. ASTM International. F2792-12a - Standard Terminology for Additive Manufacturing Technologies. Rapid Manuf Assoc. 2013;10–2.

12. Koch M. 3D printing: The Revolution in Personalized Manufacturing. Minneapolis: Lerner Publishing Group; 2018. 113 p.

13. IUPAC. Compendium of Chemical Terminology. Gold Book. 2014. 1670 p.

14. Hashmi S. Comprehensive Materials Processing. Vol. 1, Comprehensive Materials Processing. 2014. 1-52 p.

15. Ultimaker 3 Gyro timelapse - Dual extrusion with water-soluble PVA support [Internet]. Ultimaker; 2016 [cited 2018 Apr 12]. Available from: https://www.youtube.com/watch?v=oeJLLC2NJQs

16. A New Way to Heal Broken Bones: An Exoskeletal 3D Printed Cast of bones [Internet]. [cited 2018 Jul 17]. Available from: https://www.arch2o.com/new-way-heal-broken-bones-3d-printed-cast-3d-molds-exoskeletal/

17. Bandyopadhyay A, Gualtieri T, Bose S. Global Engineering and Additive Manufacturing. Vol. 10, Additive Manufacturing. 2015. 1-18 p.

18. Luo J. Additive manufacturing of glass using a filament fed process. 2017;

19. Klein J, Stern M, Franchin G, Kayser M, Inamura C, Dave S, et al. Additive Manufacturing of Optically Transparent Glass. 3D Print Addit Manuf. 2015;2(3):92–105.

20. Kotz F, Arnold K, Bauer W, Schild D, Keller N, Sachsenheimer K, et al. Three-dimensional printing of transparent fused silica glass. Nature. 2017;544(7650):337–9.

21. Klocke F, McClung A, Ader C. Direct laser sintering of borosilicate glass. Proc Solid Free Fabr Symp. 2004;214–9.

22. Khmyrov RS, Grigoriev SN, Okunkova AA, Gusarov A V. On the possibility of selective laser melting of quartz glass. Phys Procedia. 2014;56(C):345–56.

23. Gusarov A V, Protasov KE, Khmyrov RS. Manufacturing individual beads of quartz

glass via the selective laser melting of its powder. Bull Russ Acad Sci Phys. 2016;80(8):999–1002.

24. Khmyrov RS, Protasov CE, Grigoriev SN, Gusarov A V. Crack-free selective laser melting of silica glass: single beads and monolayers on the substrate of the same material. Int J Adv Manuf Technol. 2016;85(5–8):1461–9.

25. Fateri M, Gebhardt A. Jewelry fabrication via selective laser melting of glass. ASME 2014 12th Bienn Conf Eng Syst Des Anal ESDA 2014. 2014;1:1–5.

26. Manob G. Processing and Characterization of Lithium Aluminosilicate Glass Parts Fabricated By Selective Laser Melting. 2003;

27. Manob G, Lu L, Fuh JYH, Cheng YB. Selective Laser Melting of Li2O.Al2O3.SiO2 (LAS) Glass Powders. Mater Sci Forum. 2003;437–438:249–52.

28. Fateri M, Gebhardt A. Selective Laser Melting of soda-lime glass powder. Int J Appl Ceram Technol. 2015;12(1):53–61.

29. Fateri M, Gebhardt A, Thuemmler S, Thurn L. Experimental investigation on Selective Laser Melting of glass. Phys Procedia. 2014;56(C):357–64.

30. Gan MX, Wong CH. Properties of selective laser melted spodumene glass-ceramic. J Eur Ceram Soc. 2017;37(13):4147–54.

31. Aboulkhair NT, Everitt NM, Ashcroft I, Tuck C. Reducing porosity in AlSi10Mg parts processed by selective laser melting. Addit Manuf. 2014;1:77–86.

32. Khan M, Dickens P. Selective Laser Melting (SLM) of pure gold. Gold Bull. 2010;43(2):114–21.

33. Li R, Liu J, Shi Y, Wang L, Jiang W. Balling behavior of stainless steel and nickel powder during selective laser melting process. Int J Adv Manuf Technol. 2012;59(9–12):1025–35.

34. Tolochko NK, Mozzharov SE, Yadroitsev IA, Laoui T, Froyen L, Titov VI, et al. Balling

processes during selective laser treatment of powders. Rapid Prototyp J. 2004;10(2):78–87.

35. Gu H, Gong H, Pal D, Rafi K, Starr T, Stucker B. Influences of Energy Density on Porosity and Microstructure of Selective Laser Melted 17- 4PH Stainless Steel. Solid Free Fabr Proc. 2013;37:474–89.

36. Liverani E, Toschi S, Ceschini L, Fortunato A. Effect of selective laser melting (SLM) process parameters on microstructure and mechanical properties of 316L austenitic stainless steel. J Mater Process Technol. 2017;249:255–63.

37. Yadroitsev I, Bertrand P, Smurov I. Parametric analysis of the selective laser melting process. Appl Surf Sci. 2007;253(19):8064–9.

38. Mercelis P, Kruth J. Residual stresses in selective laser sintering and selective laser melting. Rapid Prototyp J. 2006;12(5):254–65.

39. Kasperovich G, Haubrich J, Gussone J, Requena G. Correlation between porosity and processing parameters in TiAl6V4 produced by selective laser melting. Mater Des. 2016;105:160–70.

40. Shaw B, Dirven S. Investigation of porosity and mechanical properties of nylon SLS structures. M2VIP 2016 - Proc 23rd Int Conf Mechatronics Mach Vis Pract. 2017;

41. Saarinen J, Van de Vrie R. Printed Optics Usher in New Era of Manufacturing | Features | Dec 2014 | EuroPhotonics. 12-2014. 2014.

42. Taylor RE. Thermal Expansion of Solids. 1st ed. Materials Park: ASM International; 1998. 293 p.

43. Drive CP. Accommodating Expansion of Brickwork. 2006;(November):1–11.

44. Petrucci, R.H.; Harwood, W.S. and Herring F. General Chemistry: principles and modern applications 10th ed. Igarss 2014. 2002.

45. Donaldson EC, Alam W. Wettability. Wettability. 2008.

46. Shartsis L, Smock AW. Surface Tensions of Some Optical Glasses. J Am Ceram Soc. 1947;30(4):130–6.

47. Michael Ashby HS and DC. Materials: Engineering, Science, Processing and Design. Materials and Manufacturing Processes. 2008.

48. CES Edupack 2017. Cambridge: Granta Design Limited; 2017.

49. ASTM. Standard Test Method for Transparency of Plastic Sheeting 1. Astm. 2015;

50. ASTM Int. Standard Test Methods for Tension Testing of Metallic Materials 1. Astm. 2009;

51. Ashby MF. Materials Selection in Mechanical Design. Design. 2005;

52. Brittain HG, Florey K. Analytical Profiles of Drug Substances and Excipients: Preface. Analytical Profiles of Drug Substances and Excipients. 1992;

53. Carr RL. Evaluating flow properties of solids. Chem Eng. 1965;

8 Table of Figures

9 Appendix

9.1 Sipernat D17 Specification Sheet

SIPERNAT®

Product information

SIPERNAT ® D 17

Characteristic physico-chemical data*)

Properties and test methods	Unit	Value
Particle size, d50 Laser diffraction following ISO 13320-1	µm	10.0
Loss on drying 2 h at 105°C following ISO 787-2	%	≤ 6.0
pH value 5 % in water/methanol 1:1 following ISO 787-9	-	8.0
Wettability by methanol internal method	%	≥ 52
Carbon content elemental analysar LECO following ISO 3262-19	%	1.7
Sieve residue 63 µm Alpine following ISO 8130-1	%	≤ 1.0
Tamped density not sieved following ISO 787-11	g/l	150
Loss on ignition 2) 2 h at 1000°C following ISO 3262-1	%	≤ 6.0
SiO_2 content 3) following ISO 3262-19	%	≥ 97
Na content 3) internal method	%	≤ 1.2
Fe content 3) internal method	ppm	≤ 400
Sulfate content 1) internal method	%	≤ 1.0
HACCP / FAMI-QS	-	only feed
Package size (net)	kg	15

1) based on original substance
2) based on dry substance (2 h/105°C)
3) based on ignited substance (2 h/1000°C)
*) The given data are typical values. Specifications on request.

Registrations

SIPERNAT ® D 17

CAS-No.	68611-44-9
EINECS (Europe)	exempted (defined as polymer, therefore not listed)
TSCA (USA) AICS (Australia) DSL (Canada)	registered
PICCS (Philippines) IECS (China)	registered
ENCS (Japan)	registered
KECI (Korea)	registered
NZIoC (New Zealand)	registered

SIPERNAT ® represents a specific product range of precipitated silica, aluminium and calcium silicates.

SIPERNAT ® D 17 is a hydrophobic silica and not wettable by water. Its primary application is as anti-caking agent.

- fire extinguishing powders (anticaking)
- manufacture of defoamers / antifoams (fast foam destruction)
- chemicals (flowability, anticaking)
- HTV / RTV-2C / LSR silicone rubber (reinforcing filler)

Safety and handling

Information concerning the safety of this product is listed in the corresponding Material Safety Data Sheet, which will be sent with the first delivery or upon updating.

Such information is also available from: Evonik Industries AG, Product Safety Department, E-Mail: sds-im@evonik.com . We recommend to read carefully the material safety data sheet prior to the use of our product.